

ELECTRON SPIN RESONANCE DETERMINATION OF THE EFFICIENCY
OF FREE RADICAL PRODUCTION IN BIOLOGICAL MEMBRANES
BY VARIOUS TYPES OF IONIZING RADIATION

A THESIS

Presented to

The Faculty of the Division of Graduate
Studies and Research

by

Henry L. Fisher, Jr.

In Partial Fulfillment

of the Requirements for the Degree

Doctor of Philosophy

in the School of Nuclear Engineering

Georgia Institute of Technology

May, 1973

ELECTRON SPIN RESONANCE DETERMINATION OF THE EFFICIENCY
OF FREE RADICAL PRODUCTION IN BIOLOGICAL MEMBRANES
BY VARIOUS TYPES OF IONIZING RADIATION

Approved: 1 1 /

V. A. Heise, Chairman

F. W. Chambers, Jr.

D. S. Harmer

J. A. Knight, Jr.

Date approved by Chairman: May 24, 1973

ACKNOWLEDGMENTS

Research described in this thesis was accomplished through the joint cooperation of the School of Nuclear Engineering and the School of Biology at the Georgia Institute of Technology. Facilities in the Engineering Experiment Station: the Georgia Tech Research Reactor, the Cesium-137 Gamma Exposure Facility, the Machine Shop, and the Ceramic Materials Laboratory contributed to the accomplishment of this work.

The author expresses his sincere appreciation to Dr. J. J. Heise, thesis advisor, for his suggestions, help, and advice in planning and carrying out this research project. His support of this effort contributed immensely to its success. Gratitude is expressed to members of the reading committee, Professor F. W. Chambers, Jr., Dr. D. S. Harner, and Dr. J. A. Knight, Jr., for their assistance and guidance. Gratitude is also extended to Dr. G. G. Eichholz whose reviews and advice were most helpful.

Support of the author by the U. S. Public Health Service and the Environmental Protection Agency is gratefully appreciated. Thanks are extended to Dr. J. A. Auxier and other members of the Health Physics Division at the Oak Ridge National Laboratory for their interest and consultation on instrumental aspects.

Thanks also go to Dr. M. E. McLain, Jr. for radiological technical support and for supplying the uranium-235 nitrate, to Dr. D. E. Wrege for data processing assistance, to Mr. R. M. Boyd and staff of the Georgia

Tech Health Physics Section for radiological safety and for dosimetry assistance, to Mr. B. D. Statham for the design and construction of the necessary electronic equipment, to Grady Memorial Hospital for the supplies of blood, and to the staff of the School of Ceramic Engineering for processing the ruby rod.

The format and typing of this thesis are the accomplishments of Mrs. Lydia S. Geeslin to whom my gratitude is extended.

TABLE OF CONTENTS

	Page
ACKNOWLEDGMENTS.	ii
LIST OF TABLES	vi
LIST OF ILLUSTRATIONS.	vii
SUMMARY.	xi
Chapter	
I. INTRODUCTION.	1
II. BIOLOGICAL MEMBRANES.	5
Membrane Structure.	5
Membrane Function and Composition	6
Erythrocytes.	8
III. IRRADIATION STUDIES OF MEMBRANES AND COMPONENTS	11
Amino Acids	11
Proteins.	12
Lipids.	15
Energy Migration.	16
Radiation Damage, Enhancement, and Protection.	17
Temperature Effect.	18
Trapping of Free Radicals	20
Saturation Dose	21
Linear Energy Transfer.	23
Membranes	25
IV. ELECTRON SPIN RESONANCE	30
Interactions of Electrons with a Microwave Field	30
Microwave Power Saturation.	33
Limitations to the ESR Method	34
V. INSTRUMENTATION AND EQUIPMENT	36
Electron Spin Resonance Spectrometer.	36
Microwave Cavity.	38
Data Recording System	41
Irradiation Facilities.	44

TABLE OF CONTENTS (Concluded)

Chapter	Page
VI. EXPERIMENTAL METHODS.	46
Membrane Preparations	46
Sample Preparation.	47
Radiological Dosimetry.	53
Electron Spin Resonance Measurements.	56
Quantitative Radical Determination.	60
VII. RESULTS AND DISCUSSION.	64
ESR Spectra of Unirradiated Membranes	64
ESR Spectra of Gamma Irradiated Membranes	72
ESR Spectra of Neutron Plus Gamma Irradiated Membranes.	85
ESR Spectra of Alpha Irradiated Membranes	90
ESR Spectra of Fission Product Irradiated Membranes	95
ESR Spectra of Controls	99
Power Saturation.	106
Radical Production and G-values	111
VIII. CONCLUSIONS AND RECOMMENDATIONS	137
Conclusions	137
Recommendations	143
Appendices	
I. FREE RADICAL BUILD-UP	146
II. COMPUTER PROGRAMS	150
ESR Spectral Integration.	150
Base Line Correction Program.	153
Power Saturation Program.	156
Radical Build-up Program.	158
BIBLIOGRAPHY	161
VITA	170

LIST OF TABLES

Table	Page
1. Membrane Sample Characterization.	49
2. Source Characteristics.	51
3. Comparison of Changes in Spectrometer Sensitivity and Q	59
4. Microwave Power Saturation Factors.	108
5. Relaxation Times from Saturation Measurements.	110
6. Constants for the Radical Build-up Equation.	114
7. G-values for Radical Production	114
8. Free Radicals Generated by Ionizing Radiation	147

LIST OF ILLUSTRATIONS

Figure	Page
1. Reaction Processes Following Absorption of Ionizing Radiation.	2
2. Assembly Drawing of Adjustable Ruby Standard.	39
3. ESR Data Recording System	42
4. ESR Spectra of Lyophilized Membranes at 200 mW at Room Temperature; Scan Time 4 min, Field Center 3385 G, Modulation Amp 10 G, Freq 9.55 GHz.	66
5. ESR Spectra of Oven-Dried Membranes at 200 mW at Room Temperature; (a) and (c) before Irradiation, (b) after 0.875 Mrad Gamma Irradiation.	67
6. ESR Spectra of Lyophilized Membranes at 200 mW at 77°K.	70
7. ESR Spectra of Lyophilized Membranes after 0.875 Mrad Gamma Radiation at Room Temperature; (a) at 200 mW, (b) at 0.5 mW; Spectrosil Tube, (c) at 200 mW, (d) at 0.5 mW.	73
8. ESR Spectra of Lyophilized Membranes after 0.916 Mrad Gamma Radiation at 77°K; (a) at 200 mW, (b) at 0.5 mW; Spectrosil Tube, (c) at 200 mW, (d) at 2 mW	75
9. ESR Spectra of Lyophilized Membranes after 0.816 Mrad Gamma Radiation at 77°K and after Annealing at Room Temperature; (a) at 200 mW, (b) at 2 mW; Spectrosil Tube, (c) at 200 mW, (d) at 2 mW.	77
10. ESR Spectra with Error Range of 1.5% Aqueous Membrane Solution after 0.816 Mrad of Gamma Radiation at 77°K at 200 mW; (a) at End of Irradiation, (b) Five Days Later	79
11. ESR Spectra with Error Range of 1.5% Aqueous Membrane Solution after 0.816 Mrad of Gamma Radiation Plus One Day Storage at 77°K; (a) at 0.5 mW, (b) at 200 mW	80
12. ESR Spectra after 0.816 Mrad Gamma Radiation at 77°K at 200 mW; (a) of 1.5% Membrane Solution, (b) of 48% Membrane Solution	82

LIST OF ILLUSTRATIONS (Continued)

Figure	Page
13. ESR Spectra of 48% Membrane Solution after 0.816 Mrad Gamma Radiation at 77°K after Annealing at Room Temperature; (a) at 200 mW, (b) at 5 mW.	84
14. ESR Spectra of Lyophilized Membranes at 200 mW at Room Temperature; (a) after n+γ Exposure, (b) before Exposure, (c) Spectrosil Tube after n+γ Exposure.	86
15. ESR Spectra of Lyophilized Membranes at Room Temperature after n+γ Exposure; (a) at 0.5 mW, (b) Spectrosil Tube at 200 mW	87
16. ESR Spectra of Lyophilized Membranes at 200 mW at 77°K; (a) after n+γ Radiation, (b) before Irradiation, (c) Spectrosil Tube after Irradiation	88
17. ESR Spectra of Lyophilized Membranes at 77°K; after n+γ Radiation; (a) at 1 mW, (b) at 200 mW, (c) Membranes at 200 mW before Irradiation, (d) Spectrosil Tube at 200 mW.	89
18. ESR Spectra of Lyophilized Membranes after n+γ Exposure at 77°K after Annealing at Room Temperature; (a) at 1 mW at 77°K; at 0.5 mW, (b) at Room Temperature, (c) after 4 Days at Room Temperature.	91
19. ESR Spectra of Lyophilized Membranes at Room Temperature; (a) at 200 mW before Irradiation; after 2.63 Mrads Alpha Radiation, (b) at 0.5 mW, (c) at 200 mW, (d) at 200 mW after 6.5 Days Storage.	92
20. ESR Spectra of Lyophilized Membranes at 77°K; after 1.77 Mrads of Alpha Radiation; (a) at 200 mW, (b) at 1 mW, (c) at 200 mW before Irradiation.	93
21. ESR Spectra of Lyophilized Membranes at 200 mW after 1.77 Mrads of Alpha Radiation at 77°K after Annealing at Room Temperature; (a) after 4 Days at Room Temperature, (b) at 77°K, (c) at Room Temperature.	94
22. ESR Spectra of Lyophilized Membranes at Room Temperature, after 2.68 Mrads Fission Product Radiation; (s) at 0.5 mW, (b) at 200 mW, (c) at 200 mW before Irradiation	96
23. ESR Spectra of Lyophilized Membranes at 77°K, after 1.80 Mrads of Fission Product Radiation; (a) at 1 mW, (b) at 200 mW, (c) at 200 mW before Irradiation.	97

LIST OF ILLUSTRATIONS (Continued)

Figure	Page
24. ESR Spectra of Lyophilized Membranes at 200 mW after 1.80 Mrads of Fission Product Radiation at 77°K after Annealing at Room Temperature; (a) at 77°K, (b) at Room Temperature, (c) after 4 Days at Room Temperature.	98
25. ESR Spectra of Irradiated Spectrosil Tubes at 200 mW at Room Temperature; (a) and (c) Unirradiated, (b) Fission Product Irradiated, (d) Alpha Irradiated.	101
26. ESR Spectra of Irradiated Spectrosil Tubes at 1 mW at 77°K; (a) after Fission Product Radiation, (b) after Annealing at Room Temperature, (c) after Alpha Radiation	103
27. ESR Spectra of Hydrogen Radicals in Spectrosil Tubes at 1 mW at 77°K; (a) after Alpha Radiation, (b) after Fission Product Radiation	105
28. Build-up of Free Radicals at Room Temperature in Gamma Irradiated Membranes Dried at 80°C, HDM Sample.	115
29. Build-up of Free Radicals at Room Temperature in Gamma Irradiated Lyophilized Membranes, FDM-1 Sample.	116
30. Build-up of Free Radicals at 77°K in Gamma Irradiated Lyophilized Membranes, FDM-2 Sample	118
31. Build-up of Free Radicals at 77°K in Gamma Irradiated 1.5% Membrane Solution, LM Sample, and in Water, HS Sample	120
32. Build-up of Hydrogen Radicals at 77°K in Gamma Irradiated 1.5% Membrane Solution, LM Sample, and in Water, HS Sample	123
33. Build-up of Radicals at 77°K in Gamma Irradiated 48% Membrane in Aqueous Solution, 50-50 Sample.	124
34. Build-up of Free Radicals at Room Temperature in n+γ Irradiated Lyophilized Membranes, N-1 Sample.	126
35. Build-up of Free Radicals at 77°K in n+γ Irradiated Membranes, N-2 Sample	127
36. Build-up of Free Radicals at Room Temperature in Alpha Irradiated Lyophilized Membranes, A-1 Sample.	130

LIST OF ILLUSTRATIONS (Concluded)

Figure	Page
37. Build-up of Free Radicals at 77°K in Alpha Irradiated Lyophilized Membranes, A-2 Sample	132
38. Build-up of Free Radicals at Room Temperature in Fission Product Irradiated Lyophilized Membranes, F-1 Sample.	133
39. Build-up of Free Radicals at 77°K in Fission Product Irradiated Lyophilized Membranes, F-2 Sample.	135

SUMMARY

Radiation damage to the plasma membrane, a component necessary for cellular existence, was studied by observing free radicals produced by radiation of different qualities. Membranes were separated from hemolysed red blood cells and exposed to gamma, neutron, alpha, and fission product radiations. Exposures and measurements were made at both 77°K and room temperature. Free radical measurements were made with an electron spin resonance spectrometer operating at about nine GHz and equipped with an analog to frequency converter, permitting storage of the spectrum in a 400 channel scaler. The digitalized spectrum was subsequently analyzed with a computer where background and baseline corrections could be made.

Free radical yields in lyophilized membranes varied inversely as the LET of the radiation. At room temperature the initial yield for gamma radiation was five radicals/100 eV while for alpha radiation the yield was 0.6 and for fission product radiation the yield was 0.03. The build-up of radicals was generally linear with dose although radical saturation was apparent in a few samples. At 77°K hydrogen radicals were observed in samples exposed to gamma rays but not to high LET radiation. However, the yield was quite low, being about 0.001 radical/100 eV.

The g-values for free radicals produced by radiation were close to that of the free electron. Membrane samples containing water exposed to gamma rays exhibited larger g-value shifts than dry samples. Large shifts were also observed for dry samples exposed to high LET radiation at 77°K

and annealed at room temperature.

From the ESR spectra it was concluded that the radicals observed at room temperature are not the primary radicals produced by the radiation. Radical reactions were also observed to continue over a period of hours or days. Since the yield of free radicals in membrane material is sufficiently high, radicals are likely involved in producing membrane damage. The exact pathway by which this occurs remains to be explored.

CHAPTER I

INTRODUCTION

It is well known that ionizing radiation causes damage in biological systems. This damage is associated with the amount of energy absorbed, the type or linear energy transfer (LET) of the radiation, and the particular biological or cellular system exposed. Although the magnitude of the effect depends on total dose and often on dose rate, the basic or elementary stages between the absorption of energy and the expression of biological effect are just beginning to be elucidated. It is thought that chemical species with an unpaired electron or free radicals, which are usually very reactive and have excess energy, may be an important link in many radiobiological processes.

Since the plasma membrane is necessary for cellular existence and has been associated with such processes as protein and DNA synthesis, the mechanism by which radiation causes damage to this structure should be investigated. The primary objective of this research was to determine the build-up of free radicals in such membranes as a function of radiation dose. The electron spin resonance (ESR) method of detecting free radicals was chosen because of its sensitivity, non-destructiveness, and its applicability to opaque samples.

The primary reaction steps leading to biological damage after the absorption of ionizing radiation as given by Dertinger and Jung (1970) are reproduced in Figure 1. The free radicals which are usually observed

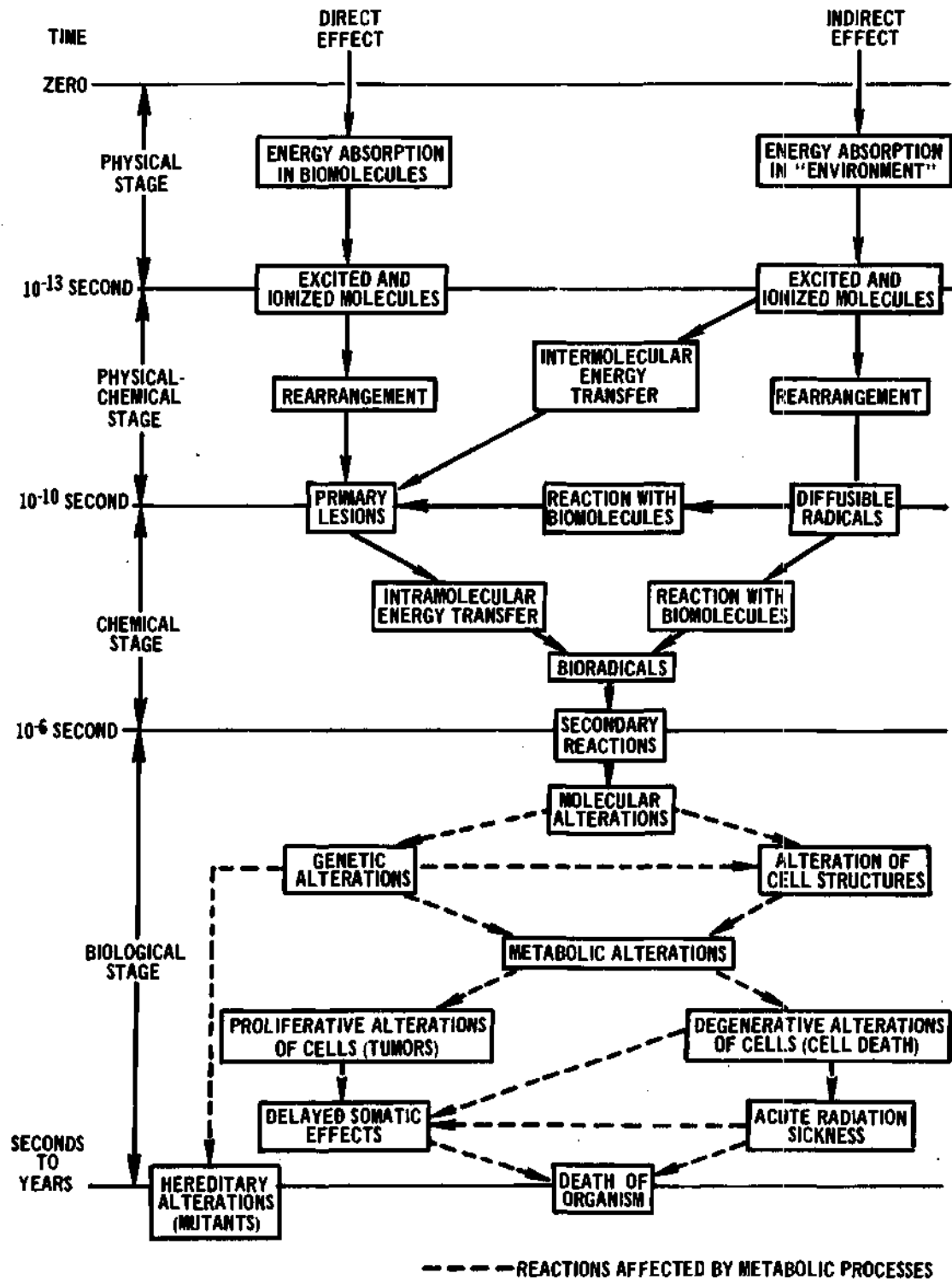


Figure 1. Reaction Processes Following Absorption of Ionizing Radiation

occur in either the early physical, physical-chemical, or chemical stages. Under physiological conditions these stages are usually completed within 10^{-6} seconds after radiation absorption. Cooling the biological systems to low temperatures may slow or stop reactions; this in turn may permit examination of free radicals. Some free radicals may also be observed days after irradiation even at room temperature. Another method for production of short-lived free radicals in sufficient quantity to be observed involves the use of intense or pulsed radiation. In the present study the quantity of free radicals produced as a function of dose was determined at both room temperature and at 77°K.

Although free radicals are usually very reactive, they may be stabilized in unsaturated symmetrical aromatic molecules or in biopolymeric structures which can result in slow decay over a long period of time under physiological conditions. Such effects were observed in the experiments to be described. Biological damage may be produced without the formation of free radicals anywhere in the sequence. The reaction pathways in Figure 1 are a simplified diagram of a complex network of pathways. Therefore, the production of a free radical in one branch of the pathway may have little or no relation to a biological effect produced at the end of another pathway. Although these are serious limitations, it is expected that determination of free radical processes may help explain some of the processes by which ionizing radiation is absorbed and affects a biological system.

It is the purpose of this dissertation to compare the quantity of free radicals produced by radiation of various qualities or with various

CHAPTER II

BIOLOGICAL MEMBRANES

Some of the characteristics of the sample material, the plasma membrane, are described in this chapter. These characteristics may or may not have a bearing on the efficiency of free radical production by ionizing radiation. However, a knowledge of the static and dynamic characteristics peculiar to membranes provides a better foundation from which to interpret the experimental results.

Membrane Structure

The first study on cell membranes by E. Overton (1895) deduced that lipids were likely to be an important component of the membrane (Hendler, 1968). In 1925 Gorter and Grendel attempted to extract and quantitatively determine the lipid content of erythrocyte membranes (Gorter and Grendel, 1925). From this analysis it was apparent that the area of a monolayer of the extracted lipids was twice the surface area of the erythrocytes which implies that membranes have a bimolecular lipid layer.

In the 1930's a very low value for the surface tension of membranes was obtained by a number of investigators. Since this could not be accounted for by the lipid model of the membrane, it was postulated that the lipid base was coated with two layers of protein (Danielli and Harvey, 1935). These facts were the basis of a model of membrane structure

(Danielli and Davson, 1935). Measurement of the electrical capacitance and impedance of cell membranes produced further evidence in support of this model (Höber, 1945).

With electron microscopy it was possible to observe some structural detail in membranes and this led to the concept of the unit membrane as the basis for biological membranes in general (Robertson, 1959,1964,1966). The unit membrane is described as a three layered sandwich, the middle layer consisting of lipids and a layer on each side consisting of protein. Each layer is about 2.5 nm thick. There is also evidence which has led to other models such as the discrete globular model (Sjöstrand, 1963 a,b), which may have protein molecules embedded in or extending into a sea of lipids. It has also been suggested that the hydrophobic side of some globular proteins may be able to nestle into the lipid bilayer (Dewey and Barr, 1970). Although there are several models of such structures (Lucy, 1968), the difficulty of interpreting the experimental data and deducing the in vivo structure results in inadequate support for any model (Korn, 1966).

Membrane Function and Composition

The oldest idea of the function of the plasma membrane was that it was a structural container with the ability to selectively permit the passage of materials into and out of the cell. Recent experiments extended this idea to include an active transport mechanism. These experiments have indicated that surface components along with specific enzymes and proteins are involved (Pardee, 1968).

The erythrocyte membrane has been associated with various enzymes,

antigens, and blood group markers (Dowben, 1969; Watkins, 1967).

Membranes play a very important role in the conduction of nerve impulses, and energy transfer and conversion in vision and photosynthesis. Additionally, membranes have been linked with amino acid transport (Kostyo, 1964), protein synthesis (Spiegelman, 1958), and DNA replication and transcription (Sinsheimer, 1968).

It has been known since the 19th century that membranes were composed of proteins and lipids. However, the nature of the bonding between protein and lipid, as well as the geometrical arrangement has yet to be determined with certainty. Suggestions for such bonding include hydrogen bonding, coulombic bonding, or hydrophobic bonding of fatty chains (Chapman, 1969). Since a knowledge of membrane composition can help in the formulation of valid models of membrane structure and function, determination of the lipid composition of various types of membranes has been done. Of the three classes of lipids, phospholipids, glycolipids, and sterols, animal cell membranes generally contain all three types, while plant and bacterial cells usually do not contain sterols (Rouser et al., 1968). As many as a dozen specific lipids have been determined in the plasma membranes, endoplasmic reticulum, and membranes of mitochondria, nucleus and the Golgi apparatus. Variations in lipid composition for the various types of membranes, for the same type of membrane from different types of cells, and for different species have been tabulated (Rouser et al., 1968; Nelson, 1967). Many determinations of the lipid composition of the plasma membrane of human erythrocytes have been reported (Rouser et al., 1968; Ways and Hanahan, 1964; Weed et al., 1963; Dodge et al.,

1963). Of the total lipids the average sterol content, which occurs solely as cholesterol, is 25 percent, the average content of total phospholipids is 56 percent, and the average glycolipid content, which for animal cells occurs as spingolipids, is 19 percent. Any variation in composition with age, sex, or blood type is obscured by a wide range of the normal biological variation (Rouser et al., 1968).

Erythrocytes

The purpose of the experiment was to analyze the radiation products in a representative or model plasma membrane.

The erythrocyte membrane was chosen for the experimental material because erythrocytes are readily available in sufficient quantities and have been thoroughly studied with respect to metabolism and membrane permeability. Additionally, the membrane is easily isolated, particularly as intact red blood cell ghosts.

Human erythrocytes have a life span of about 120 days. By differential centrifugation to separate the various age cells, it has been shown that with increasing age there is a decrease in enzyme activities, in the rate of glucose utilization, in the lipid content, and in potassium concentration and increase in sodium concentration, and an increase in osmotic fragility (Pranker, 1961). Apparently normal cell death is not due to merely the depletion of energy reserves but is probably due to the inability of the cell to replace vital protein or lipid constituents (Yunis and Yasminch, 1969). In vitro aging was reviewed and concluded to be different from in vivo aging (Yunis, 1969). The in vitro aging has been identified with a loss of energy potential due to a decrease in

various phosphate esters, primarily adenosine triphosphate (Huennekens, 1960).

The constitution or structure of the erythrocyte membrane has yet to be well defined. One model suggests that the erythrocyte consists of a homogeneous liquid surrounded on the outside by a membrane. Another interpretation is that the erythrocyte is a sponge consisting of a membrane-like framework or stroma surrounded by a membrane and impregnated with hemoglobin solution (Seitz, 1969). Electron microscopic investigations place the thickness at about 10 nm although considerable variability is not uncommon. After hemolysis the erythrocyte "ghost" is entirely empty and balloon-like but the intact erythrocyte has a dense internal structure (Bernhardt, 1952).

The normal red blood cell contains about 18×10^{-17} moles/cell of sulfhydryl groups (Rothstein, 1970). The function of sulfhydryl groups in membrane structure is not precisely known. It is known that x-irradiation will increase the number of sulfhydryl groups in red blood cell ghosts and that many membrane functions are disrupted by the addition of sulfhydryl-binding, or altering chemicals (Rothstein, 1970). Although sulfhydryl groups in membranes are ubiquitous, not all sulfhydryl groups have the same physiological function. In erythrocyte ghosts, three types of sulfhydryl groups have been identified (Rothstein and Weed, 1963). These three types, based on their reactivity with various chemical agents are the maximal binding for: N-ethylmaleinide, chlormerodrin, and H_3Cl_2 .

N-ethylmaleinide reacts the most readily with reactive sites and is able to bind 1.4×10^{-17} moles/cell or seven percent of the sulfhydryl

groups in the membrane. Chloromerodrin can react with 4.2×10^{-17} moles/cell, or 23 percent, and H_3Cl_2 can react with 18×10^{-17} moles/cell or all the sulfhydryl groups. The chloromerodrin-bound sulfhydryl groups will inhibit the transport of ATPase as will those bound with H_3Cl_2 , but not those bound by N-ethylmaleinide, indicating that the intermediate reactive sulfhydryl groups are essential for ATPase transport (Rothstein and Weed, 1963). With increasing mercuric binding, there is observed a sequence of no effect, followed by ATPase transport inhibition, followed by an increase in K^+ permeability, followed by inhibition of sugar uptake, followed by a non-specific increase in permeability (Rothstein and Weed, 1963). The initial "no effect" and the absence of an observed physiological effect associated with N-ethylmaleinide binding prevents the assignment of a specific membrane function to the most reactive sulfhydryl groups. It is conjectured that these most reactive but physiologically unresponsive sulfhydryl groups may protect against traces of heavy metals or free radicals (Rothstein and Weed, 1963). Thus, the action of sulfhydryl groups in the radiological effect in membranes should be considered when free radical mechanisms are involved.

CHAPTER III

IRRADIATION STUDIES OF MEMBRANES AND COMPONENTS

Irradiation studies of membranes and membrane components by chemical and physical methods have been proceeding for some time. Although the purpose of the work described in this thesis is to directly detect radiation produced free radicals, it will be useful to consider these related works in drawing conclusions about radiation effects. Direct detection of free radicals in classes of biological materials, which are constituents of membranes, has also been done and the results compiled. It is of some interest to determine how free radical production will be affected by the particular arrangement of these components in the membrane. This can be done by comparing results from intact membranes with results from membrane components. For these reasons and to place the present work in perspective, the results of prior irradiation studies on membranes and their components will be briefly reviewed in this chapter.

Amino Acids

Twenty five amino acids have been exposed to 10^6 to 10^7 Roentgens of x-rays (Gordy, 1959) and all gave detectable radicals. Not only were radicals detected, but the ESR spectra were hundreds of gauss wide indicating strong orbital coupling of the electron. These spectra had many resonance peaks indicating coupling of the unpaired electrons with several

protons and nitrogen nuclei (Blumenfeld and Kalmanson, 1961; Gordy, 1959). Radicals in dry crystalline amino acids persisted for years even in the presence of air but vanished immediately if the crystals were dissolved in water (Blumenfeld and Kalmanson, 1961).

Although most x-irradiated amino acids give different characteristic ESR spectra, a pattern common to the amino acids containing sulfur suggests that the odd electron is localized on the sulfur atom (Shields and Gordy, 1958). For amino acids with ring structures, the ESR spectra were broad with unresolved structure indicating that the unpaired electron was migrating around the ring (Shields and Gordy, 1958). The linear energy transfer (LET) of the radiation greatly affects the efficiency of free radical production. Irradiating with high LET alpha radiation from ^{210}Po it was found that the number of free radicals produced per unit dose was one third to one fifth that for low LET x or gamma radiation (Kirby-Smith and Randolph, 1960,1961; Randolph, 1961). X-ray irradiation showed that free radical production in the eleven amino acids examined requires from 23 to 81 eV/radical (Miller, 1962). In amino acids containing aromatic rings, the energy required to produce a radical was greater.

Proteins

Although ESR signals are also obtained by x-irradiation of proteins, individual proteins do not produce specific spectra. There appear to be two basic spectra for most proteins, each protein exhibiting one or the other or a combination of both (Gordy, 1959). One basic spectrum is similar to that obtained from the irradiated amino acids, cystine, or

cysteine, and the other is a doublet, probably due to the interaction of an unpaired electron with a proton (Gordy, 1959). Since the energy density of the ionizing radiation is distributed uniformly over the protein molecule, there is a suggestion of energy transfer from the molecular group initially absorbing the radiation to a cystine or cysteine moiety. Gordy conjectured that the doublet in the ESR spectrum is due to an unpaired electron on one proton of the CH_2 group and the cysteine-like spectrum is mainly due to an unpaired electron associated with a sulfur atom (Gordy, 1959). It is certain that the observed spectrum is produced by highly localized spin densities such as could be produced by trapped electrons and free radicals but not from conduction electrons (Gordy and Shields, 1958). It has been reported that the disappearance of the doublet spectrum follows first order kinetics and decays more rapidly than the sulfur resonance which does not obey first order kinetics (Shields and Hamrick, 1970).

Later work in which protein was irradiated and examined at 77°K established that a unique spectrum is formed for each protein (Patten and Gordy, 1960). Apparently the radical or radicals formed are trapped in the material at this low temperature. Upon warming the spectrum changed, usually to one like that observed at room temperature and is not recoverable by lowering the temperature again.

The energy required for free radical production by x-irradiation of protein was found to vary from 14 to 160 eV/radical for the six proteins examined (Müller, 1962). The energy expended in hemoglobin was 140 eV/radical. The types of ESR spectra observed for x-irradiated proteins are limited compared to the many types observed for amino acids. Poly-

peptides which have only a few amino acids compared to protein composition, give ESR spectra upon x-irradiation that are in general neither like those of protein or amino acids (McCormick and Gordy, 1958). After irradiation of glycine and (glycyl)_n-glycine, n = 1,2,..., the ESR spectrum of glycine was different from the ESR spectrum of the polyglycines and all polyglycines had a common spectrum type (McCormick and Gordy, 1958). For short-chain polypeptides the terminal group can affect the ESR spectrum and hence the radical formed (McCormick and Gordy, 1958). These results indicate that although complex proteins may give rise to a simple ESR spectrum, the radiation chemistry of the formation of this free radical may involve many steps and be quite complex. In seven of the thirteen polyamino acids examined, it was possible to interpret the ESR spectrum as being produced by a loss of a hydrogen atom from the CHR group of the peptide chain (Drew and Gordy, 1963). In the other six polyamino acids the interpretation was not so clear. The free radicals formed probably occur in the side chain, rather than in the polypeptide backbone (Drew and Gordy, 1963). Thermal hydrogen atom bombardment produces radicals in some polyamino acids that are similar to those produced by gamma irradiation (Liming, 1969; Holroyd et al., 1970). This similarity suggests that some radicals produced in gamma irradiated protein can be formed by reaction with secondary hydrogen radicals.

When proteins containing sulfur are irradiated at 77°K very few sulfur radicals are formed (Henriksen et al. 1961, 1963 a). If the temperature is then raised to 280°K sulfur radicals begin to appear.

After x-irradiation of trypsin in a vacuum at room temperature,

atmospheric oxygen was admitted and the ESR spectrum recorded (Henriksen, 1967 a). A transient line of 13 gauss width at a g-value of 2.007 was observed and attributed to the peroxide radical.

By gamma radiolysis of dry proteins in the presence of tritiated hydrogen sulfide, it was determined that formation of carbon radicals occurred in two ways. The first occurs below 195°K and is independent of amino acid sequence, conformation, and the presence of disulfide bridges. The second occurs above 195°K and is specific for the various conformations of each protein (Riesz and White, 1970).

Lipids

Since lipids are fundamental constituents of the membrane, and since lipid peroxides can be produced by ionizing radiation, the study of peroxide radical species should be considered. Lipid peroxides are powerful oxidizing agents capable of destroying sulfhydryl proteins and sulfhydryl enzymes and can be produced with as little as 2 to 100 rads (Wills and Wilkinson, 1967). Peroxide formation is enhanced when lipids are irradiated in an aqueous emulsion rather than when irradiated dry (Wills and Rotblat, 1965). This implies that radicals formed in the aqueous phase, such as OH radicals, in conjunction with dissolved oxygen are the main promoters of peroxide formation. Compared to the lipid-aqueous emulsion, peroxide formation in a protein-lipid-aqueous emulsion under irradiation is reduced (Wills and Rotblat, 1965). Little is known about the action of peroxides in irradiated normal tissue. However, it has been speculated that these peroxides can cause spatial disorganization of membrane-bound enzymes or that peroxides broken from membrane

lipids may interfere with metabolism of other cellular components (Wills and Wilkinson, 1967).

Energy Migration

The mechanism of energy transfer has not been established, but it has been suggested that in protein electron vacancies may migrate (Patten, 1960) or that electrons may migrate through the conduction band (Blumenfeld, 1961). Other experiments indicate that the transfer of the unpaired electron in lyophilized serum albumin to the cystine residue upon warming from 77°K to 323°K is only about 50 percent efficient (Nielsen and Ramussen, 1962). Since the ESR spectra are different for proteins irradiated at 77°K and at room temperature and since the low temperature spectra are irreversibly converted to the room temperature spectra upon raising the sample to room temperature, intramolecular transfer of energy has been proposed as an explanation (Patten and Gordy, 1960). The low temperature spectrum is assumed to emanate from these radicals or from radicals formed after limited energy migration. At higher temperatures the electron or hole is assumed to migrate to specific trapping sites (Henriksen, 1969 a). The few types of radicals thus formed are assumed to produce the room temperature spectra.

It has also been suggested that there may be an intermolecular transport of energy (Henriksen et al., 1961, 1962 b, 1963 a, 1963 b; Milvy and Pullman, 1968). The expected observable results of this model are like those of the previous model. However, by adding other materials to make a mechanical mixture, it should be possible in some cases to intercept the energy being transferred between molecules and thereby in-

fluence the types of radicals that will be formed and observed.

An experiment demonstrating the clearest case for intermolecular transfer of energy was performed with Sephadex, a modified dextran containing a network of interstices and pores, and the thiol, penicillamine. The degree of mixing of the components was varied and the mixture was irradiated with 220 kV x-rays at 77°K. The ESR spectra indicated that radiation energy was transferred from Sephadex to penicillamine at 77°K and that the amount of transfer depended on the extent of contact between the two compounds (Henriksen, 1967 b). It appears that spin migration is more important than spin recombination at low radiation doses and low radical densities (Milvy, 1971).

Radiation Damage, Enhancement, and Protection

For low LET radiation the almost universal effect of oxygen is to promote detrimental biological effects. Gordy (1959) described the detrimental effect of oxygen as due to the modification of the damaged molecule by oxygen in an irreversible way. Through the use of ESR spectra, Gordy theorized that the unpaired electron produced by ionizing radiation has a high probability of eventually being located on the following groups presented in order of decreasing probability, (1) sulfur, (2) $-C = O$ group, or the (3) $-C = C-$ group. Sulfur radicals and $-C = C-$ radicals are capable of being attacked by oxygen which in turn changes the ESR spectra. However, the $-C = O$ radical is stable with respect to oxygen attack. The stability arises because of the large probability density of the unpaired electron being associated with this group which thereby generates a repulsive force between electronegative oxygen atoms (Gordy, 1959).

Alexander and Ormerod (1962) have put forward a hypothesis and given data in support of a mechanism by which radioprotective and radiosensitizing compounds function. According to this theory free radicals produced in nucleoproteins have three competing reactions which may be followed: (1) radical-radical reactions or cross-linking of DNA; (2) radical- O_2 reactions or peroxidizing of DNA; and (3) radical-cysteamine reactions producing repaired DNA and sulphur free radicals. Cysteamine is a radioprotector in the presence of oxygen, but in the absence of oxygen the repair rate is not limited by the natural sulphydryl groups present. Consequently introduction of additional sulphydryl groups by cysteamine does not increase the repair rates (Ormerod and Alexander, 1963). Although this theory is based on ESR determination of free radicals present in spermatozoa exposed to gamma irradiation with and without oxygen and/or cysteamine, the same mechanisms operate with protein except that radical-radical reactions or cross linking reactions do not occur (Alexander and Ormerod, 1962). In proteins, if oxygen is present, cysteamine is not effective since the reaction rate for peroxidization, reaction 2, is very much larger than that for reaction 3. This contrasts drastically with DNA protection. The rates of the three reactions for different substances will therefore affect the ability of oxygen to sensitize and cysteamine to repair radiation damage.

Temperature Effect

The temperature of the sample during irradiation may have important consequences on the experimental results. It might be expected that there would be a temperature dependence of the production of secondary free

radicals after radiation absorption since the chemical reaction coefficients may be temperature dependent. When a comparison is made of amino acids irradiated at 77°K and 300°K, it is usually found that the ESR spectra are different. But when the low temperature sample is warmed to 300°K, the radicals obtained are usually the same as those obtained in the sample irradiated at 300°K (Patten and Gordy, 1961 a). This result is also true for cystine and bovine-serum albumin (Libby et al., 1961) and for nucleosides (Müller et al., 1964 a). Additional differences in the radicals produced at 77°K as compared to those produced at 300°K are: (1) the hyperfine structure is usually not as broad nor as easily resolvable as at room temperature; (2) the hyperfine structure, when resolvable, consists of fewer components at 77°K; (3) more different types of radicals are formed at 77°K than at room temperature (Patten and Gordy, 1961 a). These observations lead one to conclude that, at low temperature, the free radicals formed consist of single atoms or small groups that have high symmetry and are relatively unstable (Patten and Gordy, 1961 a).

The trapping of radicals is a function of temperature. For example, it has been found that the OH radical is trapped in pure ice at 77°K while the trapping of H[•] radicals requires a lower temperature between 4.2°K and 77°K, depending on the matrix (Piettev et al., 1959). Many radicals, especially from complex organic compounds, may persist for months at room temperature. The matrix within which a free radical finds itself will also have an effect on the radical lifetime.

Irradiation of water, glycine, and water/glycine solutions at 77°K

leads to the conclusion that only the direct effect of the radiation on glycine produced glycine radicals (Henriksen, 1962 a). The free radicals produced in the water component of the water/glycine solutions could be observed, however. The yield of glycine type radicals in gelatin is three times higher when irradiated in vacuum at 300°K than at 77°K (Müller, 1962). This may be due to quenching of reactions producing these radicals at 77°K.

Trapping of Free Radicals

Trapping of free radicals will depend on the availability of trap sites, the diffusion of radicals, and the stability of the radical with respect to energy transfer and chemical reactions. Radical species present in acids, bases, and neutral solutions after x-irradiation at 77°K have been observed (Henriksen, 1964). He observed H[•] radicals and solvated electrons in alkaline solutions, H[•] radicals in acid solutions, and solvated electrons in neutral solutions. The OH radical was observed in all solutions. The state of the matrix also affects the observable species (Ten Bosch, 1967). In general, glassy samples trap two to four times as many total radicals as polycrystalline ones (Henriksen, 1964, 1969 b). Specific radicals such as H[•] radicals may, however, be trapped more efficiently in alkaline polycrystalline matrices than in glassy ones.

Not only does the state of the matrix affect the yield of radicals but it can also influence the kind of radical formed. The type of radical formed by gamma irradiation of a frozen solution of cysteamine is dependent on the dissociative state of the molecule as measured by the pH prior to lyophilization (Copeland and Swartz, 1969).

Saturation Dose

It is not uncommon for the build-up of radicals to cease at doses of a few Mrad. Such behavior is called radical saturation. Since the number of free radicals produced at saturation is smaller by orders of magnitude than the number of molecules capable of becoming radicals, saturation is not due to a depletion of the number of molecules which are candidates for becoming free radicals unless there are differences between these candidates which at present are not apparent. If the number of radical trapping sites were limited or the distance between radical pairs were limited because of radical-radical reactions, then the saturation level would depend on the concentration of radicals in the material. However, it has been found that in some cases the saturation value does not depend on the radical concentration (Zimmer and Müller, 1965). This furnishes support for the direct destruction of radicals by the radiation. Furthermore, the concentration of radicals at saturation might be several times smaller in the case of alpha irradiation as compared to gamma irradiation (Müller et al., 1964). For many substances, the radical yield was found to fit the function (Müller, 1963; Rotblat and Simmons, 1964):

$$N = N_{\infty} [1 - \exp(-\lambda D)]$$

where N_{∞} is the saturation radical concentration,

D is the radiological dose, and

λ is the probability of radical destruction per unit dose.

This equation originated from the assumption that the radiation destroys radicals in addition to producing them. However, the cause of

radical saturation has not yet been satisfactorily established for all substances.

The saturation concentration of free radicals depends on the temperature of the sample. When methanol was irradiated at 4°K, it was found that 20 percent more free radicals could be trapped than when irradiation was done at 77°K (Alger, 1960). Additionally, it was found that the evolution of hydrogen gas from solid methanol undergoing irradiation was proportional to energy absorbed even for doses up to ten times the dose that would cause radical saturation (Alger, 1960). Thus the hydrogen may be formed by molecular processes, although radical involvement cannot yet be eliminated.

Single crystals of alanine, after irradiation to radical-saturation concentration with cobalt-60 gamma rays, were deuterated selectively at only the radical site. This sample when given a second saturation dose of 2×10^7 R was found to have no deuterium labeled radicals (Snipes and Horan, 1967). It was concluded that in this case of radical saturation the radical production rate was not zero and that saturation was due to radical destruction by the radiation. Thus at saturation the production and destruction rates were equal.

Free radical destruction by radiation has been measured directly by ESR. Some compounds when irradiated at room temperature and at 77°K produce different radicals with different ESR spectra. If these radicals are stable, and if the spectra from the two radicals can be separated, then a sample irradiated at room temperature and cooled to 77°K will exhibit only the room temperature radical. If irradiation is carried out

again at this point, only the 77°K radicals will be produced and in addition the destruction of the room temperature radicals can be observed. Using this procedure it has been determined that radical destruction follows first order kinetics or decreases exponentially with dose (Horan and Snipes, 1969). Since the G-value for radical destruction by only the direct effect was extremely high, it was concluded that energy absorbed some distance from the radical was able to affect radical destruction. Such a mechanism might be explained through population of electron-hole energy conducting states or through diffusion of hydrogen atoms (Horan and Snipes, 1969), although the last mechanism is doubtful and does not operate in some cases (Horan and Snipes, 1970). Thus, saturation appears to be due to an equivalence of radical production and destruction rates under irradiation in some compounds. Subsequent experiments of this type in which the irradiation was performed on N-acetyl-DL-valine at various temperatures showed that the radical destruction process is temperature dependent, perhaps indicating that several energy transfer pathways of radical destruction are operative (Horan and Snipes, 1971) or that several first order kinetic processes exist (Henriksen, 1971).

That observed radicals can account for only part of the biological inactivation is deduced from saturation experiments. Inactivation of bacteriophage DNA was exponential up to five megarads while free radical saturation occurred at about two megarads (Hoff and Koningsberger, 1970).

Linear Energy Transfer

In amino acids not possessing aromatic rings the yield of free radicals per unit radiation dose was found to be about a factor of six

lower for alpha irradiation than for gamma irradiation (Müller et al., 1964). For those containing aromatic rings the yields were approximately equal. For glycine, the yield from polonium-210 alpha irradiation was about 0.3 that for cobalt-60 gamma irradiation (Kirby-Smith and Randolph, 1960). This effect was attributed to a wastage of energy or energy dissipation into non-productive modes and radical recombination from overly dense ionization of high LET radiation.

The existence of free radicals along with a biological effect provides little support connecting the two in a cause and effect relationship. A stronger case may be made if one is able to influence the sequence of events leading to free radical production and then compare any resulting change in biological effect. One example would be to vary the spatial distribution of energy absorption by using ionizing radiation of various LET values.

The free radical yield in the enzyme trypsin has been determined for LET values ranging over four orders of magnitude (Henriksen, 1966 a). The radical yield curve is constant up to about $200 \text{ MeV cm}^2/\text{g}$, but then declines until it has decreased by a factor of 2.4, at about $10^4 \text{ MeV cm}^2/\text{g}$. The type of radicals observed was independent of LET. The shape of this yield curve is similar to the enzymatic inactivation curve as a function of LET. This lends support to the hypothesis that free radicals are involved in the sequence of steps leading from the absorption of radiation to biological damage. Subsequent studies using amino acids, peptides, proteins, and nucleic acid components produced similar results. For these materials the relative yield of radicals at a LET of $1.6 \times 10^4 \text{ MeV cm}^2/\text{g}$ was a factor of two to five lower than the yield at LET values be-

low 200 MeV cm^2/g (Henriksen, 1966 b).

High LET radiation may affect free radical reactions by creating a high temperature region or thermal spike around the particle track. By irradiation of amino acids with charged particle beams of electrons, and helium, carbon, neon, and argon ions, Henriksen et al. (1970) found that no ESR spectra changes occur with increased LET. The conclusion is then that the classical thermal spike theory does not apply to radical formation or secondary reactions at 77°K.

The radical yield for $\text{H}_2\text{O}_2\text{-H}_2\text{O}$ glass was a factor of five lower for 5.7 MeV alpha particle irradiation compared to 250 kV x-ray irradiation (Smith and Wyard, 1961). A decrease in yield with increasing LET would be expected due to radical recombination for densely packed radicals.

In addition to the high concentration of radicals produced by high LET radiation, the high temperatures in heavy charged particle tracks or thermal spikes may be important in determining the type and number of radicals formed and trapped. Using alpha and gamma radiation, the decomposition yield of alkali nitrate crystals at several temperatures has been determined (Hochanadel, 1962). The yield for the high LET radiation was found to parallel that produced by low LET radiation in combination with increased sample temperature (Hochanadel, 1962).

Membranes

It may be possible for ionizing radiation to kill a cell by rupturing the plasma membrane as a lysozyme enzyme probably does. However, there is also evidence that the cell membrane remains unruptured after radiological doses that otherwise would kill the cell.

Human erythrocytes have been irradiated with doses to 40,000 rads of cobalt-60 gamma rays (Cividalli, 1963). Little or no effect on osmotic fragility, glucose utilization, glutathione content, cell volume, water content, or hemolysis was observed. However, in the cells given 40,000 rads, there was a 50 percent loss of potassium from the irradiated cell within 48 hours after irradiation which was attributed to damage to the plasma membrane structure (Cividalli, 1963). Control losses were about 10 percent. The potassium decrease was linear with dose. The lost potassium was partly replaced by sodium. Bresciani et al. (1964 a) also observed that there was an increase in the sodium influx upon irradiation and postulated that there was either an increase in the mobility of carriers in the membrane or an increase in the total number of carriers due to irradiation. Subsequent studies showed that there was an inhibiting effect on the active sodium transport mechanism which was due to an interference with the "pumping" mechanism in the membrane and not due to any enzyme or energy deficiency within the cell (Bresciani et al., 1964 b).

Using doses to 500 krad, Myers et al. (1966) have concluded that the change in potassium and sodium concentrations in erythrocytes is due mainly to an increase in passive ion flux rather than to a decrease in active transport (Myers and Bide, 1966). They also conclude that the major site of damage leading to hemolysis is the exterior surface of the plasma membrane, although lipid peroxide formation in the membrane was observed (Myers and Bide, 1966). It was also noted that the elimination of sulfhydryl groups including those in the membrane, produced a three-fold increase in erythrocyte sensitivity to subsequent radiation (Myers and

Bide, 1966). Others have similarly concluded that sulfhydryl groups of proteins on the erythrocyte surface and inside the cell are the radiation target (Shapiro et al., 1966; Sutherland et al., 1967). Using potassium flux as an indicator and x-irradiation of erythrocytes in solution, it has been found that at least 50 percent of the membrane damage is due to the action of OH radicals (Nakken, 1966). The species O_2^- , H_2O , $e_{\alpha q}^-$, H , N_2O^- do not cause any significant membrane damage indicating that up to 50 percent might be due to the direct effect of the radiation on the membrane (Nakken, 1966). The action of OH radicals may be to attack aromatic amino acids or sulfhydryl groups in the external surface of the erythrocyte membrane.

Using erythrocytes irradiated with cobalt-60 gamma rays, the uptake of sodium was measured (Shapiro and Kollmann, 1968). Agents which block surface sulfhydryl groups were radiomimetic but when employed together with radiation reduced the expected effect. Agents which did not alter the number of surface sulfhydryl groups did not alter the radiation effect while agents which increased the number of surface sulfhydryl groups increased the radiation effect. Agents which alter the hemoglobin inside the cell did not alter the radiation effect. The number of sulfhydryl groups on the cell decreased on irradiation. Irradiation also increased the uptake of other monovalent cations but did not affect the uptake of divalent cations or nonionic substances (Shapiro and Kollmann, 1968). The radiation target appears to be a fraction of the sulfhydryl groups in the membrane and the damage is not merely non-specific disruption of membrane integrity but is the production of a chemical change affecting

only monovalent cation permeability (Shapiro and Kollmann, 1968; Kollmann et al., 1969). An increase in the passive uptake of sodium-22 in human erythrocytes at 0°C has been observed for gamma doses as low as 25 rad (Kankura et al., 1969). This increase was partially suppressed if the cells were incubated at 37°C after irradiation or if the radioprotectants AET or MEA were added prior to irradiation. It was also concluded that since the sulfhydryl reductase system does not function under the experimental conditions of incubation at 37°C, sulfhydryl groups in the cell membrane might not be related to the recovery process (Kankura et al., 1969). Altman et al. (1970) have since reviewed the effects of radiation on erythrocytes and their membranes.

For other membrane systems, some investigators have reached different conclusions. When yeast cultures are protected with cystamine, the K^+ leak rate was identical whether 30 or 99 percent of the possible binding sites on the membrane were occupied by cystamine (Stuart and Standard, 1968). This suggests that extracellular radical scavenging by cystamine or a radioprotective mechanism at the membrane surface is operating. This type of membrane damage is not responsible for reproductive cell death (Myers and Karazin, 1968). The fraction of the sulfhydryl groups lost from the plasma membrane of intact erythrocytes amounts to about 20 percent for a 100 kilorad exposure, while the loss from erythrocyte ghosts is about twice as great (Sutherland and Fihl, 1968). Incubation for one hour at 37°C restored 60 percent of the lost sulfhydryl groups in the intact cells but no recovery was observed in the ghosts. This demonstrates that active metabolism can reduce membrane disulfide and thereby restore

some of the lost sulfhydryl groups. Lipid peroxides occur in erythrocyte ghosts after moderate radiation doses but hardly occur at all in intact erythrocytes until the most radiosensitive sulfhydryl groups (about 15 percent of the total) have disappeared (Sutherland and Pihl, 1968).

Through the use of hamster cells irradiated with electrons of 3 to 50 keV energies, there has come the hint that the nuclear membrane or a thin shell close to the nuclear membrane may be the major radiosensitive region (Zermeno and Cole, 1969). The biological effect observed for this experiment was the clone-forming ability of the cells. If the RBE of electrons in the region of interest were included in the model, the sensitive region would be thicker (Zermeno and Cole, 1969).

X-irradiation of erythrocytes renders them more susceptible to attack by trypsin and other proteolytic enzymes (Myers, 1970). This susceptibility was attributed to disorganization of the membrane lipoprotein structure by x-rays probably through cleavage of disulfide bonds thus exposing hidden arginine and lysine groups to enzymatic attack. However, much of this disorganization is repairable by intact erythrocytes.

CHAPTER IV

ELECTRON SPIN RESONANCE

Interactions of Electrons with a Microwave Field

Consider an electron, a particle with a spin of one half, immersed in a magnetic field of intensity H . According to quantum mechanics, there are two energy states in which the electron can reside. These states correspond to the two possible orientations of the spin vector, either in the same direction or in opposition to the direction of the applied field. The resulting energy difference, ΔE , between the two states is given by

$$\Delta E = h\nu = g\beta H$$

where g is the spectroscopic splitting factor¹

β is the magnetic moment of the electron

H is the applied magnetic field intensity

ν is the frequency of a photon of energy E

If a population of electrons is immersed in a suitable microwave field, resonance absorption of energy will occur when the microwave frequency is the same as the frequency associated with the difference in energy levels. From the above equation, it is apparent that this difference in energy levels depends on the strength of the applied magnetic field.

¹The dimensionless g -value defined here is not to be confused with the G -value (radicals/100 eV) or radical production coefficient. G is also the abbreviation of the unit of magnetic field intensity, Gauss. The g refers to a gram in the ordinate of Figures 28-39.

For an electron $\beta = \frac{eh}{4\pi mc} = .927 \times 10^{-20}$ erg/Gauss; for a free electron, $g = 2$ classically or $g = 2.0023$ with relativistic corrections. For electrons interacting with electric fields in atomic orbitals, in localized molecular orbitals, or in crystal lattices, g will take on other values and the resonance condition will be satisfied. To obtain the distribution of electrons between the energy states, Fermi-Dirac statistics may be used. However, when the interaction between the unpaired electrons in different atoms is small, Boltzmann statistics provides a good approximation. Thus the ratio of the number of electrons in the higher energy state to the number in the lower state at thermal equilibrium is

$$\frac{N_h}{N_l} = e^{-g\beta H/kT}$$

where k is Boltzmann's constant and T is the absolute temperature.

From this equation it is apparent that $N_h < N_l$. It may also be noted that for all but the very lowest temperatures $g\beta H \ll kT$ so that $N_h \approx N_l$. Thus there is an excess, but only a slight excess of electrons in the lower energy state. It is this difference in populations upon which ESR spectroscopy depends. Upon applying microwave energy of frequency ν , transitions between the two energy states will be induced. Since there are a larger number of electrons in the lower state, there will be more absorptive transitions than emissive transitions. If resonance absorption is to continue, there must be a mechanism other than the incident radiation, which will allow the electrons in the upper state to lose energy and drop back to the lower state.

Two such mechanisms are that of spin-lattice interaction or the conversion of spin energy into thermal lattice vibrations and the spin-spin interaction where the spin energy is transferred to other electrons or to nuclei (Assenheim, 1966). If there are no such mechanisms, the populations of the two levels will become equal. In such a case there would be no observed power absorption. This condition is known as power saturation and must be taken into consideration when attempting to calculate N_l or N_h from power absorption measurements. Upon removal of the microwave field, spin-lattice interactions will tend to again establish equilibrium conditions at a rate described by the thermal relaxation time. A sample with a long thermal relaxation time will thus saturate at a low value of microwave field power. Another effect of the thermal relaxation process is to determine the width of the absorption line. From the uncertainty principle, $\Delta E \Delta t \approx h$, which indicates that for a long thermal relaxation time the characteristic width of the absorption line will be small. Thus the thermal relaxation time places limits on both the absorption line width and also its intensity by restricting the microwave power that may be used.

In free radicals the spin-orbit coupling is small due to the strong quenching of orbital motion by molecular asymmetry, and almost never produces significant broadening of the spectral lines (Ingram, 1958). In certain cases, however, other interactions will permit the transfer of spin energy to the lattice without having a strong spin-orbit coupling (Ingram, 1958). Often the main contribution to spectral line width for free radicals in solids is due to the dipolar interaction

between the unpaired electrons and protons (Wyrd, 1969 a). In liquids, the free radical may be tumbling so as to average out the anisotropic portion thereby producing very narrow lines (Wyrd, 1969 a). Many lines due to the hyperfine interaction may then be visible. Broadening may be observed in polycrystalline materials. If the resonant line or g-value is different for the different orientations of a single crystal in the magnetic field, then for a polycrystalline sample of the same material, there will be a superposition of all lines in the spectrum usually resulting in a very broad line.

Microwave Power Saturation

Microwave power saturation causes two types of broadening. In both cases microwave power is absorbed by transitions from the lower to higher energy level and if the mechanisms for conversion of spin energy to thermal energy are not sufficiently rapid, then a decrease in microwave power absorption will occur. Sharp lines are broadened because of the uncertainty principle and by a change of the spin population from thermal equilibrium. In the case of homogeneous broadening, the largest power absorption occurs in the center of the line and hence the greatest decrease in microwave power absorption will occur here upon saturation. The center will be flattened, relative to the sides of the line and produce an apparent broadening of the line. The second type of broadening is inhomogeneous broadening. This is produced by unresolved hyperfine components and inhomogeneities in the magnetic field. Saturation occurs separately and in the same proportion for each component line. Therefore the shape or width of the line will not change upon saturation but the intensity of the absorption line will decrease.

Limitations to the ESR Method

Some of the typical features of ESR spectra produced by radiation have been discussed by Livingston (1958) and are listed here. If exposure of a diamagnetic substance to radiation produces paramagnetism, then at least two species must have been formed. If the spectrum from only one species is observed, then the reasons may be: (a) two identical radical types were produced; (b) the resonance may be in a different portion of the spectrum than where one has scanned; (c) one type of radical may have disappeared through chemical reaction; (d) the line width may have been so great as to have been indiscernible from the baseline level; or (e) the transition giving rise to the ESR spectrum could be forbidden. Line width is an important factor in analyzing a spectrum. Large line widths may be due to: (a) short thermal relaxation times; (b) overlapping of many lines from polycrystalline samples that occur because of anisotropy, (c) dipole-dipole or radical-radical interactions when radicals are close together; (d) interaction with magnetic nuclei; and (e) short lifetime of the radical. In addition, the sensitivity of the ESR method is so great that trace impurities may be a source of radiation produced radicals (Livingston, 1959).

Since there may be ESR signals from the unirradiated material, it is necessary that the ESR spectrum of an unirradiated control sample be subtracted from the resonance spectrum after irradiation. Additional signals may also arise from the irradiated sample container. Using different containers for irradiation and ESR measurement, or subtracting the ESR signal of an irradiated container from that of container plus sample

are possible solutions to this problem. Not only do free radicals give ESR signals but also paramagnetic ions, conduction electrons, and atoms in the triplet state. However, the production of paramagnetic ions by irradiation of biological materials is highly unlikely (Zimmer, 1961). Although conduction electrons are produced under irradiation, their ESR spectral lines are so broad that there is little interference with the measurement of the sharper lines from free radicals (Zimmer, 1961). Similarly, ESR spectral lines of triplet state atoms are usually so broad that no interference is encountered in limited scans about $g = 2.0$.

CHAPTER V

INSTRUMENTATION AND EQUIPMENT

Electron Spin Resonance Spectrometer

The electron spin resonance spectrometer consists of a klystron signal source operating at x-band ($f \approx 9.5$ GHz). The microwave radiation is incident on a sample of about 0.2 cm^3 volume in a resonant cavity. This cavity and sample are immersed in a magnetic field, the intensity of which can be varied or scanned over a selected range. Variations in the microwave energy absorbance or more properly the derivative of the absorbance of the sample as the magnetic field is scanned, are obtained with a rectifying crystal detector. This signal is displayed on an X-Y recorder moving synchronously with the field scan.

Electron spin resonance measurements were made with a Varian Model E-3 spectrometer. In this unit magnetic fields up to 6000 Gauss were produced by a four inch diameter electromagnet with a 1.2 inch gap. Magnetic field stability or regulation was one part in 10^6 and homogeneity was ± 35 mG over the volume of sample in the cavity. Magnetic field indication was accurate to within four Gauss of the absolute value, while resetting of the field could be done to within 0.1 G. The magnetic field scan range accuracy was ± 5 mG ± 0.2 percent of the scan range and the scan range linearity was ± 0.5 percent of the scan range. Scan ranges of 25 mG to 10 kG were available but normally the 100 G and 1000 G ranges

were used. The magnetic field was modulated with a 100 kHz sine wave. The peak to peak modulation amplitude could be varied from 5 mG to 40 G. Since the total absorptive area was sought, a modulation amplitude of 10 G was normally used. To obtain finer resolution much lower modulation amplitudes were used. This was accompanied by a corresponding loss in spectrometer sensitivity since the output signal is proportional to the product of the derivative of the absorption curve times the modulation amplitude.

Samples examined at room temperature were contained in four mm O.D. sample tubes which were inserted into the microwave cavity. Examinations at 77°K were carried out with a quartz Dewar filled with liquid nitrogen inserted into the cavity. Sample tubes were inserted into this Dewar. For room temperature measurements a magnetic field centered on 3385 G was generally used. The cavity resonance frequency was about 9.54 GHz. The cavity configuration for the 77°K measurements caused resonance to occur at 9.06 GHz. The corresponding magnetic field setting was 3220 G. Stability of the klystron frequency at cavity resonance by the AFC circuit was one part in 10^6 . Radiofrequency power incident on the cavity could be continuously varied from 0.5 mW to 200 mW.

Microwave Cavity

The microwave cavity is rectangular, having inside or resonance dimensions of 2.29 cm H x 1.02 cm W x 2.54 cm D, operates in the TE_{102} mode. Its unloaded Q is rated at 7000. All the samples used were cylinders extending through the cavity. The signal intensity from a point sample would vary from zero to a maximum with distance toward the center

of the cavity. For a line sample the effective signal is 0.39 times that for the same sample concentrated at the center of the cavity. Since both unknowns and standards were line samples the correction was the same for both and therefore no resultant correction needed to be applied. However, assumption in each case was that the spins or free radicals are distributed uniformly throughout the cylindrical sample.

Since only one sample could be inserted into the cavity at a time, the standard and unknown were examined alternately. There is a possibility that the dielectric loss of these samples would not be the same and therefore change the Q of the cavity. To account for this, the cavity was modified so that an auxiliary sample could be inserted into the cavity at the same time as the one being examined. Following the approach of Singer (1959) a ruby containing Cr^{+++} was chosen as the auxiliary sample. An adjustable ruby standard was desirable since rotation of the ruby trigonal axis with respect to the magnetic field would permit placement of the ruby resonance at a convenient location in the ESR spectrum and not interfere with that of the sample being examined. Additionally, provision for translation of the ruby through the cavity wall would permit the intensity of the ruby signal to be adjusted. For these adjustments a micrometer arrangement similar to that of Thompson and Waugh (1965) was constructed.

An assembly view of the adjustable ruby standard apparatus is shown in Figure 2. The ruby which was cemented onto the end of the guide rod was one-eighth inch in diameter by about one half-inch long. All other parts of this assembly were made of brass except the micrometer

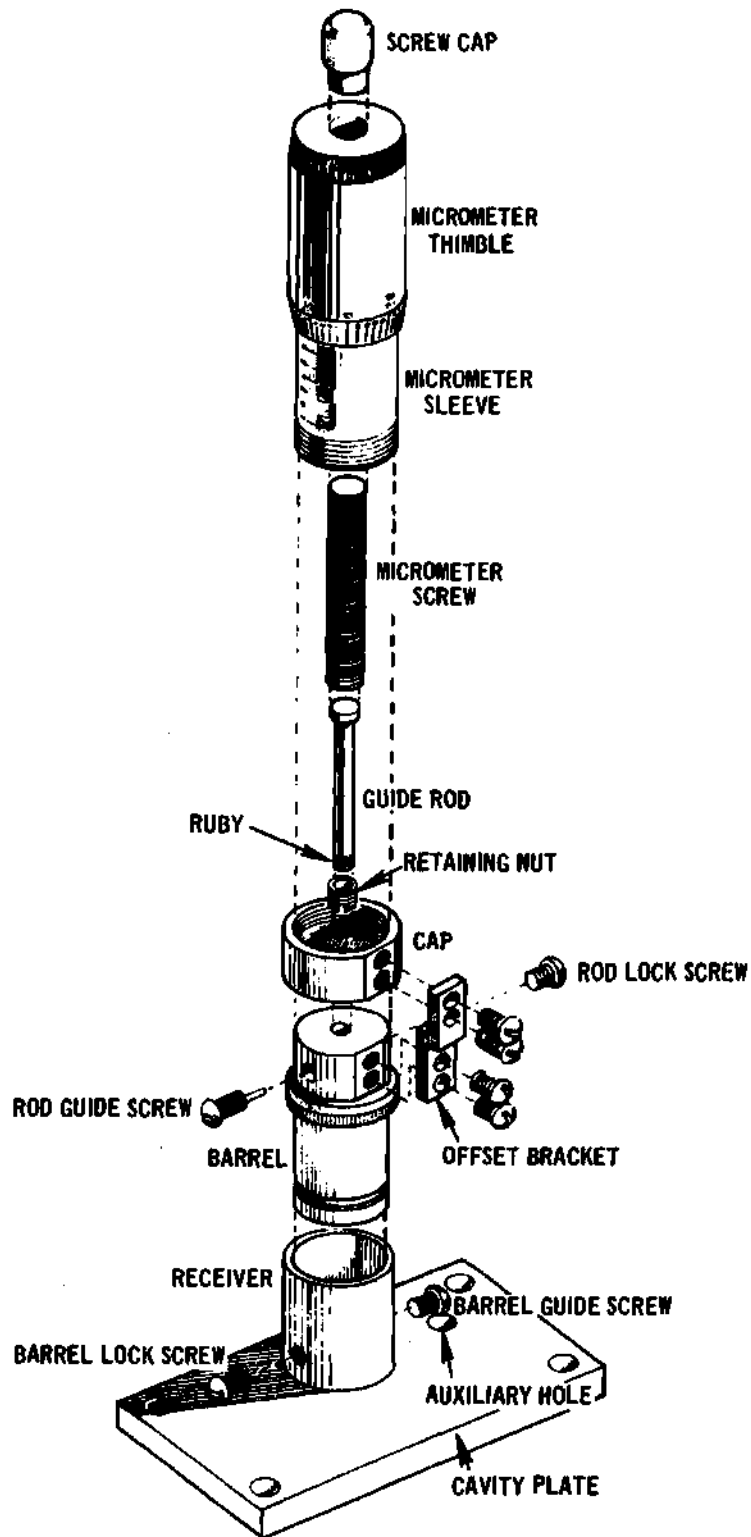


Figure 2. Assembly Drawing of Adjustable Ruby Standard

barrel, micrometer sleeve, and screw cap which were plastic. These plastic parts were taken from an ordinary laboratory micrometer buret. The receiver was silver soldered to the one-fourth inch thick cavity plate. To obtain a conducting surface on the side of the cavity plate which faces into the microwave cavity, this assembly was given a heavy silver plating followed by a gold protective plating by a commercial plating concern. In addition to the hole through which the ruby passes into the cavity, another hole labeled the auxiliary hole in Figure 2 permitted entry into the cavity. This hole, 3/32 inch in diameter, opened into the lower right hand corner of the cavity and permitted insertion of a micropipette into the cavity. The pipette when filled with an aqueous solution of Fremy's salt (potassium peroxyamine disulfonate, $K_2NO(SO_3)_2$) provided g-value markers in the ESR spectrum.

The barrel of the assembly was free to rotate in the receiver, thereby changing the ruby crystal axis with respect to the magnetic field. Both the barrel guide screw and barrel lock screw were seated in the annular groove in the barrel. The raised annulus of the barrel with a diameter equal to that of the outside receiver diameter was inscribed with calibration marks so that the angle of the ruby could be determined. The rod guide screw ran in a slot along the guide rod while the rod lock screw functioned from the side 180° away. The guide rod traveled through a hole in the cap, barrel, and cavity plate. The retaining nut screwed into inside threads in a counter-sunk hole in the end of the micrometer screw. A sliding fit of the knob at the tip of the guide rod permitted the guide rod to move only linearly while the micrometer screw was in

rotation as well as linear motion. The micrometer screw engaged the threads in the micrometer sleeve and was fastened to the micrometer barrel with the aid of the screw cap. Barrel and cap were fastened together in the offset bracket. The cavity plate and receiver alone were fastened to the front of the microwave cavity in place of the standard plate. A silver gasket was used between this plate and cavity and the screws were carefully torqued to four inch-pounds in one fourth inch-pound increments. The barrel with the remainder of the components assembled to it was inserted into the receiver. Rotation of the barrel changed the ruby crystal axis with respect to the magnetic field and allowed the ruby lines to be placed at convenient locations in the ESR spectrum. Rotation of the micrometer barrel moved the ruby rod into and out of the cavity, varying the intensity of the ruby signal.

Data Recording System

In addition to the spectrometer, from which graphical output spectra were obtained, a system for digitally collecting the output data is shown in Figure 3. The ESR voltage signal from the spectrometer receiver was converted to a pulsed output by a voltage to frequency converter whose repetition rate is proportional to the input voltage. These pulses are the input to a Technical Materials Corporation, TMC 404, 400 channel pulse height analyzer, operated in the scaler mode. The channel advance for this scaler is derived from the internal scan pulses which drive the spectrometer X-Y recorder and scan the magnetic field in the ESR spectrometer. The number of these pulses from the spectrometer is divided by 14 to obtain the required number of pulses to advance the scaler.

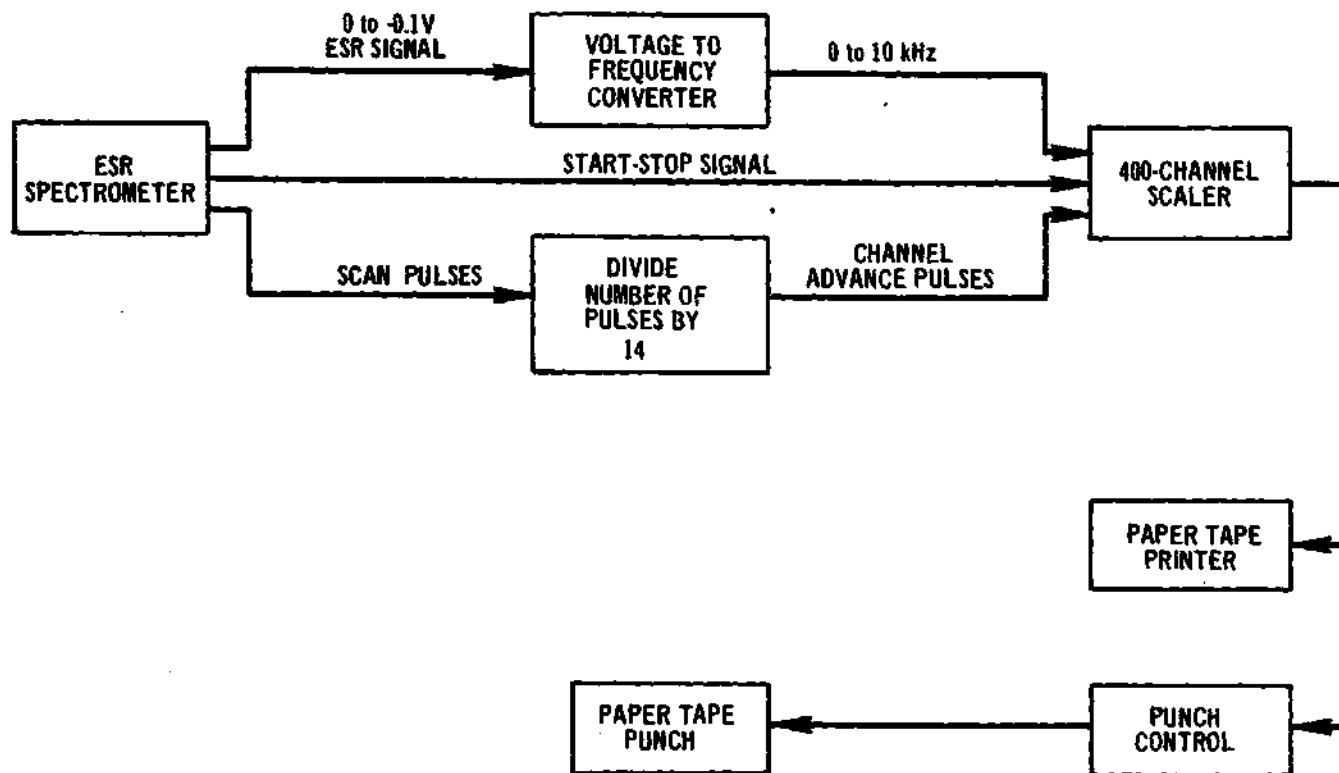


Figure 3. ESR Data Recording System

Stop-start signals are also coupled from the spectrometer to the scaler through relays. This permits synchronization as well as multiple scans to be made.

The voltage-to-frequency (V to F) converter consists of an operational amplifier/integrator feeding a unijunction level detector (Ben-Yaakov, 1968). The pulse divider consists of a series of flip-flops. Both units had RC input and output circuits to tailor the signals to match the adjoining equipment.

The response of the V-to-F converter was measured with a stable voltage source, a Hewlett Packard HP3440 A, 5-digit voltmeter, and a HP 5216 A, 7-digit frequency counter. The linearity of the output frequency with respect to the input voltage was within 0.01 percent full-scale frequency, within 0.04 percent of the theoretical frequency in the upper 90 percent of its working voltage, or within one Hz over the entire range. Stability of the output frequency from start-up to five minutes later was 0.06 percent of the measured frequency. Frequency stability over 250 seconds was within 0.0035 percent full scale, within 0.035 percent of the theoretical frequency over the upper 90 percent of its working voltage, or within 0.35 Hz over the entire range. Long-term stability over 24 hours was 0.013 percent full scale or within 1.3 Hz over the entire range. The effect of temperature on frequency was measured from 15°C to 40°C. The zero intercept was within 0.5 Hz of the origin and the variation in slope was within 0.2 percent over this temperature range. Transient response was measured by applying a voltage step or voltage pulse and measuring the response with an oscilloscope. One pulse

was produced for every 1.7 millisecond-volts. Recovery from voltage transients may take as long as one millisecond.

The ESR data collected in the scaler were printed on tape with a TMC 500 P printer. It was also punched on paper tape by a Tally 420 perforator driven by a TMC 520 tape, punch, read, control unit. This data tape was then read into a Digital Equipment Corporation PDP-8/I computer for data processing.

Irradiation Facilities

Exposures to gamma radiation were performed with a 8,050 Curie (January, 1972) cesium-137 source. This source consists of 12 cylindrical brass encapsulated sources arranged in an annular ring around a central two inch diameter exposure tube. The dose rate in this tube is constant over about four inches length. Samples exposed at room temperature were held by cork retainers in a brass sample carrier and inserted into the central exposure tube. Exposures at 77°K required a glass Dewar which was contained in the carrier. This Dewar, with 0.9 inch inside diameter, 1.4 inch outside diameter, and 5.5 inches long, could contain enough liquid nitrogen for 20 minutes on continuous exposure for the membrane samples before refilling was necessary.

Exposures requiring neutrons were performed in the Biomedical Exposure Facility of the Georgia Tech Research Reactor. The beam port, four inches in diameter, provided neutrons primarily of thermal energy. Exposures at room temperature and 77°K were done simultaneously by placing samples on both the inside and outside of the Dewar. The Dewar consisted of a cube of urethane into which was placed a 7.5 inch diameter

by 10 inch long opened top cylindrical aluminum container with wall thickness of 0.04 inch. The aluminum container was surrounded by eight inches of urethane on four sides, by 16 inches in the rear, and by three fourths inch in front on which the neutron beam was incident. Joints in the urethane were cemented with Dow mastic Number 11 and were kept clear of the direct beam. Samples exposed at room temperature were retained on the outside of the Dewar by a urethane jig in the top portion of the neutron beam. Samples exposed at 77°K were retained inside in the front and adjacent to the aluminum can in the lower portion of the neutron beam. When precooled this Dewar could contain more than enough liquid nitrogen for exposures of one hour duration.

CHAPTER VI

EXPERIMENTAL METHODS

Membrane Preparations

Membranes were prepared by hemolyzing human red blood cells. The whole blood obtained from a local hospital had 63 ml of citrate phosphate dextrose (CPD) anticoagulant added per 450 ml of blood. The chemical composition per 100 ml of CPD was 327 mg citric acid, 2.63 g sodium citrate, 222 mg monobasic sodium phosphate, and 2.25 g dextrose. Blood was stored at 1°C and all centrifugations were done in a Sorvall RC-2 automatic refrigerated centrifuge at this same temperature.

In developing a procedure for obtaining red blood cell membranes, or ghosts, methods used by a number of investigators were considered (Danon, 1956; Weed et al., 1963; Dodge et al., 1963; Porzig, 1969). The procedure used here most closely follows that of Dodge et al. (1963), since the hemoglobin content of the lyophilized ghosts can be reduced to less than one percent on a dry weight basis. There were no losses of lipids in the procedure although there was some non-hemoglobin, non-lipid nitrogen loss, presumably protein in nature.

Buffer solutions were prepared from reagent grade chemicals. Stock solution "A" consisted of a 0.155 M solution of $\text{NaH}_2\text{PO}_4 \cdot \text{H}_2\text{O}$. Stock solution "B" consisted of a 0.103 M solution of $\text{Na}_2\text{HPO}_4 \cdot 7\text{H}_2\text{O}$. Both of these solutions were 310 ideal milliosmolar. An isotonic buffer solution at pH 7.4 was prepared by mixing 27.6 ml of solution "A" and 100 ml

of solution "B". The hemolyzing solution, prepared by mixing 64.5 ml isotonic buffer with 935.5 ml distilled water, was 20 ideal milliosmolar.

In a 50 ml centrifuge tube, 40 ml of blood was centrifuged for 20 minutes at 1000 X gravity. The plasma and buffer coat was removed by aspiration. To the precipitate, isotonic buffer solution was added to give a total volume of 45 ml. After resuspension and gently washing, the cells were centrifuged at 1000 X gravity for 20 minutes and the precipitated red blood cells recovered. This washing procedure was repeated two more times. To the precipitate from the third wash, isotonic buffer solution was added to make 40 ml and the cells resuspended. Five milliliters of this suspension was pipetted into each of eight centrifuge tubes to which 40 ml of isotonic buffer was added. After centrifugation at 4000 X gravity for 20 minutes, the erythrocyte precipitate was recovered and hemolyzed by adding 40 ml of hemolyzing solution to each tube. Centrifugation at 20,000 X gravity for 40 minutes followed. The supernate was decanted and the precipitate in each tube thoroughly washed four times with 40 ml of hemolyzing solution to remove hemoglobin. Each wash was followed by centrifugation at 20,000 X gravity for 40 minutes. After decanting as much of the supernate as possible from the final wash, the precipitate formed the suspension of "ghosts" that was subsequently used in preparing the samples.

Sample Preparation

Preparation of the various types of samples began with the precipitate from the final washing of the membranes. This precipitate with a water content of about 98 percent was transferred by pipette to 10 ml

glass shell-vials for drying or to ESR sample tubes in the case of samples designated LM. The ODM sample was prepared by drying the membranes in an oven at 80°C following which the dried mass was transferred to an ESR sample tube. The freeze dried samples were prepared by first freezing about one milliliter of sample at -40°C in the form of a thin shell in a 10 ml shell-vial. For this purpose a Virtis model 10-100SF shell freezer was used. These samples were then transferred to a Virtis model 10-100 unitrap freeze dryer. The vacuum source for this unit was a two stage mechanical pump and the refrigeration condenser temperature was -53°C. Samples were dried for at least six hours or until they had stabilized at room temperature for at least an hour. The dried material was transferred to ESR sample tubes or was the source of membranes for further processing in the case of the 50-50, A, and F samples.

The dried samples were placed under a vacuum of less than 0.01 Torr for at least an hour and the ESR sample tubes sealed off under vacuum with a natural gas and oxygen flame. Control tubes without samples underwent this same technique. Samples containing water were frozen and maintained in liquid nitrogen while under vacuum and during the sealing-off procedure under vacuum. The "50-50" sample was prepared by alternately introducing small quantities of freeze-dried membrane material and water into an ESR sample tube until a measured quantity of each had been introduced. This sample was also frozen before being placed under vacuum. Table 1 shows data on the samples used experimentally.

To determine the quantity of water evaporated from the membrane solution by the different drying processes, the following experiment was

Table 1. Membrane Sample Characterization

Sample Designation	Type of Sample	Type of Radiation	Irradiation Temperature (°K)	Examination Temperature (°K)	ESR Sample Tube	Total Sample Weight (mg)	Length of Sample (cm)
ODM	Oven Dried	γ	295	295	Quartz	54.6	2.40
FDM-1	Freeze Dried	γ	295	295	Quartz	48.0	2.70
FDM-2	Freeze Dried	γ	77	77	Quartz	72.9	2.40
LM	Memb in Soln	γ	77	77	Quartz	389.9 ^a	7.00
HS	Wash Soln	γ	77	77	Quartz	332.3	6.30
50-50	50% Membrane	γ	77	77	Quartz	150.5 ^b	2.30
FDM-1-S	Freeze Dried	γ	295	295	Spectrosil	94.4	2.90
FDM-2-S	Freeze Dried	γ	77	77	Spectrosil	69.1	2.50
LM-S	Memb in Soln	γ	295	77	Spectrosil	460.2 ^c	6.50
HS-S	Wash Soln	γ	295	77	Spectrosil	440.3	6.30
N-1	Freeze Dried	n + γ	295	295	Spectrosil	54.1	2.55
N-2	Freeze Dried	n + γ	77	77	Spectrosil	62.4	2.75
A-1	Freeze Dried	α + ⁷ Li	295	295	Spectrosil	110.3 ^d	2.80
A-2	Freeze Dried	α + ⁷ Li	77	77	Spectrosil	102.7 ^e	2.70
F-1	Freeze Dried	F.P.	295	295	Spectrosil	89.6 ^f	2.85
F-2	Freeze Dried	F.P.	77	77	Spectrosil	81.1 ^g	2.80

^aFreeze dried weight of membranes is 2.316 ± 0.006 % of the sample weight. ^bFreeze dried weight of membranes is 48 ± 4 % of the sample weight. ^cFreeze dried weight of membranes is 0.595 % of the sample weight. ^dBoron compound comprised 13.4 mg of the sample weight. ^eBoron compound comprises 12.5 mg of the sample weight. ^fUranium compound comprises 1.38 mg of the sample weight. ^gUranium compound comprises 1.25 mg of the sample weight.

carried out. Aliquots of the membrane solution from the last wash were placed in six shell vials. Two vials each were dried by freeze drying, oven drying at 80°C, and drying in air at room temperature. An empty shell vial control was similarly processed for each drying process. Weighing was used to determine the water loss taking into account that lost by the control. It was found that the dry weight of ghosts was 1.5 ± 0.1 percent of the wet weight for both the freeze drying and oven drying processes. After drying, the samples were allowed to stand in air at room temperature. Within experimental error there were no changes in weights of the samples up to 40 days later when measurements were discontinued. After 17 days the samples which had been drying in air had a weight of 1.1 ± 0.1 percent of the wet weight and after 40 days the value was measured as 1.2 ± 0.1 percent. It was concluded that freeze drying and oven drying at 80°C removed about the same amount of water from the membranes but a slightly greater amount would be removed by room temperature evaporation. Although the quantities of water removed by freeze drying and oven drying appear to be the same, the appearance of the dried mass is visually different in each case, and as will be shown later, the ESR spectra are very different. The freeze dried samples appeared opaque white while those dried in the oven appeared translucent.

Alpha particle irradiation was accomplished through the $^{10}\text{B}(n,\alpha)^7\text{Li}$ reaction. For thermal neutrons the alpha particle egresses with an energy of 1.47 MeV, while the lithium-7 ion has 0.88 MeV recoil energy. By integration of the reaction rate over all neutron energies in the beam, the reaction rate for non-thermal neutrons was found to be less than 0.05

percent of the total. A one g/liter solution of $K_2B_4O_7 \cdot 4H_2O$ in water was prepared and aliquots added to the membrane precipitate from the final membrane washing. This material was then freeze dried and transferred to ESR sample tubes producing the "A" samples. Of total boron, 19.8 percent is boron-10, which has a cross section for thermal neutrons of 3840 barns. Doses to the samples from the alpha particle and lithium ion are given in Table 2. Neglect of the portion of energy not deposited in the sample results in an error of less than one percent in the dose received.

Table 3. Source Characteristics

Parameter	Outside Dewar 290°K	Inside Dewar 77°K
Thermal Flux n/cm ² /sec	1.44 x 10 ¹⁰	0.969 x 10 ¹⁰
Thermal Neutron Dose (rad/sec)	0.346	0.232
Total Neutron Dose (rad/sec)	0.945	0.635
Gamma Dose (rad/sec)	0.710	0.507
Alpha + ⁷ Li Dose (rad/sec)	393	265
Fission Product Dose (rad/sec)	400	269
¹³⁷ Cs Gamma (rad/sec)	292	272

Fission product irradiation was accomplished by fissioning uranium-235 with thermal neutrons. A water solution containing one mg ²³⁵U/ml was prepared from a 93.3 percent enriched uranium compound, $UO_2(NO_3)_2 \cdot 6H_2O$. Aliquots were added to the membrane precipitate from the final membrane

washing. After freeze drying the material was transferred to ESR sample tubes producing tubes which were designated the "F" samples. Thermal fission, for which uranium-235 has a cross section of 577 barns, produces fission products with an average total kinetic energy of 162 MeV/fission. Integration of the uranium-235 cross section over the neutron energy spectrum showed that less than 0.06 percent of the fissions would be due to non-thermal neutrons. Escaping energy of the fission products is less than one percent of the total. The energy of the prompt neutrons and gamma rays might raise the dose by 0.03 percent. Similarly the energy of the beta particles and gamma rays of the fission products if integrated over all time would increase the dose by less than three percent. For the small 0.1 gram samples and the short time of a few days over which measurements were made, the error in dose due to these factors should not be more than a few percent.

After completion of all radiation exposures, the "F" samples were analyzed by gamma counting in order to determine the number of fissions that had occurred. A three by five inch NaI:Tl scintillation crystal with 400 channel analyzer was used. An ^{88}Y standard source was used for calibration. The quantity of ^{140}Ba - ^{140}La , which has a fission yield of 6.44 percent and which produces a gamma ray of 1.6 MeV energy, was determined both experimentally and by calculation. The results agreed within 20 percent, which reflects both the error involved in introducing the uranium into the sample and that due to dosimetry.

Radiological Dosimetry

For dosimetry in a mixed field of neutrons and gamma rays, an LiF:Mg thermoluminescent dosimeter (TLD) system supplied by Harshaw Chemical Company was used. To resolve the field into the neutron and gamma component, two types of detectors were used. One, the TLD-700, is depleted in lithium-6, having a lithium-7 content of 99.99 percent and a lithium-6 content of 0.01 percent. This dosimeter is primarily sensitive to gamma rays. The other dosimeter, the TLD-100, has a lithium-7 content of 92.5 percent and a lithium-6 content of 7.5 percent. This detector responds strongly to thermal neutrons through the ${}^6\text{Li}(n,\alpha){}^3\text{H}$ reaction which has a cross section of 950 barns. Some gamma sensitivity is present also but less significant.

Prior to irradiation the dosimeters were annealed at 400°C for 15 minutes to remove electron traps from previous irradiations and at 100°C for two hours to reduce low energy thermoluminescent centers. After the two types of dosimeters were irradiated simultaneously to the same mixed radiation, they were annealed at 100°C for 10 minutes to remove short-lived, low energy thermoluminescent centers. The area under the thermoluminescent glow curve was then determined with a Harshaw Model 2000 thermoluminescence analyzer which consists of a thermoluminescence detector and integrating picoammeter. A 30-second heating cycle which reached a maximum temperature of 245°C in 25 seconds was used to stimulate light emission from the dosimeter. Prior to each series of analyses, the sensitivity of the analyzer was adjusted with the aid of the internal standard light source.

Both types of dosimeters respond, at least somewhat, to both neutron and gamma radiation. Therefore the following response equations were employed:

$$C_{700} = A_{700}D_{\gamma} + B_{700}D_n$$

$$C_{100} = A_{100}D_{\gamma} + B_{100}D_n$$

Subscripts 100 and 700 refer to the TLD-100 and TLD-700. C is the net integrated charge (picocoulombs), less background, collected from the photomultiplier as the TLD's are heated. Background is obtained by activating the TLD analyzer with an unexposed TLD present. D_{γ} and D_n are the doses in rads given a small mass of tissue in the radiation field under consideration by gamma rays and thermal neutrons, respectively. A and B are constants determinable through calibration of the dosimeters and system together. The response is independent of gamma ray energy over a wide range (0.1 to 10 MeV). The cross section for lithium-6 decreases inversely as the neutron velocity to about one barn at 10 keV which permits discrimination against high-energy neutrons.

The gamma calibration coefficients, A , were determined by exposing the detectors to a 0.856 Curie cesium-137 source. The source and detectors were positioned 1.5 meters above the floor of the calibration room by a wood and Styrofoam frame. Exposures were made in air with the detectors placed 45.7 cm from the source. Thermal neutron calibration coefficients, B , were determined by using a five Curie PuBe source surrounded by a cylindrical shell of paraffin 10.2 cm thick. Gold foils, with and without

cadmium shields, established the thermal neutron flux of 2.2×10^3 n/cm²/sec at the moderator surface. The TLD's in polyethylene vials were positioned in the midplane of the source at the surface of the moderator by a polystyrene support. Solution of the response equations including allowance for the gamma field from this source, determined the B coefficients. This system of equations was then inverted to give for the analyzer and dosimeters used here:

$$D_{\gamma} = (C_{700} - 0.00133 C_{100})/0.550$$

$$D_n = (C_{100} - 0.75 C_{700})/144$$

where the units of D are tissue rads and those of C are picocoulombs.

The thermal neutron irradiation source used in this experiment was the port of the biomedical facility of the Georgia Tech Research Reactor. At the port exit the thermal flux as determined by cadmium covered gold and rhodium detectors was 1.0×10^{10} n/cm/sec (McLain, 1972). A threshold detector system employing five different foils, established that 95.5 percent of the total neutron flux was due to thermal neutrons. TLD detectors were used to determine the shape of the beam and its intensity at various distances from the port. Detectors were housed in polyethylene vials for cleanliness and mechanical protection and were supported in the beam by a lightweight polystyrene foam jig. Radially the beam intensity profile was sufficiently flat that four 4 mm diameter samples could be irradiated simultaneously and receive within two percent of the same dose. Axially along the beam the intensity decreased rapidly to 21 percent of the port exit dose at a distance of 20 cm from the port. This rapid

decrease made it imperative that the wall of the Dewar in which irradiations would be carried out should be kept thin at the beam entrance.

Dosimetry was finally carried out with the Dewar in experimental configuration, in the beam and loaded with liquid nitrogen. A matrix of TLD's was constructed by sealing the detectors into five columns and four rows in a polyethylene packet. Centers of the detectors were separated by 0.9 cm. One such matrix was placed to cover the sample positions on the outside of the Dewar and another was similarly placed inside. The results of these measurements are summarized in Table 2. Since the TLD's primarily respond to thermal neutrons, the dose from neutrons of all energies, extrapolated from the flux distribution in the bare beam, may not be as precise as the other values in the table for which the error is estimated to be ± 10 percent. It is apparent from Table 2 that the extraneous doses from neutrons and gamma rays in the beam are very small compared to the desired alpha and fission-product doses.

Dose rates for the cesium-137 gamma source, also given in Table 2, were determined with a Fricke dosimeter (Knight, 1972) at room temperature and with thermoluminescent dosimeters at both room temperature and 77°K. For this application, six EG & G TL-33 $\text{CaF}_2:\text{Mn}$ dosimeters were placed in a four mm I.D. glass tube and irradiated. For exposures at 77°K, a glass vacuum Dewar which held the sample in liquid nitrogen was placed in the radiation field. Annealing and reading procedures for these dosimeters were the same as for the lithium fluoride dosimeters.

Electron Spin Resonance Measurements

Electron spin resonance measurements were made at room temperature,

about 290°K, and at liquid nitrogen temperature, 77°K. For measurement at room temperature, the sample contained in a three mm I.D., four mm O.D. quartz sample tube was placed in the spectrometer cavity. The Varian standard sample, consisting of a 3.3×10^{-4} percent mixture of pitch in potassium chloride in a similar quartz sample tube, was similarly positioned in the cavity. Spin concentration in the standard was 1.00×10^{13} spins/cm length. All samples and standards used were line samples, spanning the entire cavity, about 2.5 cm. This standard produced an approximately Lorentzian line shape centered at $g = 2.0028$. For measurements at 77°K, a quartz vacuum Dewar was inserted into the cavity and filled with liquid nitrogen. A secondary standard was constructed for use at 77°K by thoroughly mixing powdered charcoal with finely ground potassium chloride. This mixture was placed in a quartz sample tube, evacuated, and sealed off. The secondary standard also had a nearly Lorentzian line shape and a g -value of 2.0030. This secondary standard as well as the pitch standard was stable over the one-year period that measurements were made.

The spin concentration in the charcoal-secondary-standard was determined by comparison with the pitch standard. In order to duplicate operating conditions at 77°K as closely as possible at room temperature, the Dewar without liquid nitrogen was used. First the pitch and then the charcoal standard were placed in the Dewar and the spectrum recorded. The scan range, scan time, and modulation amplitude were the same in each case. In each case change in cavity Q and power saturation were determined. The cavity Q with the charcoal standard was found to be 0.915 ± 0.015 times that with the pitch standard present. This lowering of the

cavity Q indicates slightly greater microwave power absorption for the charcoal standard. Saturation factors defined in the next section at 200 mW power were 1.54 for the pitch and 1.66 for the charcoal, indicating a similar molecular environment for the free radicals in these standards. At 0.5 mW both standards were determined to be unsaturated. After double integration of the derivative spectrum and correction for Q-changes and power saturation, the charcoal secondary standard was determined to have 3.52×10^{15} spins/cm. At 77°K the saturation factor for the charcoal standard was observed to be 1.01 at 0.5 mW and 2.70 at 200 mW microwave power. This increase indicates the expected increase in the spin lattice relaxation time as the temperature is lowered. It is noteworthy that the quartz Dewar concentrates or focuses the microwave field at the sample position. The ESR signal with the Dewar present is 1.78 times that without the Dewar. Additionally the presence of liquid nitrogen enhances the signal by 10 percent which is not attributable to lowering of the temperature, power saturation, or Q changes.

To account for a change of cavity Q when the sample is substituted for the standard in the microwave cavity, a ruby rod inserted into the front of the cavity provides a signal against which Q changes can be gauged. To determine the relationship between cavity Q and ruby signal intensity, the following experiment was done. A 100 microliter pipette was filled with a solution of α, α -diphenyl- β -picrylhydrazyl (DPPH) in benzene and sealed. This pipette was placed inside a quartz sample tube which was put in the cavity. The ruby was adjusted so that its signal appeared in a different region of the ESR spectrum than that of DPPH and

thus the absorption intensity of the two could be determined independently. Water, a material with high dielectric loss, was introduced into the sample tube in various amounts. DPPH and ruby signals were recorded for each of the increasing amounts of water present. As the water loaded the cavity, decreasing its Q, the DPPH and ruby signals decreased. The signal from DPPH in the sample position was found to be proportional to the square of the absorption signal from the ruby. Thus for two samples the ratio of cavity Q's including microwave field distortions is equal to the square of the ratio of ruby signal intensities.

After each sample which was to be irradiated had been prepared, it was inserted into the cavity in the configuration to be used when recording the ESR spectrum, and the ruby spectrum was recorded. After determining the area under the ruby absorption curve, the Q ratios between samples and standard were calculated and are given in Table 3.

Table 3. Comparison of Changes in Spectrometer Sensitivity and Q

Sample	Examination Temperature (°K)	Standard	Relative Absorption of Standard	$\frac{Q(\text{sample})}{Q(\text{standard})}$
ODM	295	Pitch	1.00	0.991
FDM	295	Pitch	0.98	1.000
N,A,F	295	Pitch	1.06	1.013
FDM	77	Charcoal	1.00	1.083
LM	77	Charcoal	1.06	1.003
50-50	77	Charcoal	1.08	0.948
N,A,F	77	Charcoal	1.07	1.005

At start-up and shut-down of the ESR spectrometer, usually comprising a period of a day, the spectrum of a standard was recorded to determine if

spectrometer sensitivity had changed. Such readings were usually within two percent of each other. However, there may have been some long-term changes, due to cleaning of the cavity for example, of a few percent. In Table 3 a summary of standard readings is given. The standard deviation of the population about the mean values is three percent.

Quantitative Radical Determination

For each sample the ESR spectrum in digital form was punched on paper tape for transfer to a Digital Equipment Corporation PDP-8/I computer for double integration (Appendix II). In the integration program, corrections for spectrometer gain setting, scan time, and base line position were performed. A linear base line on the derivative spectrum was used. After obtaining the absorption spectrum, results for any other linear base line could be determined by applying the base line correction program (Appendix II) without having to apply the time-consuming integration program again. Additionally, the modulation amplitude, scan range, and limits of integration were held constant or corrections applied. Cavity Q changes evaluated by a ruby rod signal source and power saturation effects were finally considered.

Power saturation was determined by obtaining ESR spectra of the radicals under investigation at a number of microwave power levels incident on the cavity. Such power levels ranged from 0.5 mW to 200 mW. Theoretical ESR absorption versus power for inhomogeneous power saturation is given by

$$Y = A \sqrt{\frac{kP}{L + kP}}$$

where Y = resonance absorption

P = incident microwave power

A and k are constants

This expression was fitted to the experimentally determined absorption by a least squares method thereby determining the constants A and k . See Appendix II for a computer program to do this. At low power levels this expression reduces to the relation for unsaturated conditions in which the absorption is proportional to the square root of the incident power. The saturation factor, F , at power, P , is defined to be the ratio of the expected absorption signal under conditions of no saturation to that under conditions of saturation. Thus $F = 1 + kP$.

The integrated area, S , under the ESR absorption curve is

$$S \sim Ng^2$$

where N = number of spins present

g = spectroscopic splitting factor.

Since the g -values of standard and unknown for free radicals are not very different, the area is taken to be proportional to the number of spins. Using the associated g -values calculated from $g = 2H/3300$, the true area and the approximate area for a constant g -value of 210 may be calculated. As an example of the error involved when neglecting g -value variation, consider two peaks located 100 G apart at 3300 G. The relative error in this case is six percent. If instead there were a uniform distribution of peaks, infinite in number, from 3200 G to 3400 G, the relative error would be 0.1 percent. For complex ESR spectra all the g -values are not likely to be known. This is the case here and no corrections for g -value

variation have been introduced. Since the free radical spectra observed here in nearly every case were within 100 G of the free electron g-value, the error involved is limited to six percent and is very likely less than one percent.

To calculate the number of spins from the integrated area under the absorption curve, the following equation was used:

$$\frac{N_u}{N_s} = \frac{A_s(0) Q_s F_u \sqrt{P_s} A_u(t) G_s T_s C_u^2 m_s g_s^2 S_s(S_s+1)}{A_s(t) Q_u F_s \sqrt{P_u} A_s(0) G_u T_u C_s^2 m_u g_u^2 S_u(S_u+1)}$$

where subscripts s and u refer to standard and unknown, respectively, and all parameters are measured at time t unless specified otherwise

N = spin concentration

A(t) = integrated absorption curve area at time t

Q = cavity Q

F = saturation factor at incident microwave power P

G = gain of spectrometer amplifier

T = time required to scan across a channel

C = magnetic field scale factor in G/channel

m = modulation amplitude

g = spectroscopic splitting factor

S = quantum spin number.

The variables T and C are included here since the number of counts collected in a channel is proportional to the time spent in scanning across the channel as well as the ESR signal intensity. $A_s(t)$ and $A_s(0)$ should

be determined with identical spectrometer settings. The areas "A" under the peaks in counts x channel² are determined by integrating with respect to the artificial magnetic field variable, i.e., channel. Some simplification of this equation results from the following facts: (1) the modulation amplitude for standard and unknown was always the same; (2) the spin quantum number of all unknown radicals was assumed to be one half, the same as the standard; (3) the g-values of standard and unknown were taken to be the same, resulting in a small error discussed above; and (4) saturation factors for standard and unknown were determined at a common microwave power. All samples used here were line samples. Therefore, the spin concentration in spins/gram is N_u/M_u where M_u , in grams/cm, is the sample mass per unit length.

CHAPTER VII

RESULTS AND DISCUSSION

ESR Spectra of Unirradiated Membranes

After the wet membrane preparations were lyophilized, an electron spin resonance signal was always produced. The form of this spectrum was essentially the same for all lyophilized samples even though inorganic materials, such as potassium tetraborate and uranyl nitrate, were added to some samples. The solution with which the membranes were finally washed contained small amounts of inorganic material which were purposely added to enhance the washing. For these materials it was calculated that the fraction of the weight of freeze dried membrane sample attributable to sodium orthophosphate, primary, was 0.7 percent and to sodium orthophosphate, dibasic, was 3.5 percent. These materials alone did not produce a detectable ESR signal. An attempt was made to determine the effect that these chemicals might have on the membrane preparations. After the last centrifugation in the standard procedure described earlier, the precipitates containing the ghosts were washed in distilled water and centrifuged at 20,000 x gravity. Four such washings were done. Although water is not as effective as the 20 milliosmolar washing solution in promoting a transfer of material across the erythrocyte membrane, these washings would reduce the concentration of the extraneous material in the extracellular fluid by a factor of about 5000. After freeze drying the ESR spectra of the ghosts prepared as described apparently were not different from those

of ghosts prepared in the normal way. Irradiation of the two types of samples with gamma radiation produced the same results for both types. The ESR spectra of samples irradiated with gamma radiation are given in Figures 4-13 while the spectra of those subject to high LET radiation are given in Figures 14-24.

The horizontal axis of the ESR spectral graphs is linear in magnetic field strength with a scale indicated by a horizontal line segment. The center of the graph of room temperature observations is 3385 G and of 77°K observations is 3220 G. Markers appear at $g = 2.0028$ for pitch, at $g = 2.0030$ for charcoal, and at $g = 2.0057$ for the center line of Fremy's salt which can be recognized by the triplet markers 13 G apart. Positions on the graph in terms of g -values can be obtained from magnetic field, H , by $g_u = g_s H_u / H_s$ where u and s indicate unknown and standard. For magnetic field values within 100 G of the resonance of the standard, a simple rule is that an increase of one Gauss is equivalent to a decrease of 0.006 in the g -value near $g = 2$. In order that all graphs may be compared, a vertical line segment gives a vertical scale in arbitrary but consistent units for all graphs in this dissertation.

The ESR spectrum of lyophilized membranes, shown in Figure 4a, consists of a broad resonance occupying a 1400 G region. The principal resonance is centered at $g = 2.2$ and there may be an additional resonance of much lower intensity at $g = 2.0$. Although the magnitude of the derivative trace in Figure 4a is low compared to that obtainable by irradiation, it extends over a large magnetic field range and consequently the integrated absorption is comparable to that obtainable with radiation. The radiation-

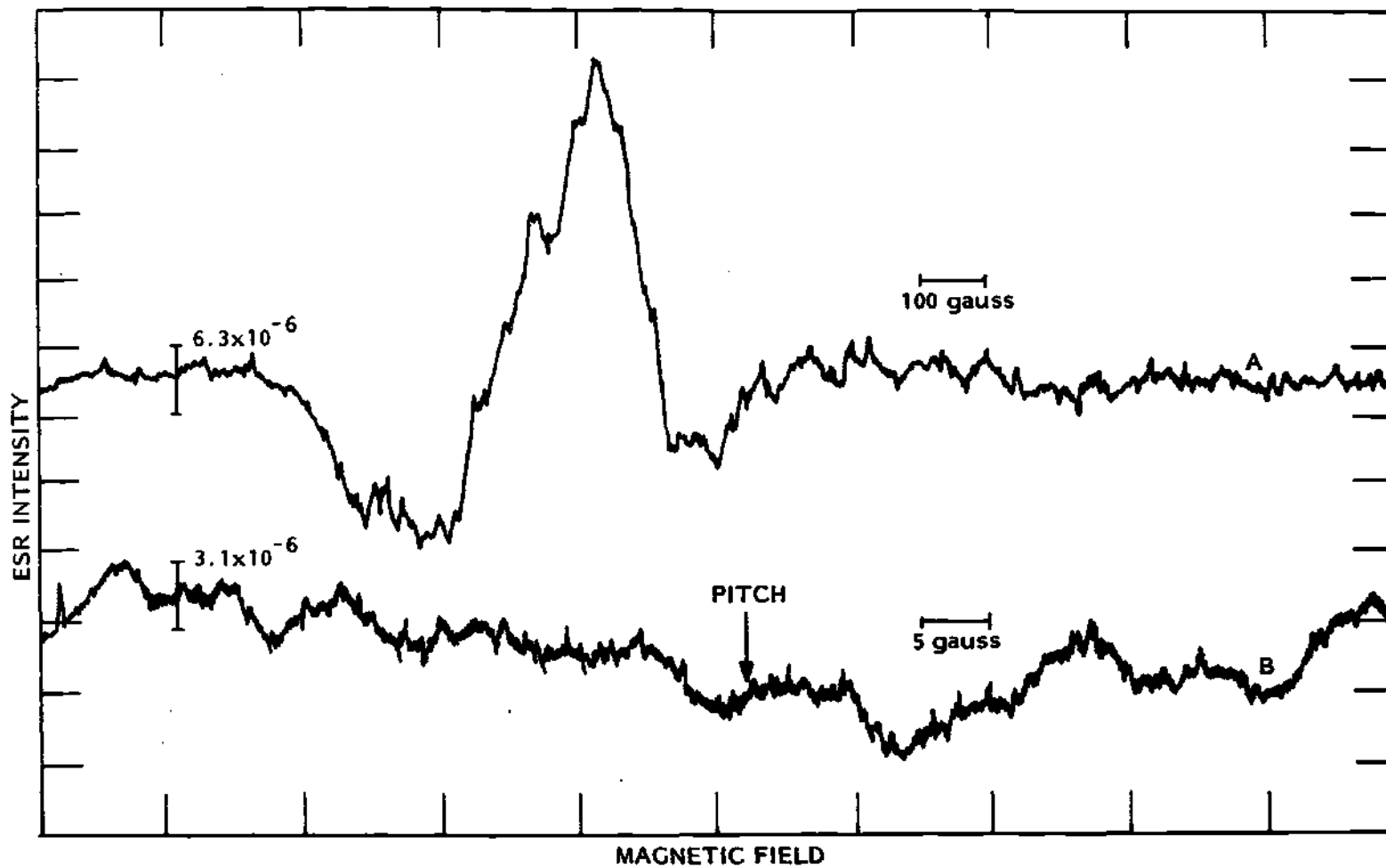


Figure 4. ESR Spectra of Lyophilized Membranes at 200 mW at Room Temperature; Scan Time 4 min, Field Center 3385 G, Modulation Amp 10 G, Freq 9.55 GHz

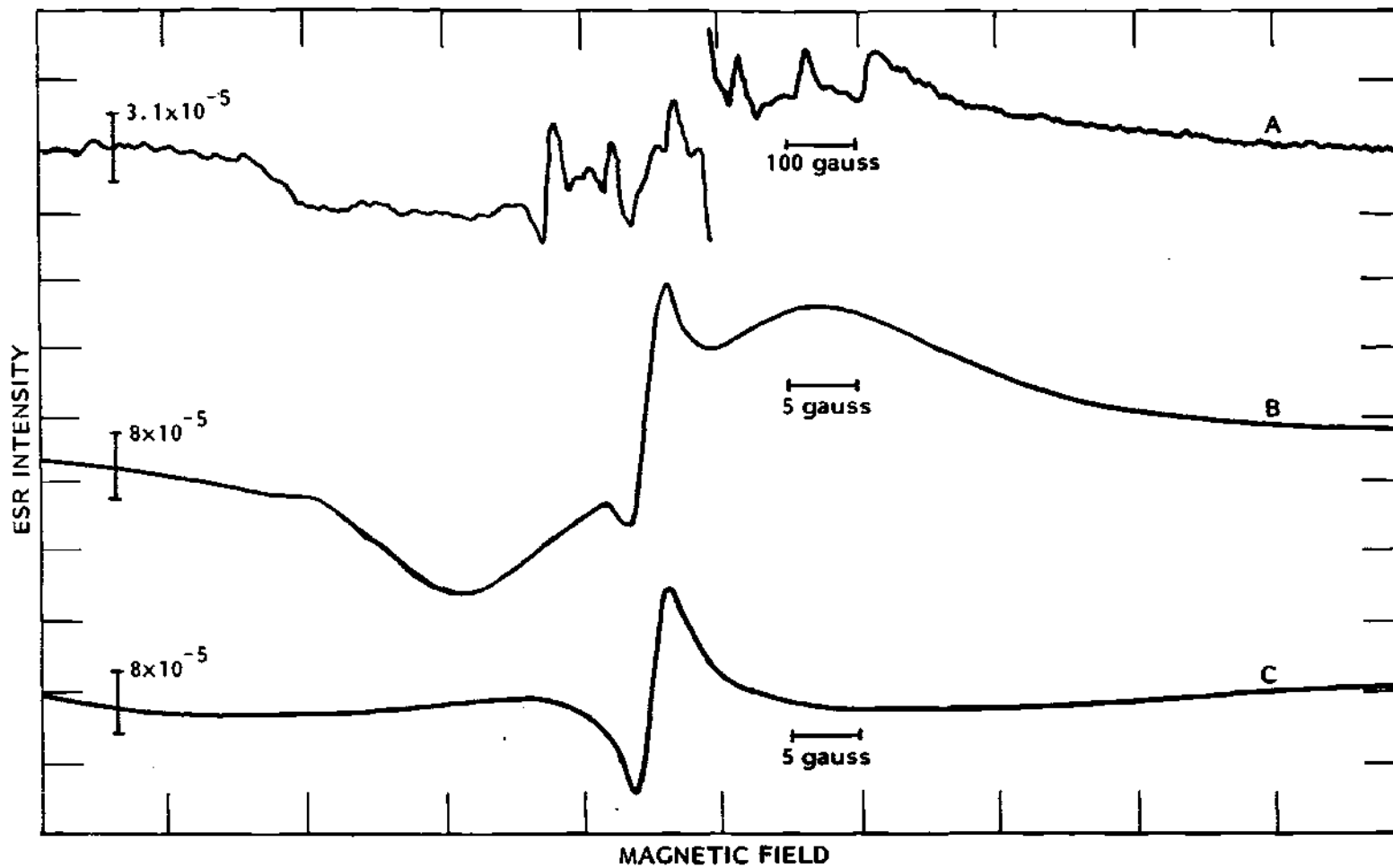


Figure 5. ESR Spectra of Oven-Dried Membranes at 200 mW at Room Temperature; (a) and (c) before Irradiation, (b) after 0.875 Mrad Gamma Irradiation

produced spectra covered only about 200 G, therefore the broad resonance shown in Figure 4a did not seriously interfere with efforts to separate the radiation-produced portion from the pre-existing spectrum.

The membranes that were dried in the oven exhibited a broad ESR spectrum covering about 1800 G. However there was much more detail present than in the case of lyophilized membranes. This absorption, shown in Figure 5a, occurs in the central 500 G and seems to be superimposed on the broad background resonance. There is a strong central resonance located at $g = 2.00$. If this peak, which has been curtailed in Figure 5a, were shown in its proper magnitude, the peak-to-peak derivative would occupy two-thirds of the entire vertical scale. This central peak is shown at reduced vertical scale and expanded horizontal scale in Figure 5c. The saturation factor of this peak was determined to be 2.16 at 200 mW. The intensity of the entire spectrum, as indicated by the vertical scale, is much greater than that of the lyophilized ghost. Correspondingly the integrated absorption is about 25 times that of the lyophilized membrane.

All samples that were irradiated with gamma rays were prepared from blood from a single donor. Similarly all samples that were irradiated with other than gamma radiation were prepared from blood from a single but different donor. There was not sufficient blood from a single donor to prepare all the necessary samples. The ESR spectrum of lyophilized ghosts from a second donor is given in Figure 14b. It is similar to the one described previously in having a broad unresolved character with a resonance at $g = 2.2$. However, this spectrum has a second broad peak at about $g = 2.06$. The possible resonance at $g = 2.0$ seen in the first

batch of samples was not present or was reduced below the level of detection in the second batch.

Freezing the lyophilized ghosts in liquid nitrogen produced an ESR spectrum different from that of the ghosts held at room temperature. This spectrum, having a broad unresolved resonance at about $g = 2.06$, is displayed in Figure 6. For the 1.5 percent membrane in water solution frozen at 77°K, no ESR resonances were detectable except possibly for a small narrow peak at $g = 2$. This peak was barely discernible above the noise in the spectrum. The same statements apply to the 48 percent membrane in water solution. It is apparent from Figure 18b that the resonance at $g = 2.06$ seen at room temperature in lyophilized ghosts is still present. However the resonance at $g = 2.2$ has disappeared.

These broad unresolved resonances observed in prepared membrane samples may be described summarily as follows. Freeze dried samples produce broad unresolved ESR spectra, simpler and of less magnitude than that of oven dried membrane samples. Similarly membranes, with residual water, exhibit spectra indistinguishable from background. The freeze dried samples had one or two broad resonances whose g -values were 2.2 or 2.06. Samples from one donor had a peak at $g = 2.2$ at room temperature, but at 77°K a resonance at only $g = 2.06$ was apparent. Samples from another donor had both peaks present at room temperature, but only the $g = 2.06$ peak remained at 77°K. Organosulfur radicals may have a resonance at $g = 2.06$, but this rarely occurs in unirradiated tissue (Swartz, 1972). However, their extent over a wide range of magnetic field strengths suggests the possibility that their source may be molecules in the triplet state,

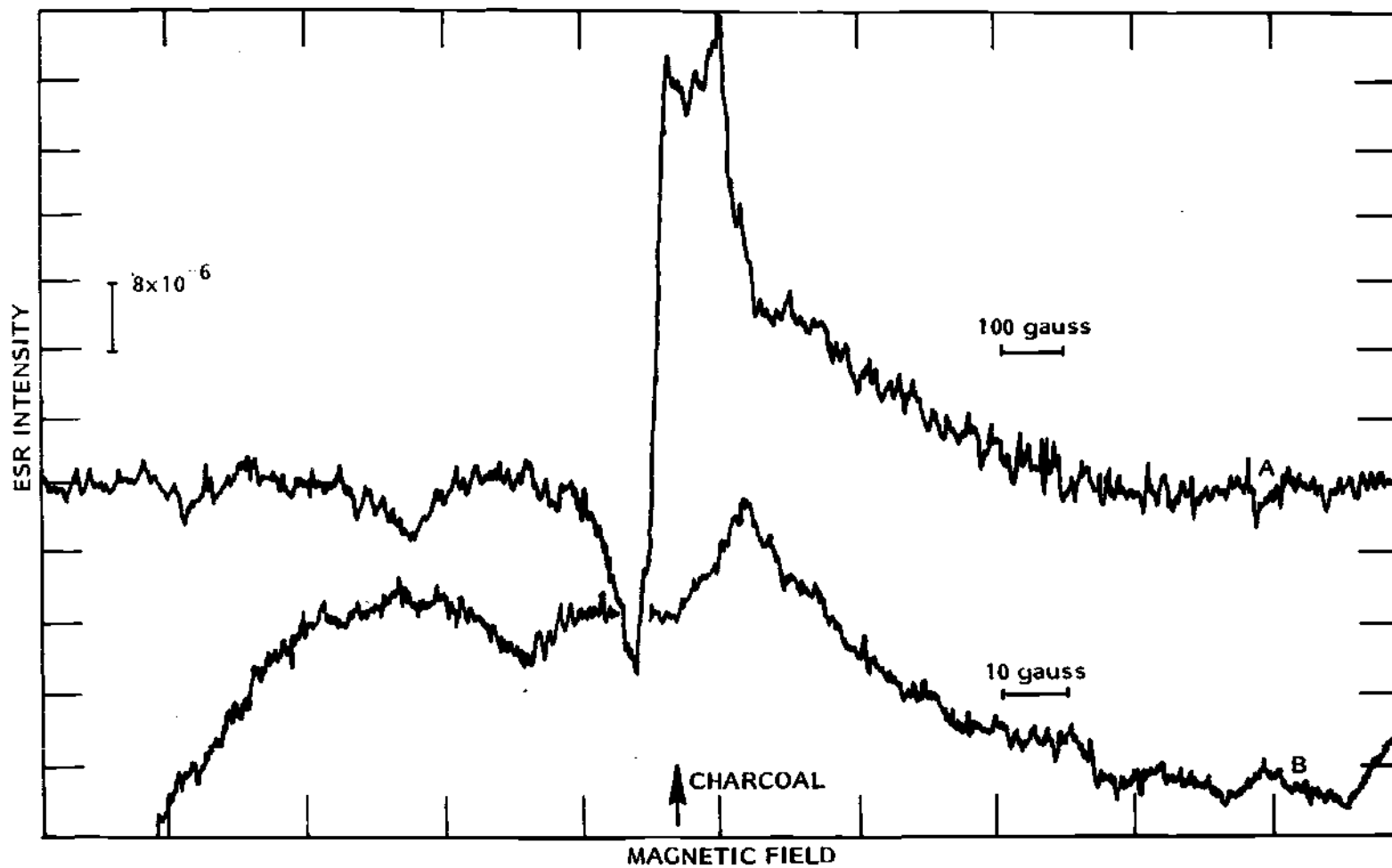


Figure 6. ESR Spectra of Lyophilized Membranes at 200 mW at 77°K

transition metal ions, or other paramagnetic species. Although less than one percent of the dry weight of the lyophilized ghost is hemoglobin, this or other extraneous material in the erythrocyte cannot be completely ruled out as a source of the ESR signals. Another candidate for these ESR signals is the reaction of the ghosts with oxygen. In transferring a sufficient quantity of membranes to ESR sample tubes after freeze drying, the membranes were necessarily in contact with air. Afterwards they were again placed and kept under vacuum. It is possible for the effect of oxygen on free radicals to be physical as well as chemical and therefore be partially or completely reversible.

The background signals present before irradiation were generally much lower than the ones produced after irradiation. Additionally, they extended over many hundreds of Gauss, whereas the radiation-generated radicals produced ESR spectra confined to within 100 G of the free electron resonance at $g = 2.0023$. These pre-existing signals served primarily as a background from which deviations produced by radiation were measured.

Although ESR signals were detectable in the wide-range scans, signals lying within 100 G of the free electron g -value were generally weak or beyond detection for the freeze dried samples. The spectra in Figures 4b, 6b, and 19c show that in pure lyophilized membrane preparations, absorption near $g = 2$ by free radicals was not detectable above the general background. The samples to which a boron or uranium compound was added, exhibited small resonances near $g = 2$ as shown in Figures 16a, 17c, 21c, and 23c, but subtraction of these small peaks from the much larger ones generated by radiation produced negligible differences. Although not shown, no free radical resonances were detectable in the 1.5

or 48 percent membrane in water solution.

ESR Spectra of Gamma Irradiated Membranes

The membranes that were dried at 80°C were irradiated with gamma rays to a dose of 875,000 rads. The background spectrum, Figure 5a, present before irradiation, did not change. The irradiation, however, produced a 27 G wide, derivative peak to peak, resonance centered at $g = 2.00$. This peak may be seen in Figure 5b surrounding the 3G wide peak present before irradiation.

Lyophilized membranes were irradiated at room temperature with gamma radiation to a maximum dose of 875,000 rads. This radiation produced an ESR spectrum limited to within 100 G of the free electron g -value. The spectrum taken at 200 mW incident power, Figure 6a, contains one broad, 27 G wide peak. From the shape of this peak, unresolved structure is suggested. This is indeed the case. When examined at 0.5 mW power, a double peak is apparent in Figure 6b. The width of the doublet is 27 G, the same as observed at 200 mW. From the Fremy's salt field markers, the g -value of the center of the doublet is 2.0030 ± 0.0008 . It is estimated that the g -value of the two peaks composing the doublet are 2.0067 ± 0.0008 and 2.0004 ± 0.0008 . Individual peak width is about 17 ± 2 G and the splitting between them about 10 ± 1 G. If this doublet is the envelope of many lines, these lines are naturally broadened beyond resolution since a trace of the spectrum at 0.5 mW and modulation amplitude of 0.1 G produced an identical double peaked-spectrum.

An empty Spectrosil tube after irradiation identical to that above, produced the low intensity spectra recorded at 200 mW in Figure 6c and at

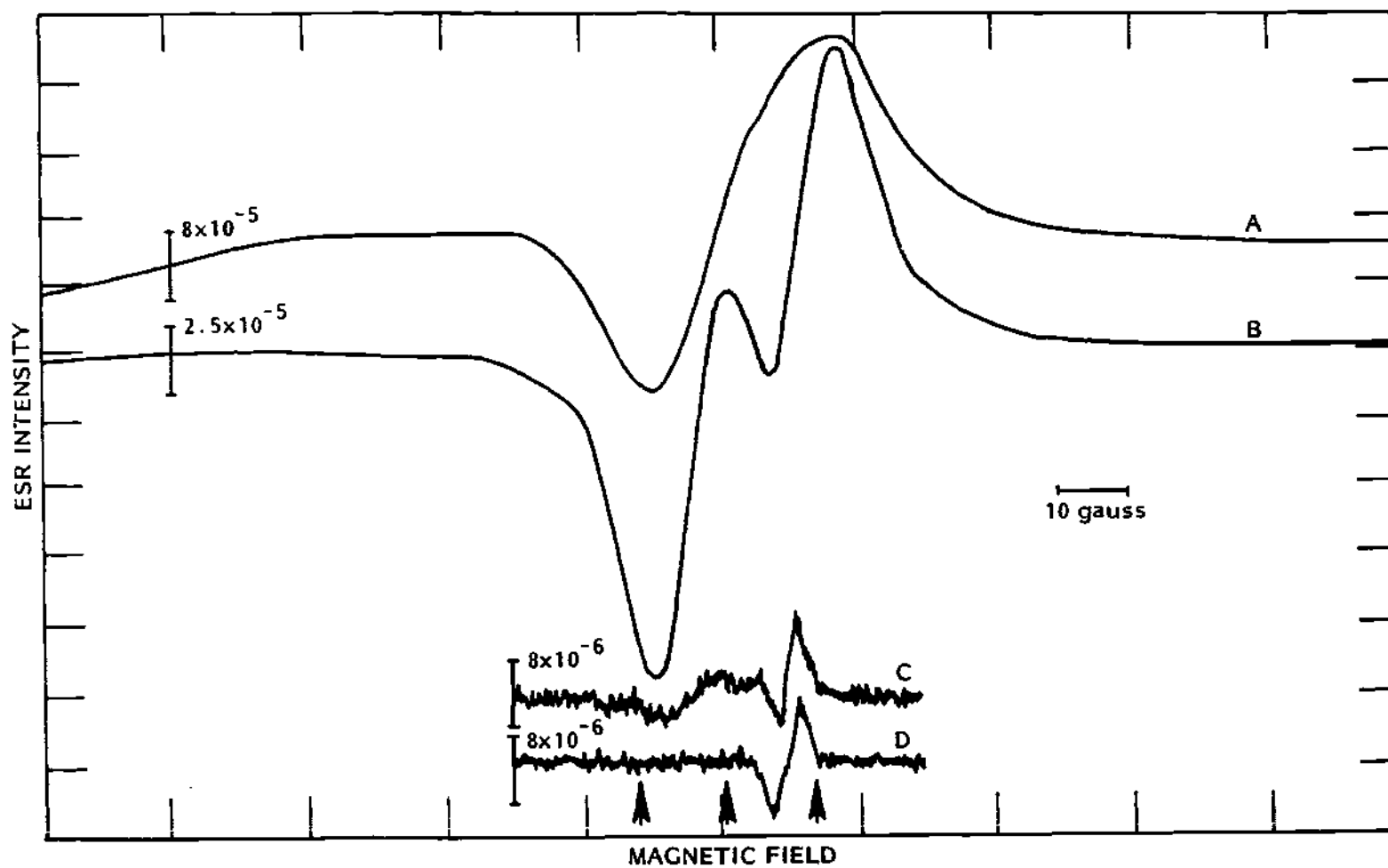


Figure 7. ESR Spectra of Lyophilized Membranes after 0.875 Mrad Gamma Radiation at Room Temperature; (a) at 200 mW, (b) at 0.5 mW; Spectrosil Tube, (c) at 200 mW, (d) at 0.5 mW

0.5 mW in Figure 6d. Two peaks are apparent, one at $g = 2.010 \pm 0.001$ and the other at $g = 2.002 \pm 0.001$. The latter one located near the free electron g -value has a peak width of about 3 G.

Lyophilized membranes, kept frozen in liquid nitrogen during both irradiation and ESR measurement, received a dose of 816,000 rads of gamma radiation. The ESR spectra near $g = 2$ are displayed in Figure 8b for 200 mW power and Figure 8a for 0.5 mW power. These spectra include signals from free radicals generated in the sample tube which may be seen in Figures 8c at 200 mW and in Figure 8d at 2 mW. After subtraction of the signal from the container, it is apparent that there are at least two absorption peaks for the membrane sample. Because these peaks overlap extensively, it is difficult to determine their g -values accurately. However, their approximate g -values are 2.004 and 2.015. Estimated peak widths are 19 and 26 G respectively. Scans at a modulation amplitude of 0.1 G did not reveal any additional structure. At a power of 0.5 mW only the $g = 2.004$ peak was apparent, although the shape of the curve indicated that there must be other ones present. The sample tube also exhibited a small double peak with g -values of 2.003 and 2.009, which were very nearly the same as the ones observed at room temperature.

Spectra from the ± 500 G scan of the membranes contained two peaks of width 4.5 G that were separated 505 ± 4 G apart. These were identified as being due to the hydrogen radical. Although these peaks were of low intensity compared to the central absorption peak, there were no such peaks in the sample container spectrum. Additionally there is little interference in this region of the spectrum from other resonances. The

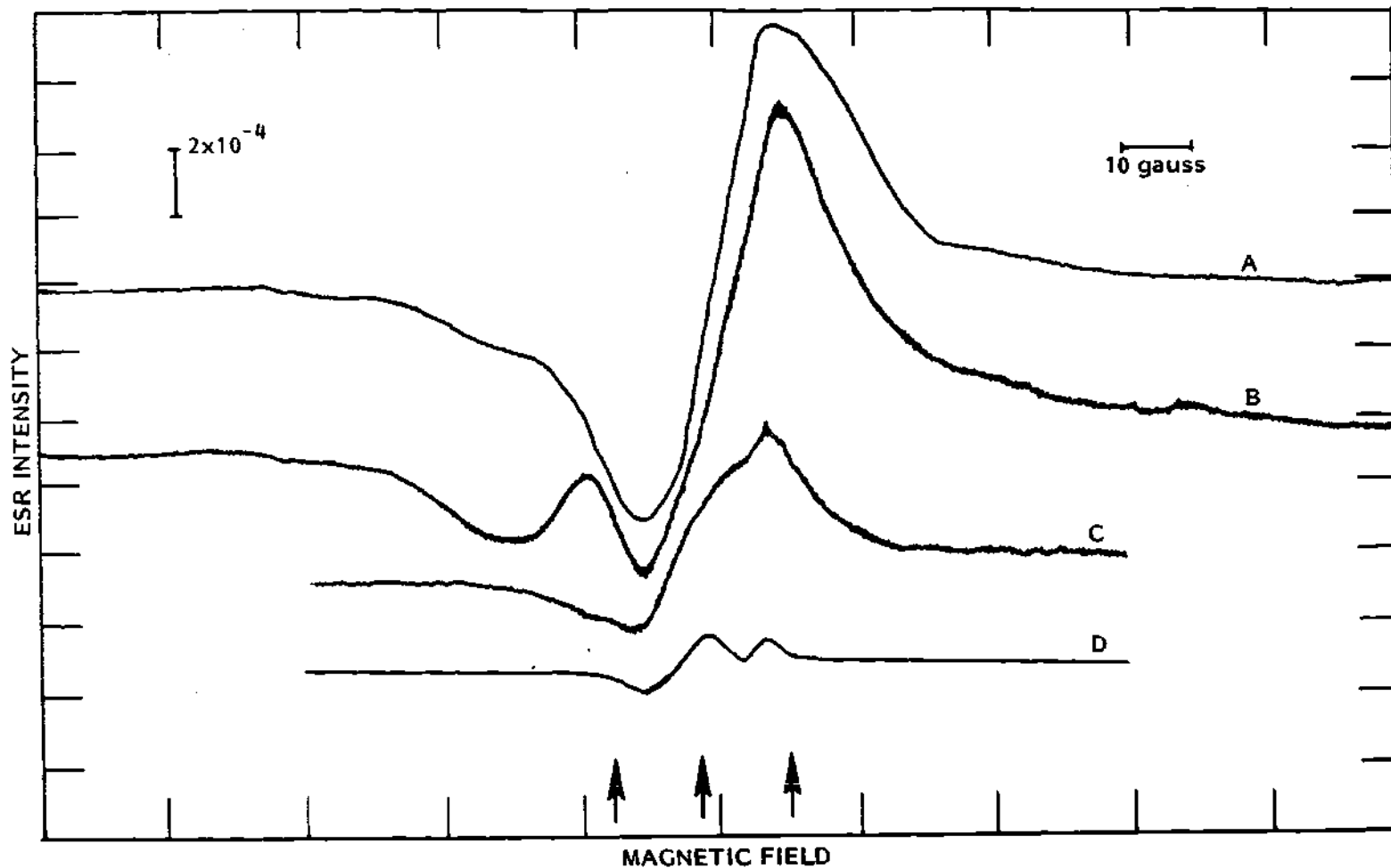


Figure 8. ESR Spectra of Lyophilized Membranes after 0.916 Mrad Gamma Radiation at 77°K; (a) at 200 mW, (b) at 0.5 mW; Spectrosil Tube, (c) at 200 mW, (d) at 2 mW

width of these peaks, about 5 G, is probably broadening due to the large modulation amplitude necessary to increase spectrometer sensitivity.

After completion of the irradiations at 77°K, the sample was removed from the liquid nitrogen and allowed to equilibrate at room temperature. The sample was then refrozen at 77°K and the spectrum recorded at 200 mW, Figure 9a, and at 2 mW, Figure 9b. Only one broad distorted peak at approximately the same location as the one occurring before the heat treatment was observed. The shape of the two peaks are noticeably different, however, with the one occurring after heat treatment being considerably reduced in magnitude. It is apparent that radical reactions occurred and that several radicals were present before and after heat treatment. The hydrogen radicals completely disappeared on heat treatment. Radicals occurring in the sample tubes decreased proportionally much more than radicals in the ghost after heat treatment. As seen in Figure 9c at 200 mW and in 9d at 2 mW, the spectra of radicals in the sample container contributed negligibly to the membrane plus container spectrum. At higher gain there was visible some small resonance about $g = 2$ in the sample tube however.

A water solution containing 1.5 percent membranes by weight was frozen at 77°K, irradiated with gamma radiation and analyzed at this temperature. A control sample consisting of the solution without membranes was treated identically. The spectra of these two were similar. However there were sufficient differences to warrant an attempt to create the difference spectrum. The difference spectrum may not be that of radicals in the membrane for several reasons. In order for this subtraction process

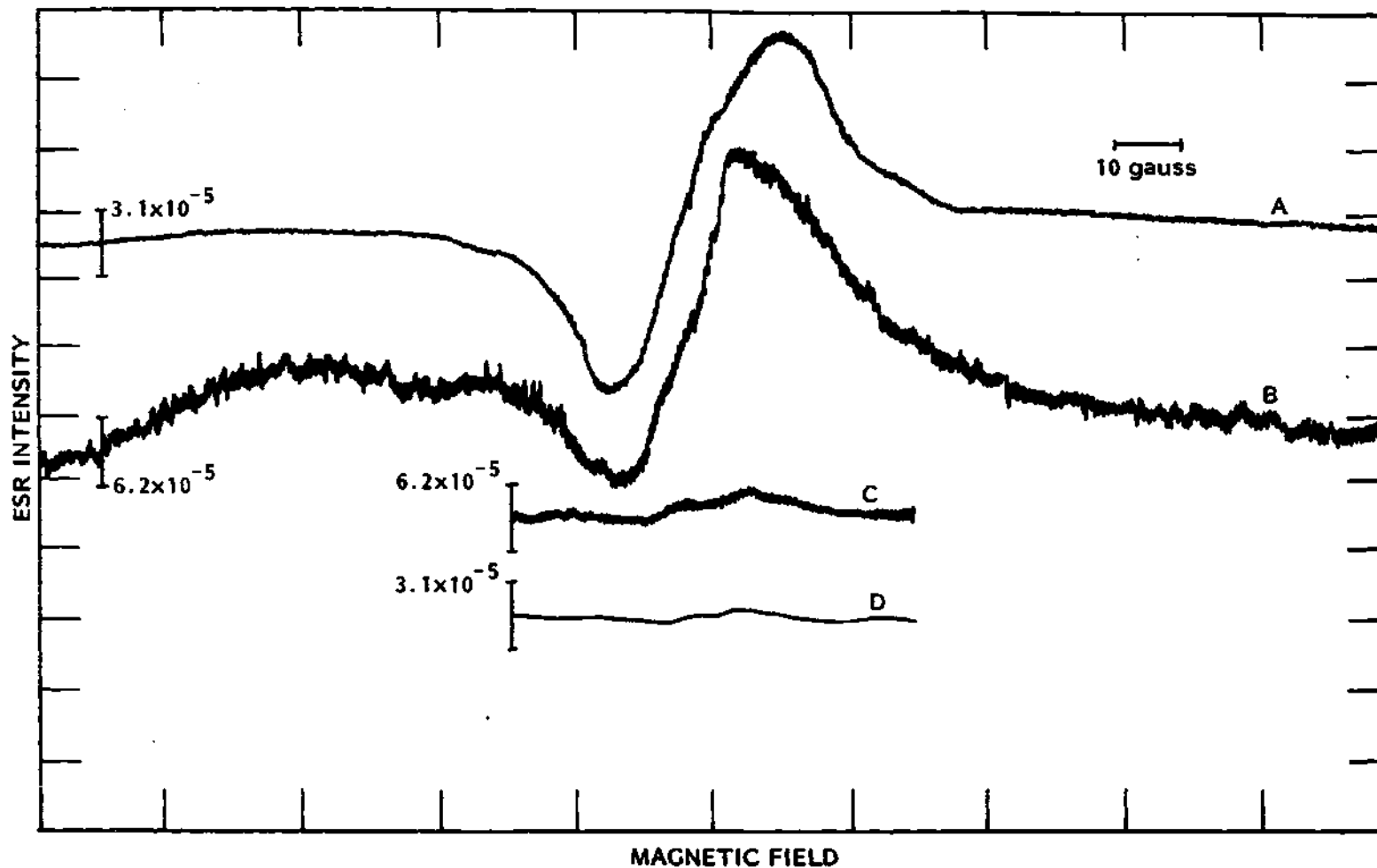


Figure 9. ESR Spectra of Lyophilized Membranes after 0.816 Mrad Gamma Radiation at 77°K and after Annealing at Room Temperature; (a) at 200 mW, (b) at 2 mW; Spectrosil Tube, (c) at 200 mW, (d) at 2 mW

to be valid, it must be assumed that the spectra from the sample and control are linearly independent; that is, they must represent linear addition of spectra from the solution and from the membrane. This is not likely to be the case. Also very large errors are probably introduced by subtracting nearly equal quantities. Since radical attack of the membrane from the solution and vice versa seems likely, the difference spectra will include a contribution from membrane radicals. Also included is a contribution from radicals in solution in the presence of membranes minus that from radicals in pure solution but not in solution in the presence of membranes.

The difference spectrum, for membranes in solution minus that for the solution alone, is presented in Figure 10a. As mentioned previously, only a very limited interpretation can be made from this spectrum. The center curve is the resulting spectrum. The upper and lower lines fix limits on the spectrum so derived, when it is assumed that the two originating spectra are subject to a five percent error. It is apparent that an error of only five percent in the recorded spectra would result in a much larger error in the difference spectrum because of their close similarity. It is estimated from Figure 10a that initially there were two peaks of about 20 G width, about 40 G apart. Their g-values are estimated to be 2.008 and 2.035. The distortion of the peaks in the spectrum is indicative of the presence of small additional resonances or of error introduced by the subtraction technique. Hydrogen radicals were also observed in the wide scan spectrum in both the membrane and control samples.

The samples were stored at liquid nitrogen temperature for a period of five days. After one day the spectrum recorded at 200 mW in Figure 11b

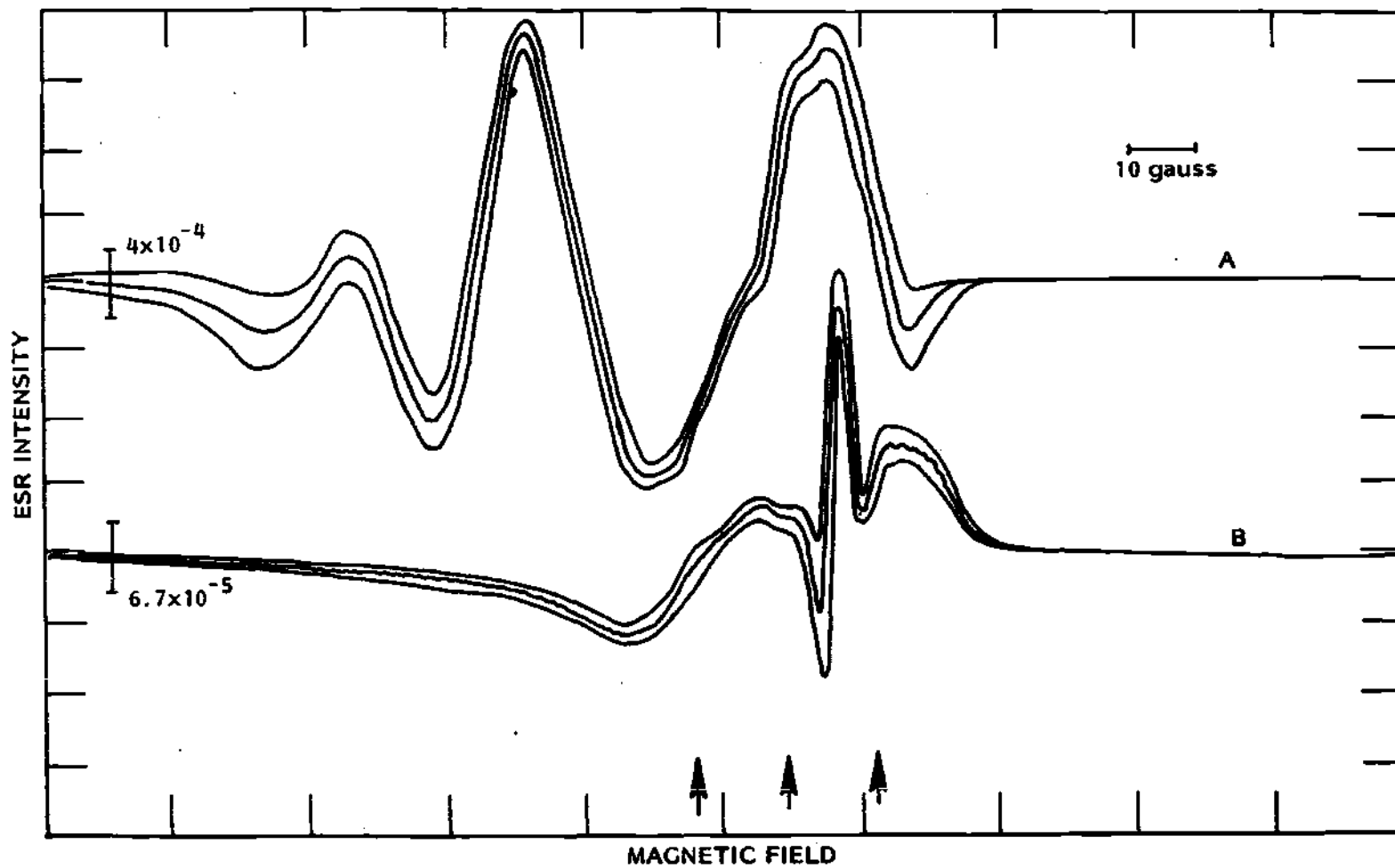


Figure 10. ESR Spectra with Error Range of 1.5% Aqueous Membrane Solution after 0.816 Mrad of Gamma Radiation at 77°K at 200 mW; (a) at End of Irradiation, (b) Five Days Later

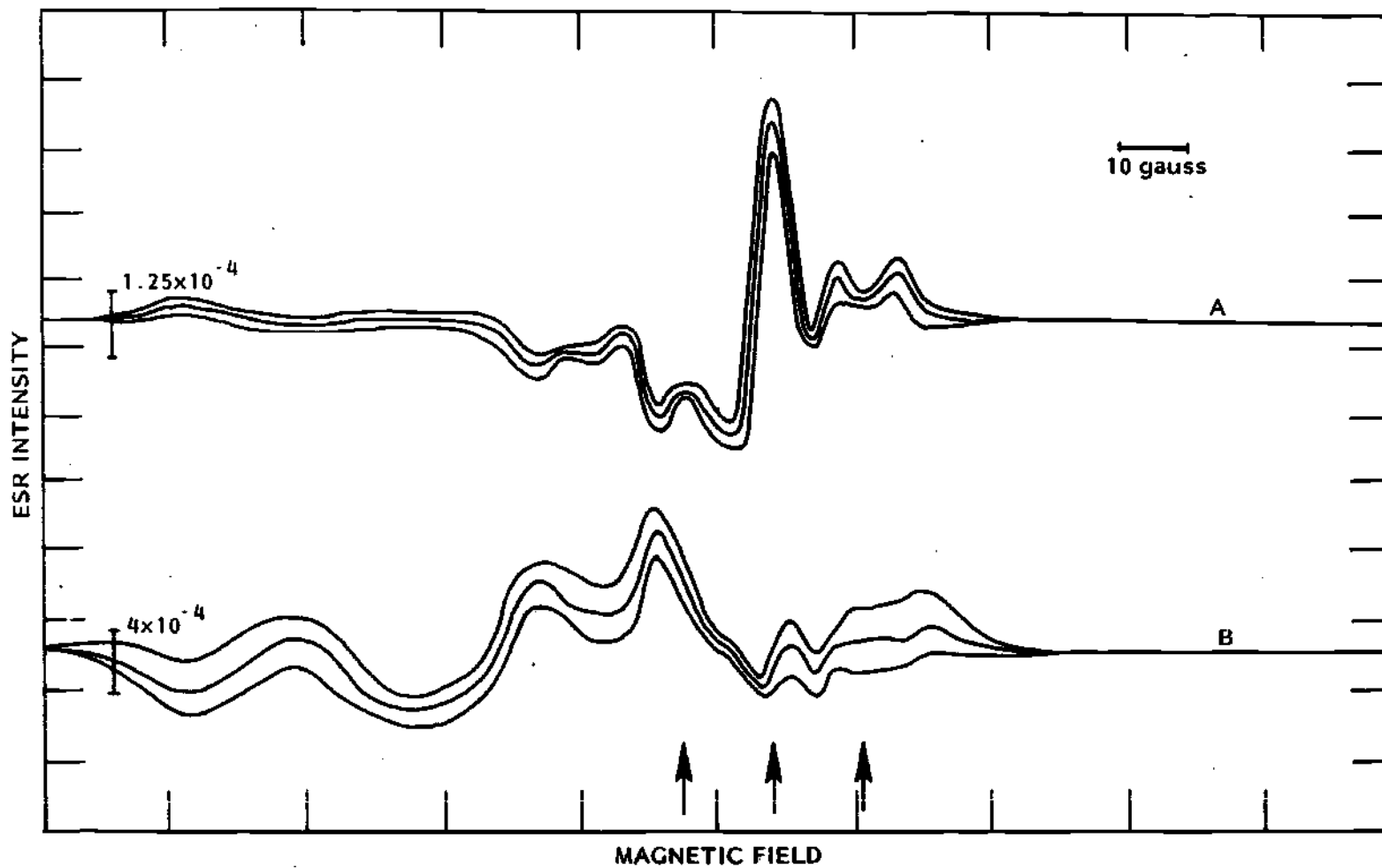


Figure 11. ESR Spectra with Error Range of 1.5% Aqueous Membrane Solution after 0.816 Mrad of Gamma Radiation Plus One Day Storage at 77°K; (a) at 0.5 mW, (b) at 200 mW

and at 0.5 mW in Figure 11a showed that radical reactions were continuing even at 77°K. The spectrum in Figure 10b was obtained after five days storage. Two peaks are apparent. One is a 30 G wide peak at $g = 2.012$ and the other is a narrow, 3 G wide one at $g = 2.002$. Either free radicals with a g -value close to that of a free electron were produced on storage or the radicals responsible for the broad initial spectrum had disappeared leaving those responsible for the free electron spectrum. The latter explanation could well be correct since there was a large decrease in amplitude of the spectrum on storage as seen in Figure 10a and 10b.

Another aqueous solution containing 1.5 percent membranes was prepared. This one was then given a gamma dose of 875,000 rads at room temperature. The sample was then frozen in liquid nitrogen and the ESR spectrum obtained at 77°K. A control consisting of the aqueous solution without membranes was treated similarly. There was very little difference in the two spectra such that any difference spectrum formed would be inconsequential.

A low concentration of membranes in solution was one of the problems that limited the effectiveness of generating the difference spectrum. To increase this concentration, lyophilization was first carried out followed by the addition of water to create a sample containing 48 percent membranes and 52 percent water by weight. This sample was frozen at 77°K and all gamma exposures and ESR measurements made at this temperature. The spectrum so created may be seen in Figure 12b. This is the spectrum in the membrane plus water mass after subtracting the spectrum

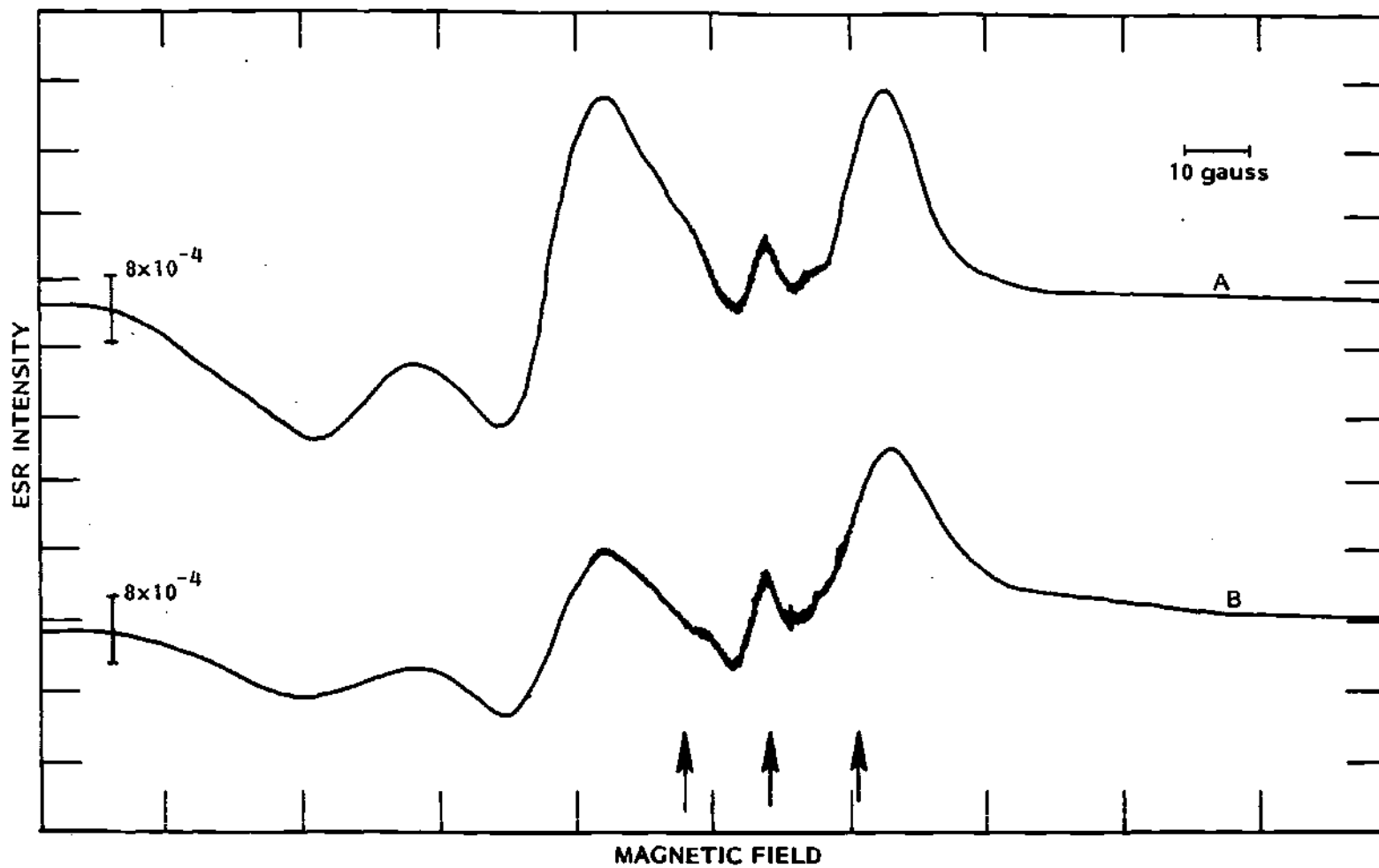


Figure 12. ESR Spectra after 0.816 Mrad Gamma Radiation at 77°K at 200 mW; (a) of 1.5% Membrane Solution, (b) of 48% Membrane Solution

generated in the sample container which was small by comparison. Apparent peaks for the broad spectrum have g-values of 2.026, 2.008, and 2.002. A spectrum for the sample containing 1.5 percent membrane in solution is shown for comparison in Figure 12a. Although there is considerable difference between the two spectra, the gross similarity is striking. Although not shown the doublet from hydrogen radicals was observed in both samples.

The sample was removed from liquid nitrogen after completion of all radiation exposures and examinations and allowed to remain at room temperature for ten minutes before refreezing at 77°K for further examination. The spectrum obtained at 200 mW may be seen in Figure 13a and that obtained at 5 mW in Figure 13b. On the unresolved background are superimposed five resolvable peaks. Because of their overlapping, it is difficult to determine the location and width of these peaks accurately. However, the estimated g-values are 2.016, 2.011, 2.005, 1.999, and 1.995. Although it is possible for these peaks to result from hyperfine splitting by the nuclear magnetic field, their separation is apparently not quite the same nor are their widths. The unresolved background spectrum is estimated to have a g-value of from 2.01 to 2.02. The broad nature of the spectrum prevents a more precise determination. Additionally it appears that the radical may be axially symmetric with a perpendicular g-value of 2.046 as indicated by the hump in the left portion of the spectrum. Axial symmetry occurs when one of the three spacial components of the g-tensor is different from the other two, which are equal. There are indications of a signal in the right portion of the spectrum, in which

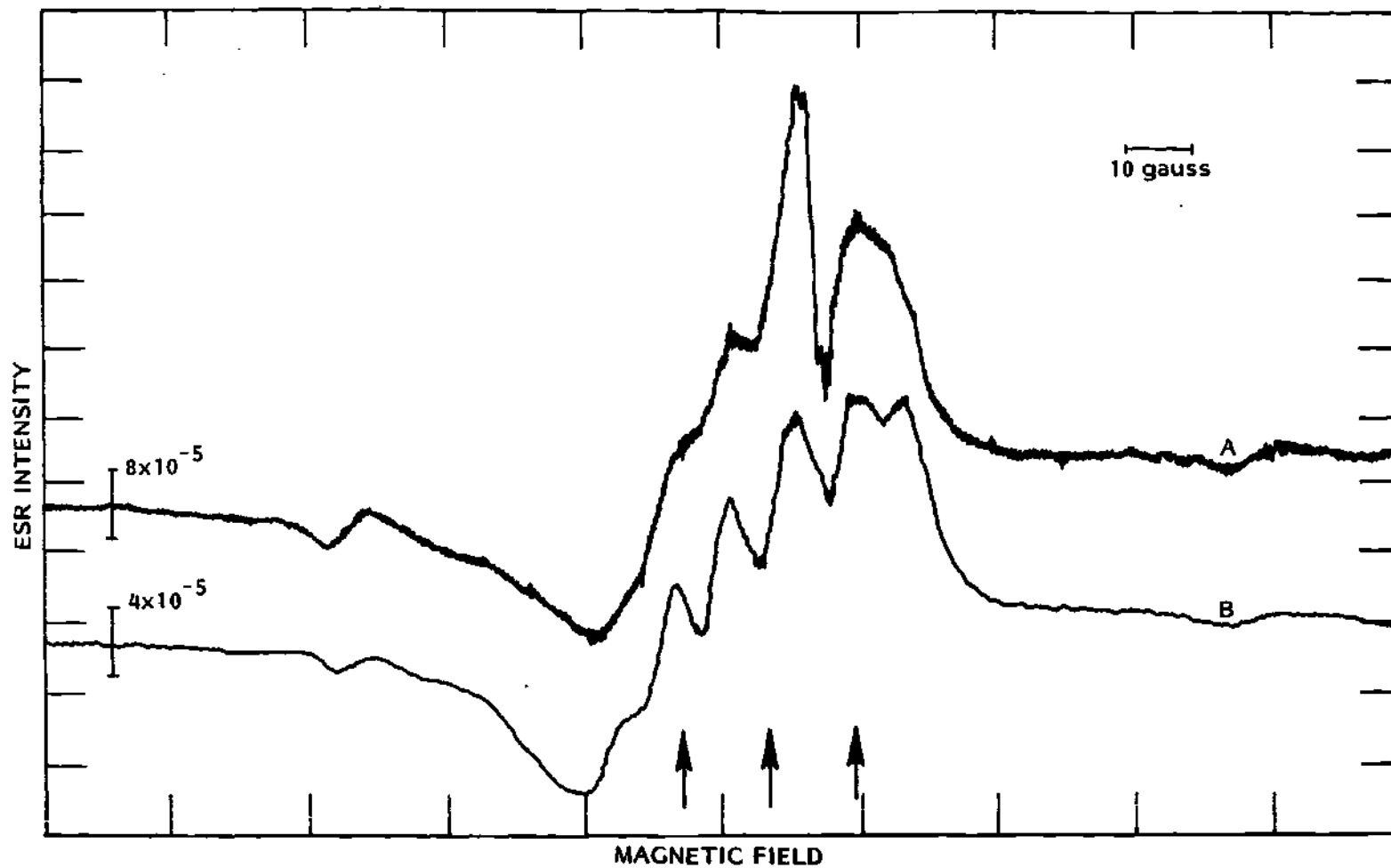


Figure 13. ESR Spectra of 48% Membrane Solution after 0.816 Mrad Gamma Radiation at 77°K after Annealing at Room Temperature; (a) at 200 mW, (b) at 5 mW

case all three g-values would be different, the third one occurring at $g = 1.960$.

ESR Spectra of Neutron Plus Gamma Irradiated Membranes

The samples that were irradiated with alpha particles or fission products required neutrons to initiate the reaction. Associated with the reactor neutron source was a gamma radiation field. The pure lyophilized membrane samples that were exposed to this mixed neutron and gamma field were used as controls for the alpha and fission product irradiated samples and in addition provide information about the radicals generated by this mixed field.

The ESR spectrum of the sample exposed to the mixed ($n + \gamma$) field at room temperature is given in Figure 14a. The apparent effect of the radiation is the production of the central peak which was absent before irradiation, (Figure 14b). This central peak seen expanded in Figure 15a has a g-value of 2.007. The spectrum did not change on storing the sample for six days at room temperature. Background radicals in the sample container are seen to be nil in Figures 14c and 15b.

For a similar sample exposed and stored at 77°K, the spectrum again consists of a single central peak as seen in Figure 16a. A portion of this signal is from the sample container itself, a spectrum of which is given in Figure 16c. These peaks may be seen in the narrow scans in Figure 17b for the sample plus container and in Figure 17d for the container only.

At 1 mW the peak in the membrane sample is seen in Figure 17a to be composed of additional unresolved peaks. From Figure 17, the approx-

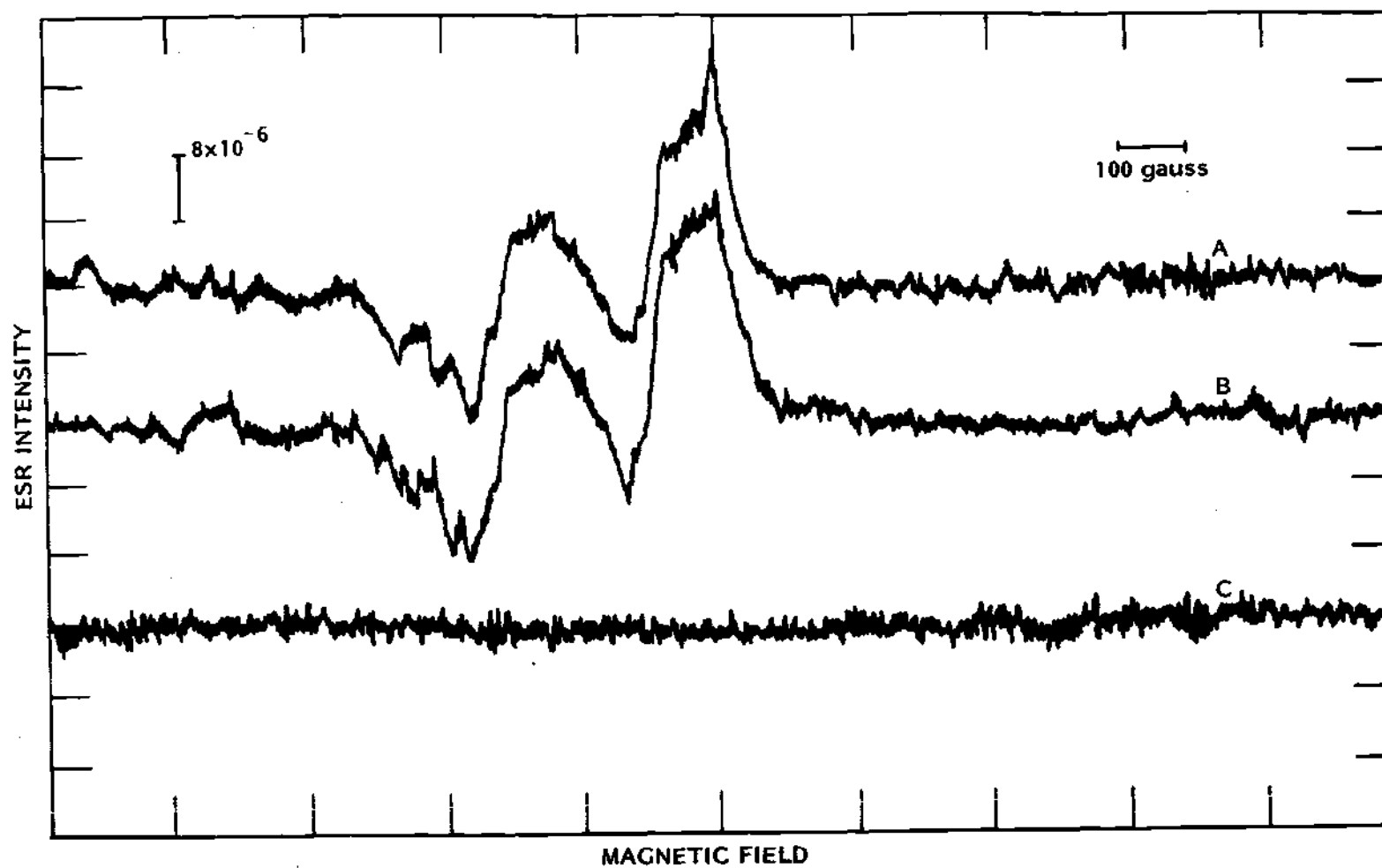


Figure 14. ESR Spectra of Lyophilized Membranes at 200 mW at Room Temperature; (a) after $n+\gamma$ Exposure, (b) before Exposure, (c) Spectrosil Tube after $n+\gamma$ Exposure

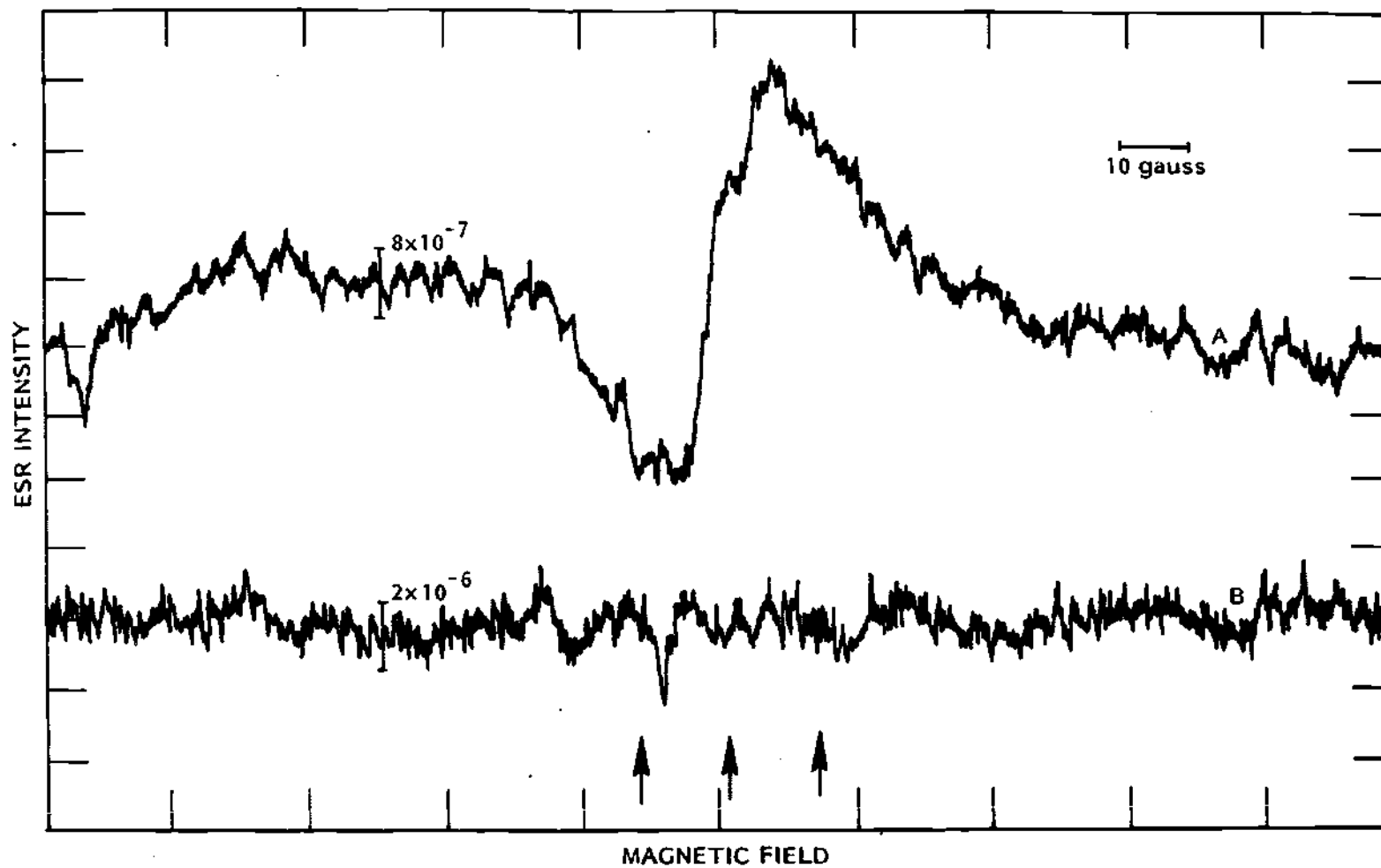


Figure 15. ESR Spectra of Lyophilized Membranes at Room Temperature after $n+\gamma$ Exposure; (a) at 0.5 mW, (b) Spectrosil Tube at 200 mW

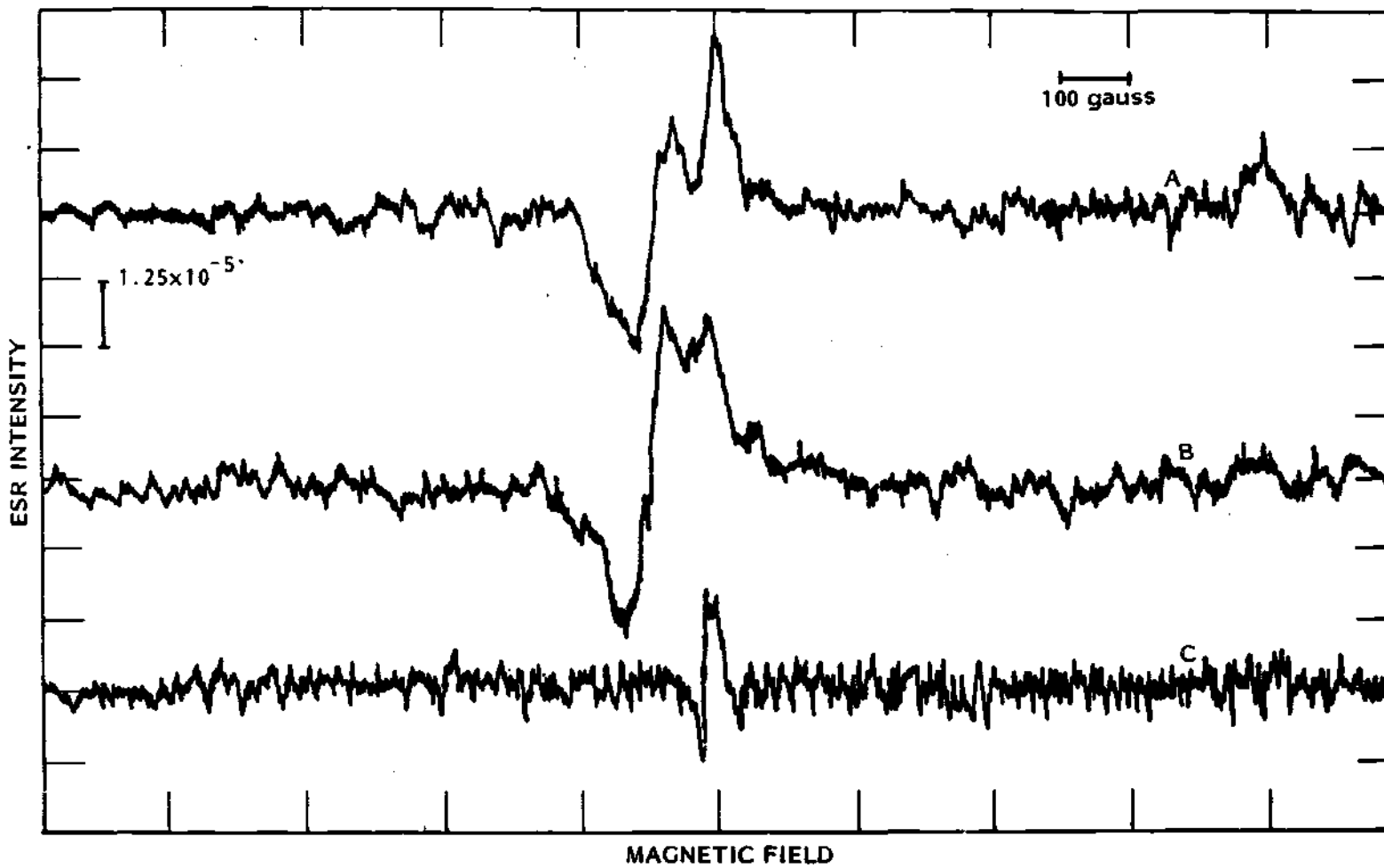


Figure 16. ESR Spectra of Lyophilized Membranes at 200 mW at 77°K; (a) after n+ γ Radiation, (b) before Irradiation, (c) Spectrosil Tube after Irradiation

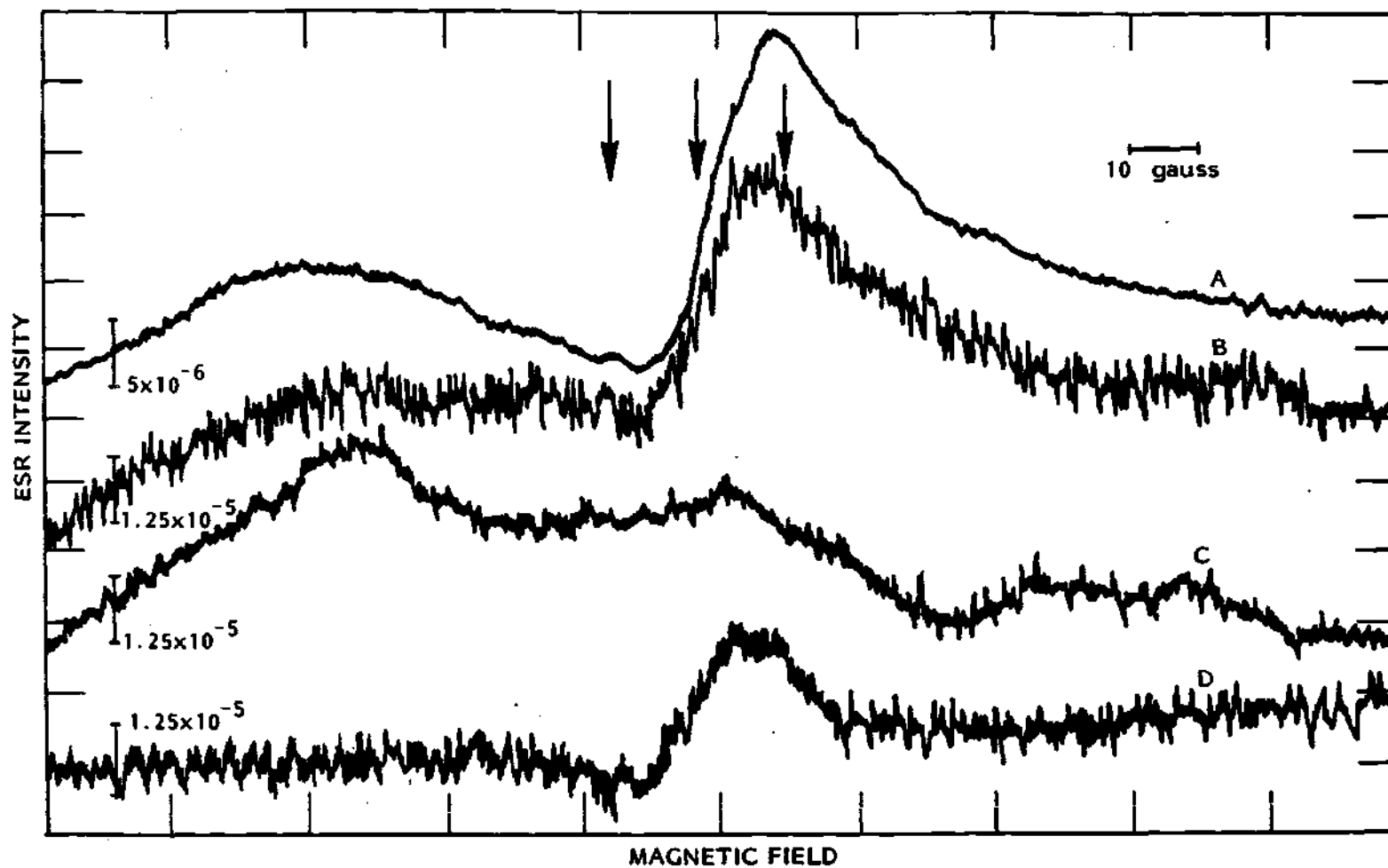


Figure 17. ESR Spectra of Lyophilized Membranes at 77°K; after n+γ Radiation; (a) at 1 mW, (b) at 200 mW, (c) Membranes at 200 mW before Irradiation, (d) Spectrosil Tube at 200 mW

imate g-value for the broad 20 G wide peak in the membrane sample is 2.004 while the peak seen in the spectrum of the sample container occurs at about $g = 2.007$. Following a period of 15 minutes at room temperature the spectrum was recorded at room temperature, Figure 18b, and the sample refrozen and the spectrum recorded, Figure 18a. The samples were once again allowed to stand at room temperature for a period of 4.8 days. The spectrum, after this period, Figure 18c, appeared similar to the one taken four days earlier. Only a single, 11 G wide peak at $g = 2.004$ was apparent. The radicals present in the sample tube disappeared on warming to room temperature.

ESR Spectra of Alpha Irradiated Membranes

The sample exposed to alpha radiation at room temperature produced a spectrum consisting principally of a 13 G wide peak when examined at 200 mW incident power, Figure 19c. When observed at 0.5 mW, Figure 19b, several unresolved peaks are indicated. These being unresolvable, the cumulative peak was 24 G wide and had a central g-value of 2.004. After storage for six days at room temperature, the spectral shape had changed, Figure 19d, and the amplitude decreased by about 50 percent indicating the continuation of radical reactions.

The spectrum of the sample exposed to alpha radiation at 77°K, Figure 20a, shows an asymmetric peak at about $g = 2.009$. Although the spectrum seen at 1 mW, Figure 20b, is somewhat different from that observed at 200 mW, the g-value of the broad peak is the same. After the sample had been at room temperature for 15 minutes, the spectrum in Figure 21c was recorded. The spectrum from the refrozen sample, Figure 21b,

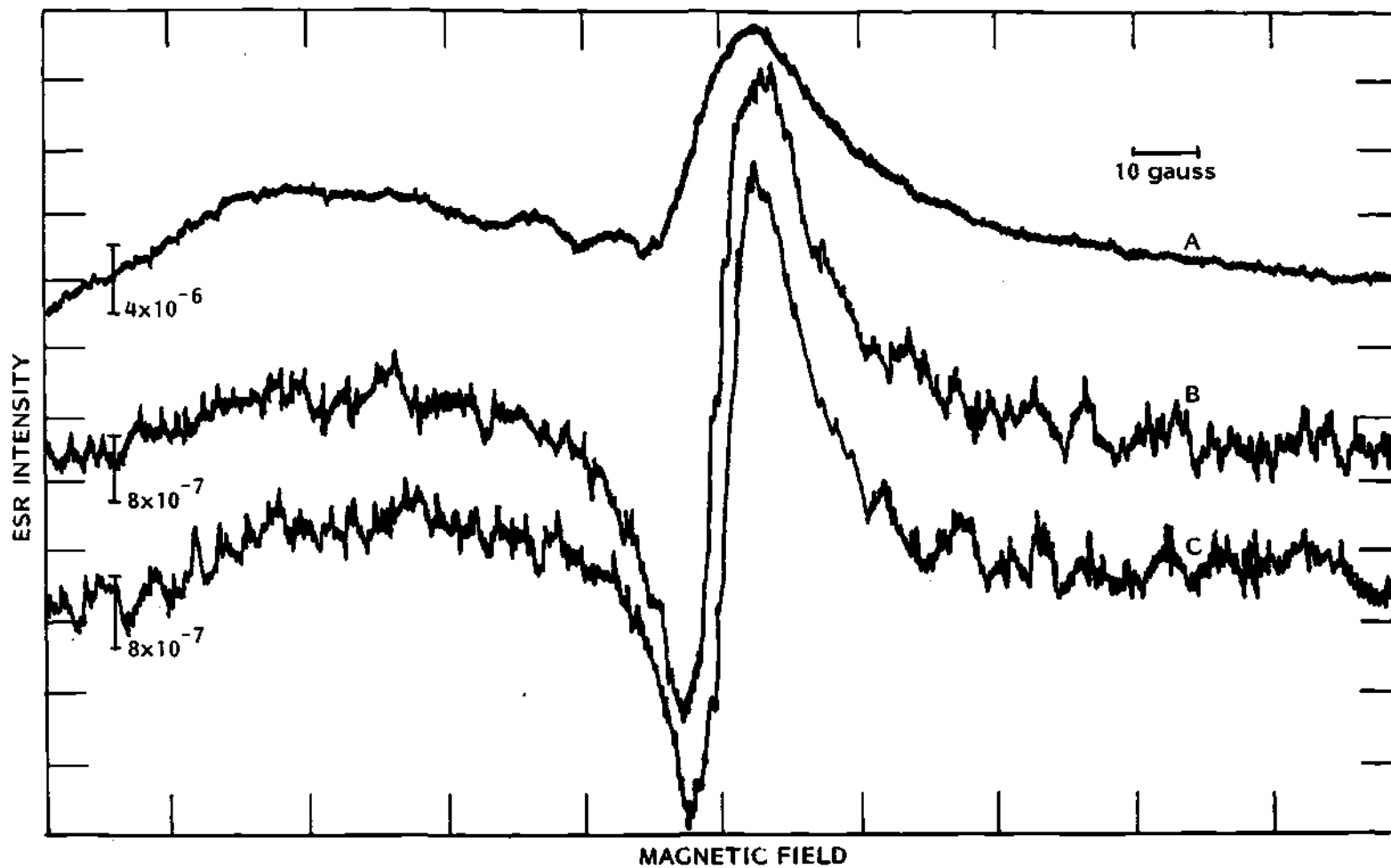


Figure 18. ESR Spectra of Lyophilized Membranes after $n+\gamma$ Exposure at 77°K after Annealing at Room Temperature; (a) at 1 mW at 77°K ; at 0.5 mW, (b) at Room Temperature, (c) after 4 Days at Room Temperature

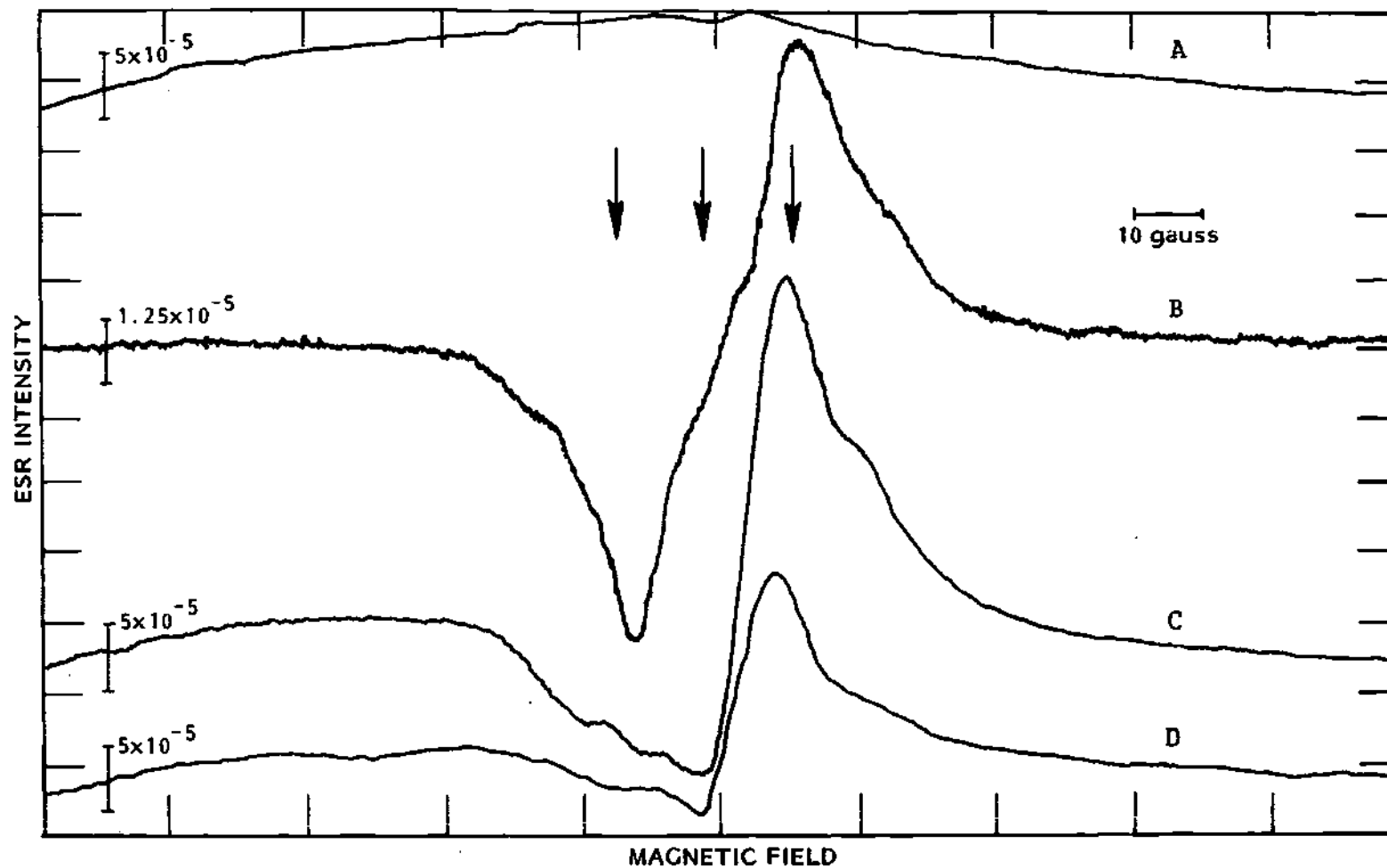


Figure 19. ESR Spectra of Lyophilized Membranes at Room Temperature; (a) at 200 mW before Irradiation; after 2.63 Mrads Alpha Radiation, (b) at 0.5 mW, (c) at 200 mW, (d) at 200 mW after 6.5 Days Storage

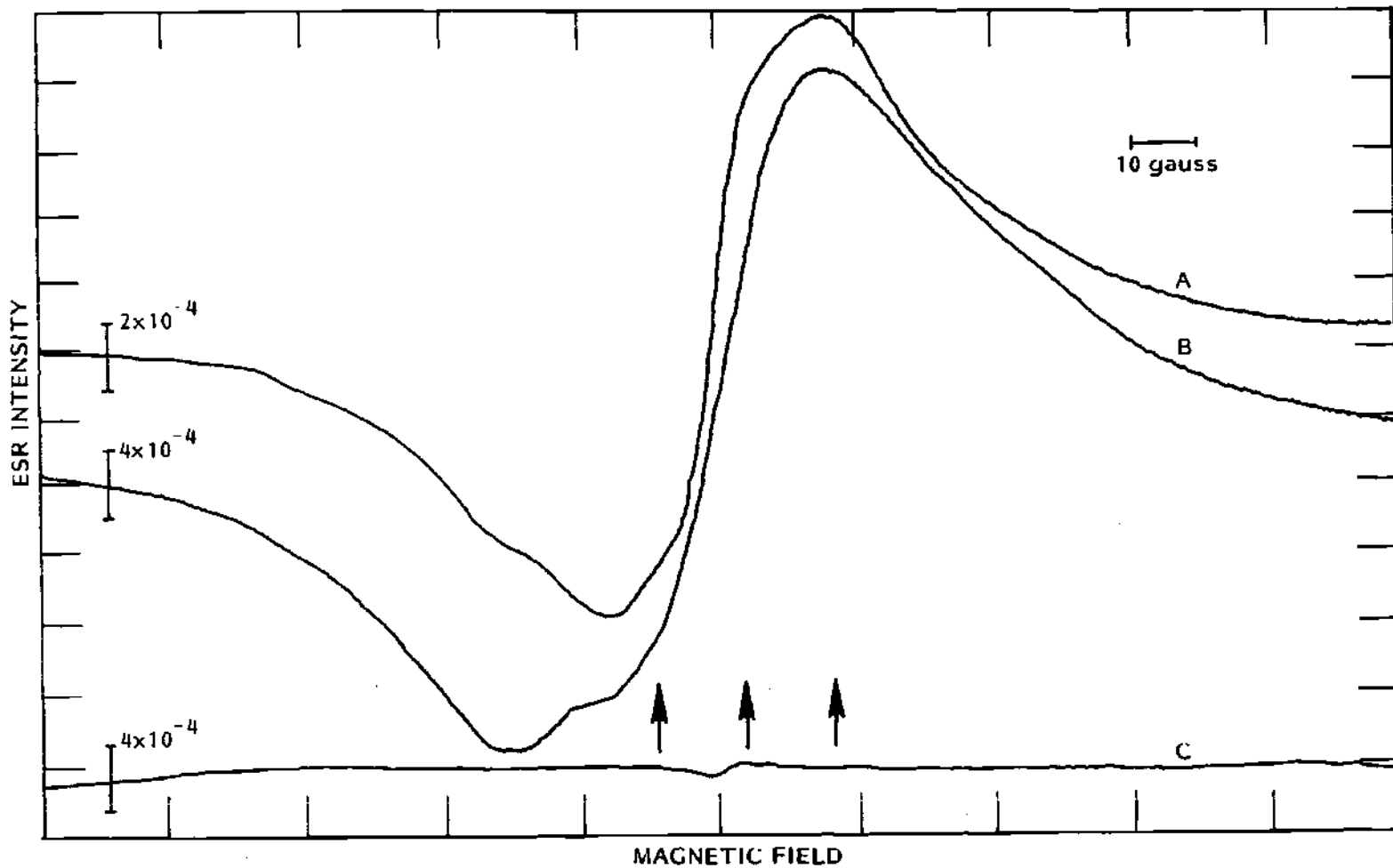


Figure 20. ESR Spectra of Lyophilized Membranes at 77°K; after 1.77 Mrads of Alpha Radiation; (a) at 200 mW, (b) at 1 mW, (c) at 200 mW before Irradiation

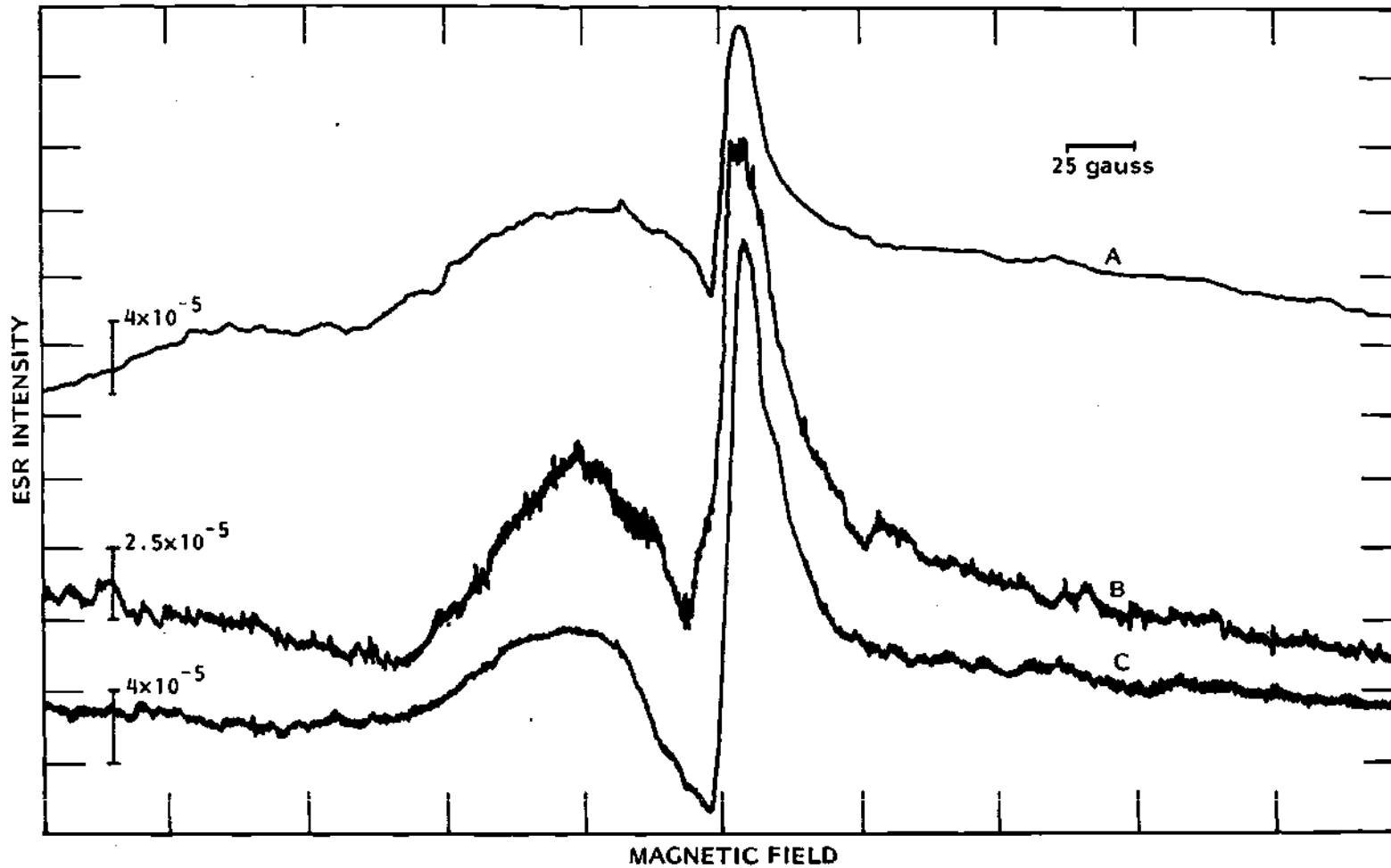


Figure 21. ESR Spectra of Lyophilized Membranes at 200 mW after 1.77 Mrads of Alpha Radiation at 77°K after Annealing at Room Temperature; (a) after 4 Days at Room Temperature, (b) at 77°K, (c) at Room Temperature

is like the one just mentioned. Whereas the spectrum at 77°K was compactly recorded on a scan range of 200 G, warming of the sample made it necessary to use a 500 G scan range to record the total spectrum. Allowing the sample to remain at room temperature for 4.8 days reduced the amplitude of the spectrum by about one half. This spectrum is shown in Figure 21a.

ESR Spectra of Fission Product Irradiated Membranes

For the fission product irradiation at room temperature, the spectrum was recorded at 200 mW, Figure 22b, and at 0.5 mW, Figure 22a. Although only one peak of about 26 G width is apparent, it is probable that there are at least two closely spaced resonances. The central g-value is about 2.006. The general low amplitude of the spectrum is apparent from the scale factor and the noise visible.

The ESR spectrum from fission product irradiation at 77°K could contain contributions from a radical with no axis of symmetry and whose g-tensor, therefore, would have three independent components, as may be seen in Figure 23b. The g-values of these components are 2.002, 2.041, and 1.960. However, the latter two components may not originate from the membrane sample as will be noted later. When the spectrum is examined at 1 mW power, Figure 23a, it is evident that there is a resonance very near the free electron g-value, independent of the previous resonance. After 15 minutes at room temperature, the sample exhibited the spectrum in Figure 24b. As in the case of alpha radiation, the spectrum broadened considerably on warming. A 500 G scan was necessary to observe the complete spectrum. The amplitude of the spectrum was much less after the

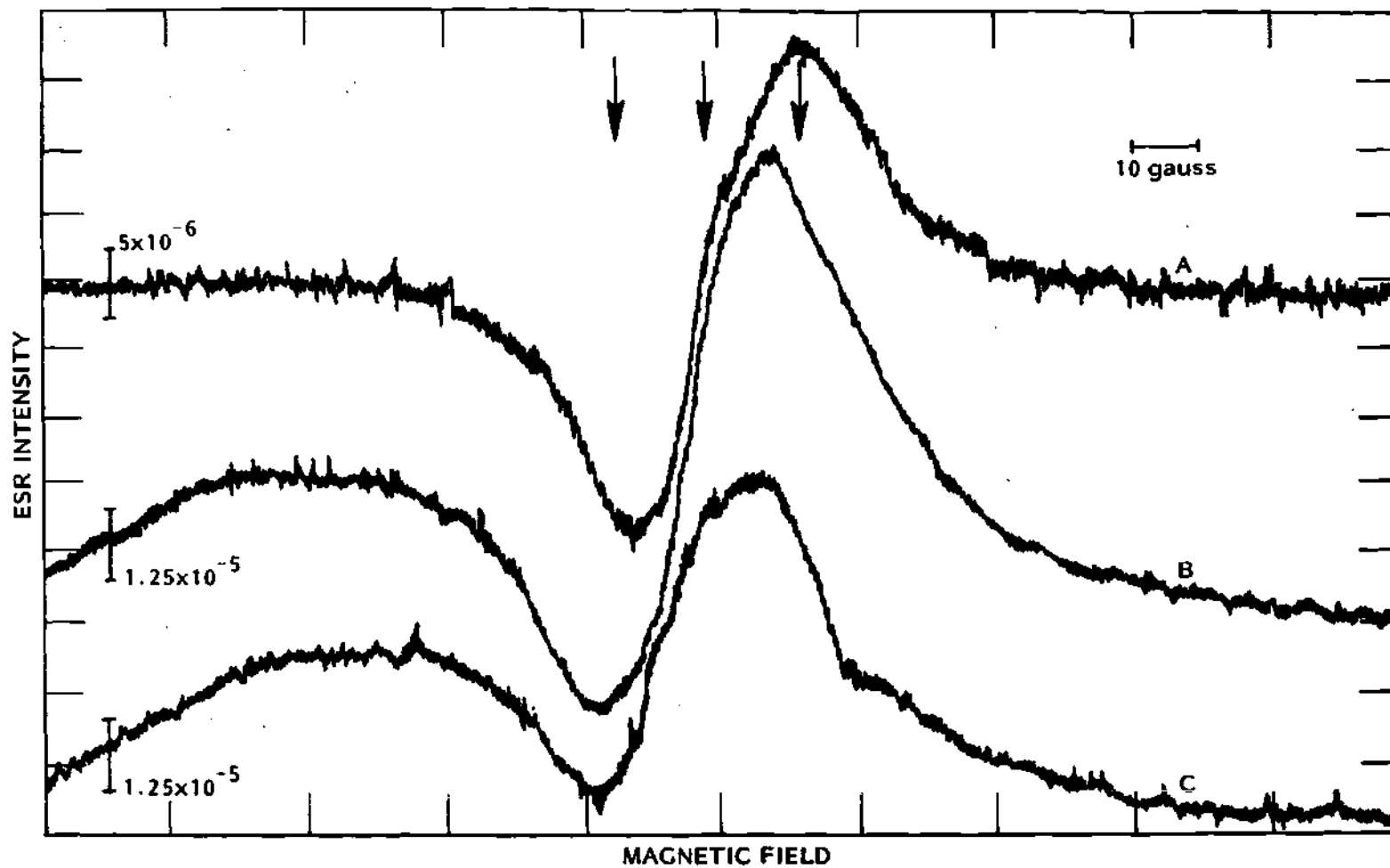


Figure 22. ESR Spectra of Lyophilized Membranes at Room Temperature, after 2.68 Mrads Fission Product Radiation; (a) at 0.5 mW, (b) at 200 mW, (c) at 200 mW before Irradiation

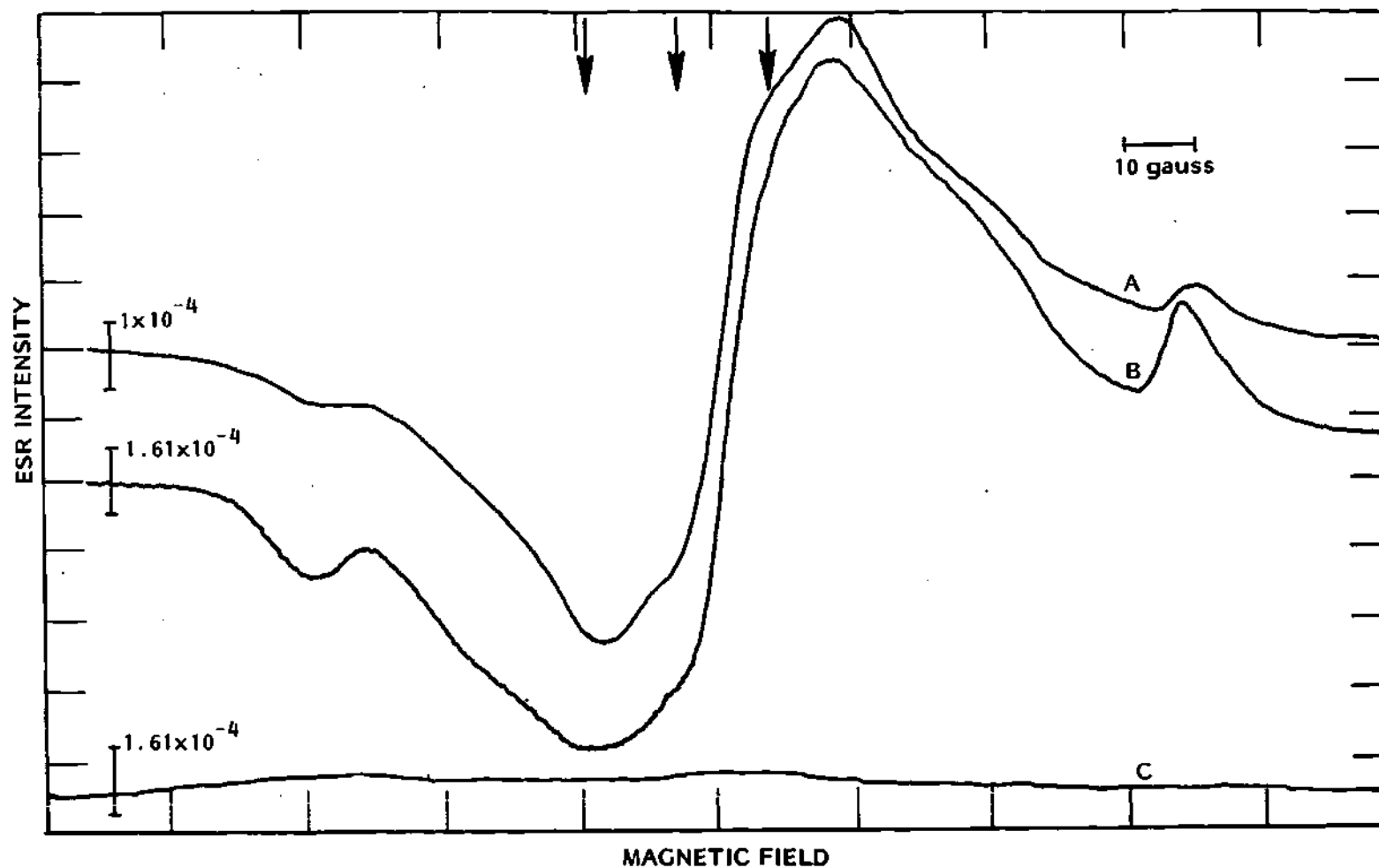


Figure 23. ESR Spectra of Lyophilized Membranes at 77°K, after 1.80 Mrads of Fission Product Radiation; (a) at 1 mW, (b) at 200 mW, (c) at 200 mW before Irradiation

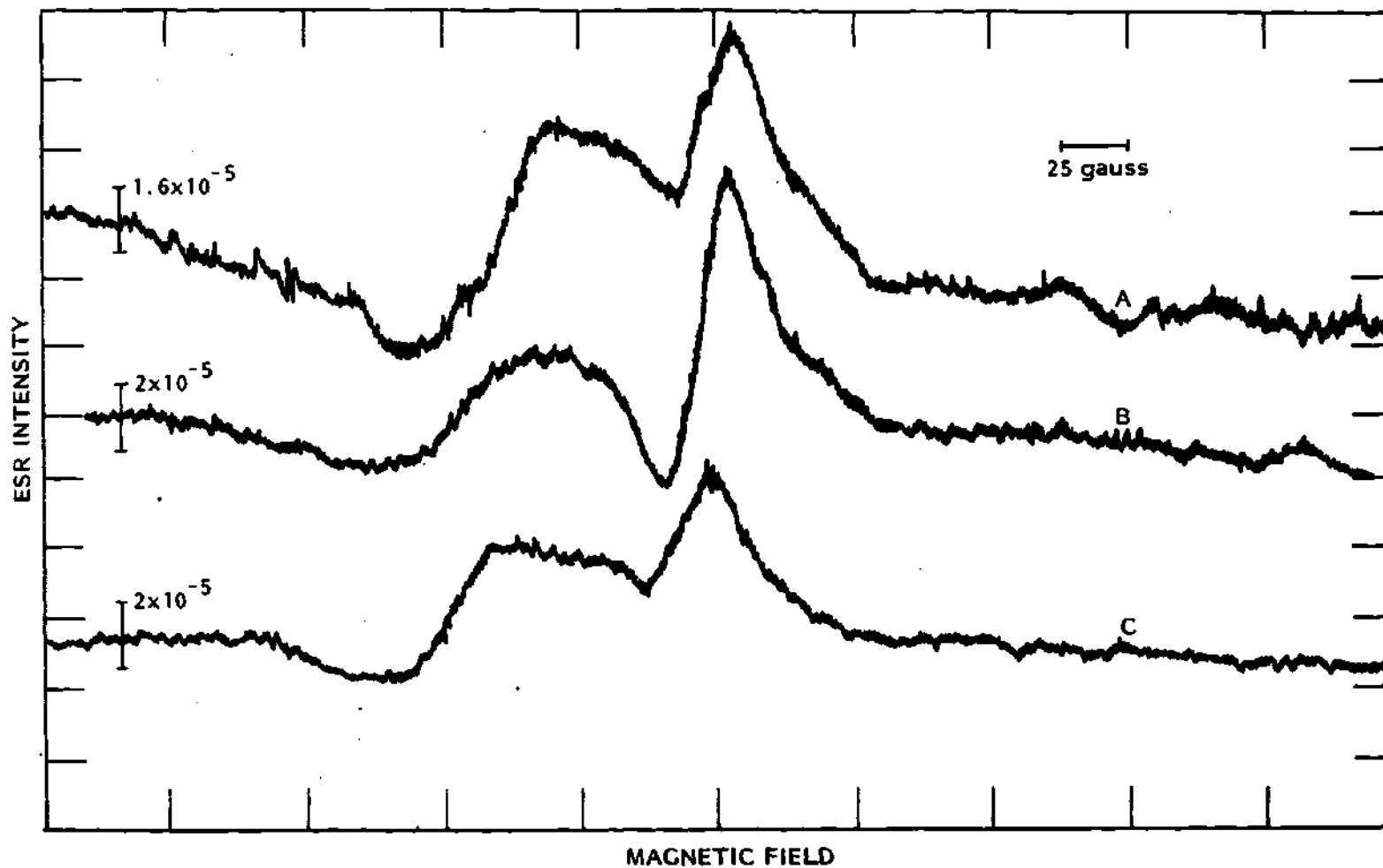


Figure 24. ESR Spectra of Lyophilized Membranes at 200 mW after 1.80 Mrads of Fission Product Radiation at 77°K after Annealing at Room Temperature; (a) at 77°K, (b) at Room Temperature, (c) after 4 Days at Room Temperature

heat treatment as indicated by the scale in Figure 24a for the refrozen sample. In these spectra a single peak near $g = 2$, predominated, with additional broad resonances at larger g -values. After 4.8 days at room temperature, the spectrum in Figure 24c was recorded. The intensity of the central peak had decreased by about a factor of two, while the accessory resonance changed little.

An attempt was made to observe hydrogen radicals in the samples exposed to high LET radiation. None was readily detected. By using maximum gain and one hour scan times, it was barely possible to discern the presence of a signal in the expected location in the sample exposed to neutron and gamma radiation at 77°K. Because of the weak signal it was not possible to determine radical quantity. Nor was it possible to distinguish that portion of the signal originating in the sample from that originating in the container. The same results were observed for the alpha irradiated and fission product irradiated samples at 77°K. However, it is unknown what fraction the alpha and fission product radiations contributed, since the components due to neutron and gamma radiation were of similar magnitude. Higher doses and/or longer scan times would be necessary to determine if hydrogen radicals are produced by high LET radiation since it is apparently very small.

ESR Spectra of Controls

The alpha and fission product irradiated samples contained small amounts of extraneous material in the form of boron and uranium compounds which were irradiated along with the membrane. Additionally these radiations deposited some of their energy in the sample container. An

effective control sample could not be developed which would allow a determination of the spectrum resulting from irradiation of these materials and simultaneously maintain the membrane sample configuration. However development of a qualitative control by deposition of the same quantity of these compounds in an empty sample tube was successful. The configuration of these controls is such that the inert material was compactly deposited, rather than distributed in bulk as in the membrane samples. The material was also deposited in a layer on the tube wall. For a given time in the radiation field, the dose deposited in the glass and in self irradiation was greater than that in these materials for the membrane samples. The unirradiated controls produced no ESR signals, only a noise spectrum.

After irradiation, all of the control samples developed at least one peak near $g = 2$. The spectra before fission-product irradiation at room temperature, Figure 25b, and after irradiation, Figure 25a, show a double peak was produced in the control samples in contrast to the broader single one in the membrane samples. With time the amplitude of the central peak of the irradiated samples decreased. After 24 hours its amplitude was 75 percent and after seven days its amplitude was 44 percent of the value immediately after irradiation. The remainder of the spectrum was constant with time.

The spectra, before and after alpha irradiation at room temperature are given in Figures 25c and 25d respectively. The single narrow peak produced here is in contrast to the broad peak with unresolved structure produced in the membrane sample. This peak's amplitude decreased to 63

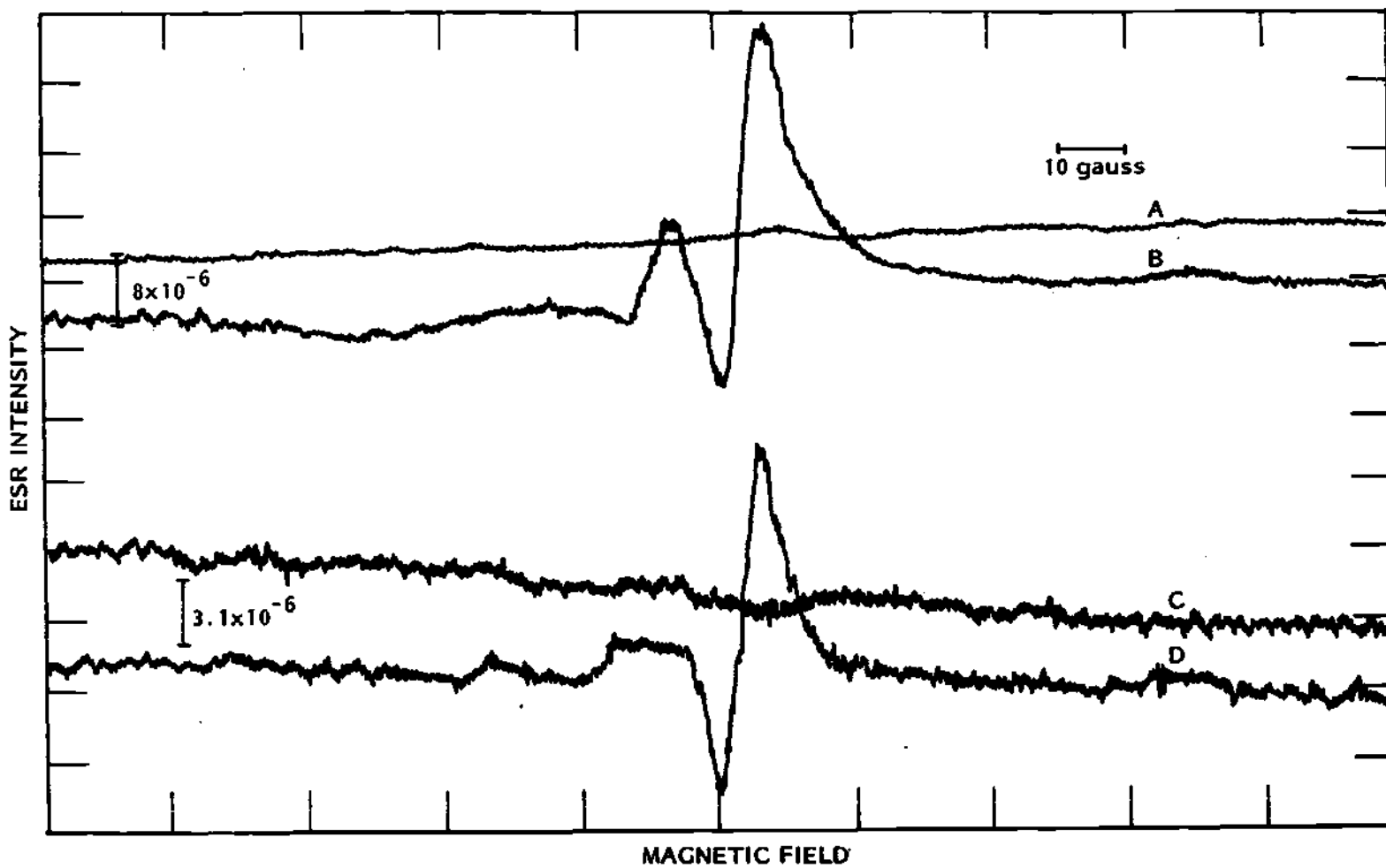


Figure 25. ESR Spectra of Irradiated Spectrosil Tubes at 200 mW at Room Temperature; (a) and (c) Unirradiated, (b) Fission Product Irradiated, (d) Alpha Irradiated

percent at 24 hours and 34 percent at seven days after irradiation.

At 77°K a broad peak developed in the alpha irradiated control, Figure 26c, which was a general feature of the membrane sample. Structure is scarce in the spectra of both sample and control. After seven days storage at 77°K, the peak amplitude had decreased 25 percent and became symmetrical, the right side resembling the previous left one. On warming to room temperature all radicals disappeared, leaving only a noise trace even at highest gain.

The control irradiated with fission products at 77°K produced a sharp peak, Figure 26a. Although this spectrum is quite unlike that observed for the membrane sample, two peaks were present at $g = 2.041$ and 1.960 , and were well separated from the central portion, in both sample and control. It seems likely that the species responsible for these components are either generated in the extraneous material or sample container or are due to fission products themselves. Storage for seven days at 77°K produced no detectable change in the spectrum. After allowing the control to stand at room temperature, Figure 26b, the sharp central peak remained but much of the accessory resonances including the two peaks just mentioned, disappeared. Although this occurred in the membrane sample too, additional resonances at larger g -values were apparent in the membrane sample.

Hydrogen radicals were barely detectable in the membrane samples exposed at 77°K. Contrastingly, in the controls exposed at this temperature, hydrogen radicals were readily detectable. A power of 1 mW, a modulation amplitude of 1 G and a scan range of 100 G were used. In the

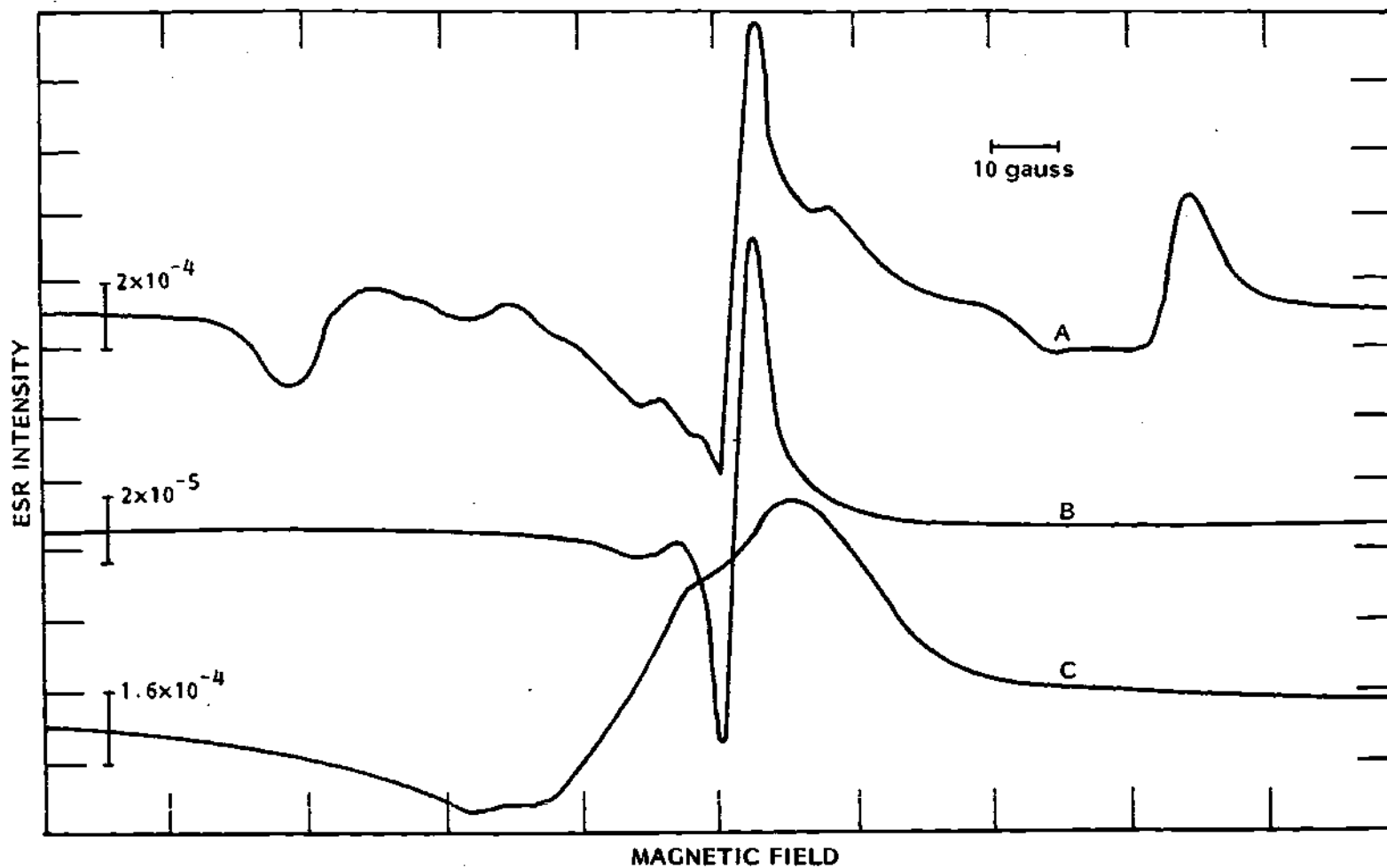


Figure 26. ESR Spectra of Irradiated Spectrosil Tubes at 1 mW at 77°K; (a) after Fission Product Radiation, (b) after Annealing at Room Temperature, (c) after Alpha Radiation

fission product irradiated control, two lines of about 1 G width, separated about 503 G apart centered at $g = 2$ were apparent, Figure 27b. This is the expected spectrum from simple hydrogen radicals. For the alpha irradiated controls, the narrow lines were again apparent. In addition, however there was a broad, 7 G wide peak superimposed at the same location as each hydrogen radical peak. The broad peak may be seen in Figure 27a. These broad peaks may be indicative of a limited interaction of the hydrogen radicals with their environments. Two different environments with different relaxation times are indicated because the narrow peak is present also. If the broad peaks are not related to the hydrogen radicals, the species producing them must have a nuclear spin and splitting constant identical to those of the hydrogen radical. The controls were stored for a period of seven days at 77°K and then re-examined. The hydrogen radical signal for both the alpha and fission product irradiated control had decreased about 15 percent from the prior measurement. The shape of the peaks had not changed.

Both the shape of the spectrum near $g = 2$ and the spectral changes on warming to room temperature were different for samples and controls. There was a prolific hydrogen radical build-up in the controls. In the membrane samples it was barely detectable. These differences as well as others based on power saturation to be discussed later, lead to the conclusion that the majority of the ESR signals observed from the membrane sample originated in the membrane. This is expected from a radiological energy deposition standpoint, if the g -value for the extraneous material is no greater than that for the membrane. Comparison of the number of

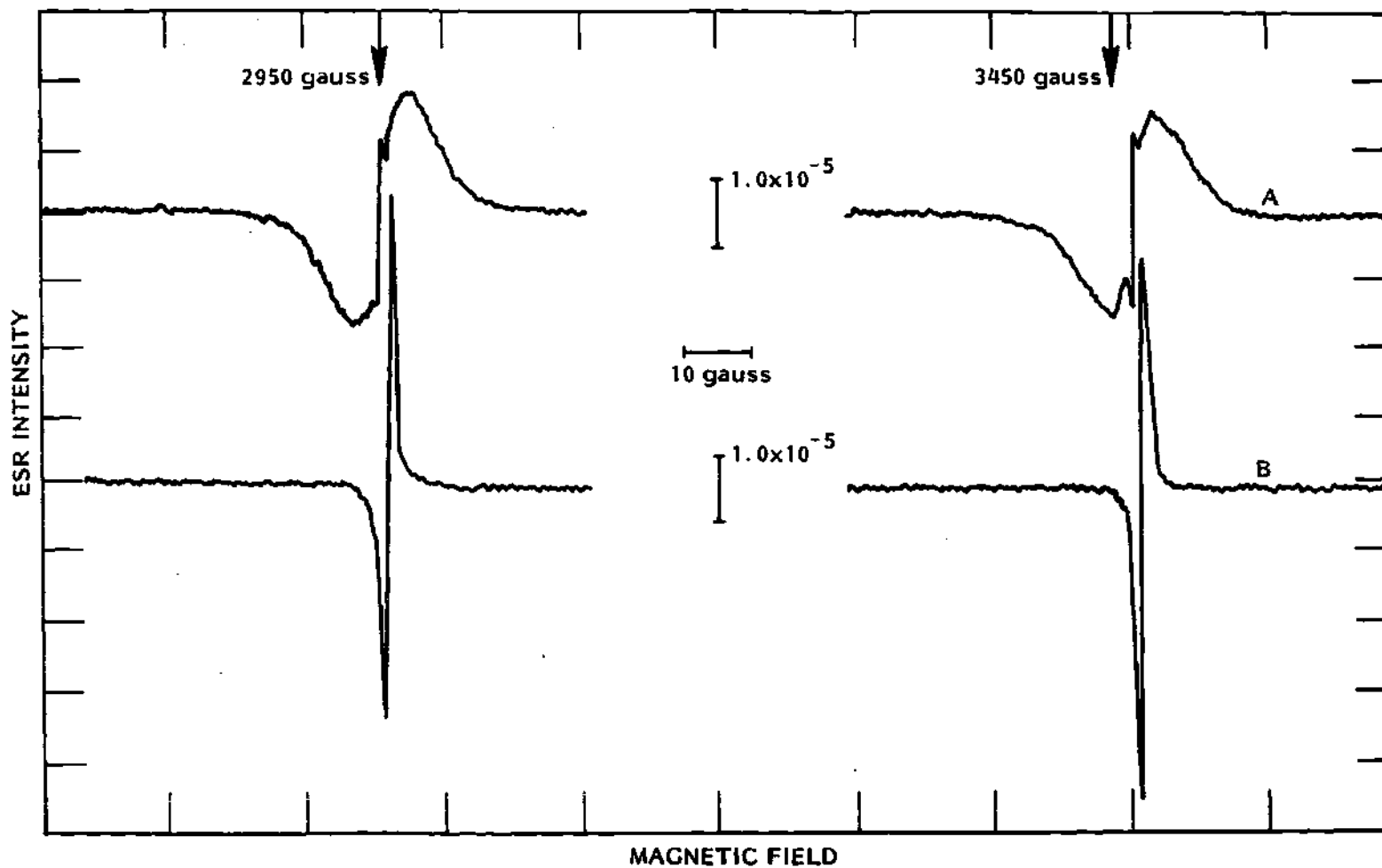


Figure 27. ESR Spectra of Hydrogen Radicals in Spectrosil Tubes at 1 mW at 77°K; (a) after Alpha Radiation, (b) after Fission Product Radiation

radicals trapped in the control versus membrane samples supports this.

Power Saturation

Power saturation is not only another parameter that must be considered in deriving radical concentrations, but it is also valuable in indicating the type of molecular environment surrounding a radical. The rate at which excess energy in the free radical or spin system is dissipated as heat to its environment is governed by the spin-lattice relaxation time, T_1 . The rate at which energy is distributed throughout the spin system is governed by the spin-spin relaxation time, T_2 . A procedure for determining these parameters has been developed (Castner, 1959).

The spectrum of the free radicals in membrane samples, as in many biological materials, consists of broad resonances from a number of superimposed lines. It was not possible, therefore, to separate the spectrum of a particular radical from the others in order to determine the underlying peak widths. For these samples only the product T_1T_2 could be determined.

The integrated power absorption, Y , is expressed by:

$$Y = A \sqrt{\frac{kP}{1 + kP}}$$

where P = microwave power input in milliwatts and A and k (mW^{-1}) are constants. This relationship is valid for inhomogeneous broadening under the assumption that the underlying linewidth is small compared to the envelope of linewidths. This same expression is obtained for the case of homogeneous broadening of g-lines and is an approximation for Lorentzian

shaped lines. Since this expression results from a single spin species, the total result for n species is obtained by summing over n such expressions, each with an independent set of constants A_i and k_i . The spectra obtained in this experiment could not be separated into contributions from individual species. The above equation for one species was applied to the entire spectrum even though there were quite probably more than one species present. The range of power available from the spectrometer was 0.5 mW to 200 mW. Over this range the fitting of this equation to the data could usually be done with no more than 10 percent error.

Table 4 shows the saturation factors for 0.5 and 200 mW incident microwave power. By the different values obtained, it is clear that saturation effects need to be taken into account in determining free radical concentration. At 0.5 mW the calculated saturation factors at room temperature are no more than 1.05, while at 77°K they are limited to 1.11 with the exception of hydrogen radicals. The large saturation factors observed for the "N" sample are suspect because of the difficulty in obtaining data at low radical concentrations and low signal-to-noise ratios. The radicals generated during irradiation at 77°K had larger saturation factors than the radicals subsequently formed after the sample had been allowed to reach room temperature and were refrozen. Hydrogen radicals had some of the larger saturation factors observed and were only measurable at 77°K. From these data, the more reactive radicals are apparently associated with larger saturation factors.

The relaxation times are related to the constants in the saturation equation by:

Table 4. Microwave Power Saturation Factors

Sample ¹	295°K 0.5 mW	Exposure 200 mW	77°K 0.5 mW	Exposure 200 mW
Pitch ²	1.00	1.54	--	--
Charcoal ²	1.00	1.66	1.01	2.70
FDM	1.01	2.86	1.04	6.15
FDM, after RT	--	--	1.03	4.84
FDM, H'	--	--	1.06	7.33
Spec. Tube	1.00	1.31	1.00	1.48
50-50	--	--	1.04	5.72
50-50 after RT	--	--	1.01	2.39
50-50, H'	--	--	1.06	7.12
LM	--	--	1.01	2.27
LM, H'	--	--	1.16	11.89
HS	--	--	1.00	1.95
HS, H'	--	--	1.16	11.68
N	1.43	20.4	1.87	22.4
A	1.03	5.12	1.06	5.23
A, after RT	--	--	1.06	4.90
F	1.05	6.27	1.11	6.87
F, after RT	--	--	1.03	3.76
Control A	--	--	1.00	1.53
Control F	1.05	6.68	1.00	1.50

¹See Table 1 for type of radiation and nomenclature.

²Standard samples not irradiated.

$$T_1 T_2 = \frac{4k}{a\gamma^2} (\text{sec}^2)$$

where

$\gamma = 1.76 \times 10^6 \text{ Gauss}^{-1} \text{sec}^{-1}$, the gyromagnetic ratio of the electron

$a = 0.0196 \text{ Gauss}^2/\text{mWatt}$ for the spectrometer used here

$$T_2 = - \frac{1}{\gamma \Delta H_{\frac{1}{2}}}$$

$\Delta H_{\frac{1}{2}}$ (Gauss) is the full width at one half the maximum of the absorption peak

This equation also applies to a system with a single spin species. If more than one species were present, then it would be necessary to include spin-spin relaxation times for all species and relaxation times between the species. For this reason and since an effective or average k rather than a k for each species present was determined, the relaxation times $T_1 T_2$ should be considered effective relaxation times. Since relaxation times for particular species may deviate from these effective relaxation times, they should be used with caution. The relaxation times so determined are given in Table 5.

The relaxation times for radicals produced at room temperature and 77°K by both gamma and fission product radiations are similar. However, after temperature treatment of the frozen samples the relaxation time for the gamma irradiated sample was 70 percent longer than that of the fission product irradiated sample. Even if the radical species were not different, the routes of reaction and radical environment are clearly different in these two cases.

The relaxation times for alpha irradiated samples were similar for both the room temperature and 77°K samples. However most membrane samples

Table 5. Relaxation Times from Saturation Measurements

Sample	Radiation	$T_1 T_2$ (sec ² x 10 ¹²)		
		295 °K	77 °K	77 °K After Room Temp.
Pitch	--	0.45	--	--
Charcoal	--	0.57	2.05	--
FDM		2.4	12.1	7.4
FDM, H'		--	29	--
LM		--	1.36	--
LM, H'		--	46	--
HS		--	.93	--
HS, H'		--	45	--
50-50		--	10.5	1.55
50-50, H'		--	16.4	--
N		136	164	--
A		8.3	8.7	7.6
F		2.4	15.2	4.3
Control A		--	.44	--
Control F		14.4	.41	--

showed an increased relaxation time at 77°K. For the same radical at room temperature and 77°K, the spin lattice relaxation time, T_1 , should be inversely proportional to temperature while the spin-spin relaxation time should be independent of temperature as a first approximation. This is demonstrated by the charcoal standard where the expected increase in relaxation time between room temperature and 77°K is about a factor of 3.8 while the observed increase was 3.6. For the neutron and gamma irradiated samples, extremely long relaxation times resulted from small changes in the absorption curve as the power is varied. Because of the low concentration of radicals in these samples, these relaxation times may be in error. The very different relaxation times for the controls and membrane samples lend support to the hypothesis that most radicals generated in the membrane sample originate in the membrane itself. It should be noted once more that because of the multitude of radicals possibly generated, the analysis of relaxation times necessarily applies to the conglomerate population of radicals, restricting the interpretations that can be made.

Radical Production and G-values

The first derivative ESR spectra were integrated twice and corrected for cavity Q changes and power saturation as described in the chapter entitled Experimental Method, in order to obtain the free radical concentration in the sample. The limits of integration were established by determining the range necessary to include all portions of the ESR derivative curve which were different from background in the case of the last or maximum radiation exposure for a particular sample. Contributions from

radicals in the sample container, which were usually less than ten percent, were subtracted. Also subtracted was the contribution of radicals initially present before irradiation in order to obtain that due solely to the radiation. The results of these measurements are given in Appendix I and in the following graphs.

In determining the radical production rate per unit of absorbed energy, the G-value, the initial change of radical concentration is needed. The radical build-up with dose may not be linear over all dose ranges, particularly at high doses. Therefore the initial linear portion at low doses is needed for this calculation. However, at very low doses the change in radical concentration may not be sufficient to permit detection. Since the desirable range where linear build-up is occurring with detectable levels of radicals was unknown, each sample was given a sequence of doses and an ESR determination made after each exposure. The cumulative dose after each exposure was about twice that after the prior exposure. In this way a large range of doses could be spanned with a manageable work load and yet one would expect to have enough significant data in some dose range to permit a determination of G-values.

The radical build-up with dose may not continue at the initial rate and radical saturation may appear. Although the cause of radical saturation is not known in each specific case, it can be due to the destruction of radicals by the radiation which is also producing them. First order kinetics appears to fit the data in most cases. When saturation was apparent, the following equation was fitted to the data:

$$N(D) = N_{\infty} (1 - \exp(- D \ln 2 / D_{\frac{1}{2}}))$$

where $N(D)$ is the radical concentration in the sample in radicals/gram

N_{∞} is the equilibrium radical concentration in radicals/gram

D is the absorbed dose in rads

$D_{\frac{1}{2}}$ is the half-value dose in rads required to produce a radical destruction probability of 0.05.

The least squares program for this fitting, in which the constants N_{∞} and $D_{\frac{1}{2}}$ were determined, is given in Appendix II. Table 6 contains the constants so determined and Table 7 contains the G-values for gross total free radical production.

The radical saturation effect is illustrated in Figure 28 by the build-up of radicals in the membranes dried in an oven at 80°C. Least squares fitting of the build-up equation to these data, shown by the curve in Figure 28, produced a half-value dose of 0.74 Mrads (Table 6). Although maximum doses of about 0.9 Mrads were attained, the initial linear portion is limited to about 36 krad. The G-value determined from this initial curve is 5.3 (Table 7).

No radical saturation is apparent for the lyophilized membrane samples irradiated with gamma rays at room temperature as shown in Figure 29. The initial radical build-up to about six krad occurred with a G-value of 5.2 (Table 7), which was about the same as for the oven dried membranes. At this dose the sample was allowed to stand overnight before resuming the exposures. The decay or removal of radicals that occurred during this period is indicated by the multiple points at 5840 rads in

Table 6. Constants for the Radical Build-up Equation

Sample	Radiation Type	Irradiation Temperature (°K)	N_{∞} Radicals/gram	$D_{\frac{1}{2}}$ Rads
HDM	γ	295	29.1×10^{17}	0.744×10^6
FDM	γ	77	2.45×10^{17}	0.189×10^6
A	$\alpha + {}^7\text{Li}$	295	11.4×10^{17}	1.09×10^6

Table 7. G-values for Radical Production

Sample	Radiation Type	Irradiation Temperature (°K)	G-value Radicals/100 eV
HDM	γ	295	5.3
FDM (initial) ^a	γ	295	5.2
FDM (final) ^a	γ	295	1.4
FDM	γ	77	2.9
FDM, H [•]	γ	77	0.0013
LM	γ	77	0.33
LM, H [•]	γ	77	0.0037
HS	γ	77	0.29
HS, H [•]	γ	77	0.0064
50-50	γ	77	0.59
50-50, H [•]	γ	77	0.0017
N	$\gamma + n$	295	$0.83--2.4^a$
N	$\gamma + n$	77	1.5^a
A	$\alpha + {}^7\text{Li}$	295	0.60
A	$\alpha + {}^7\text{Li}$	77	0.88
F	F.P.	295	0.030
F	F.P.	77	0.43

^aSee text.

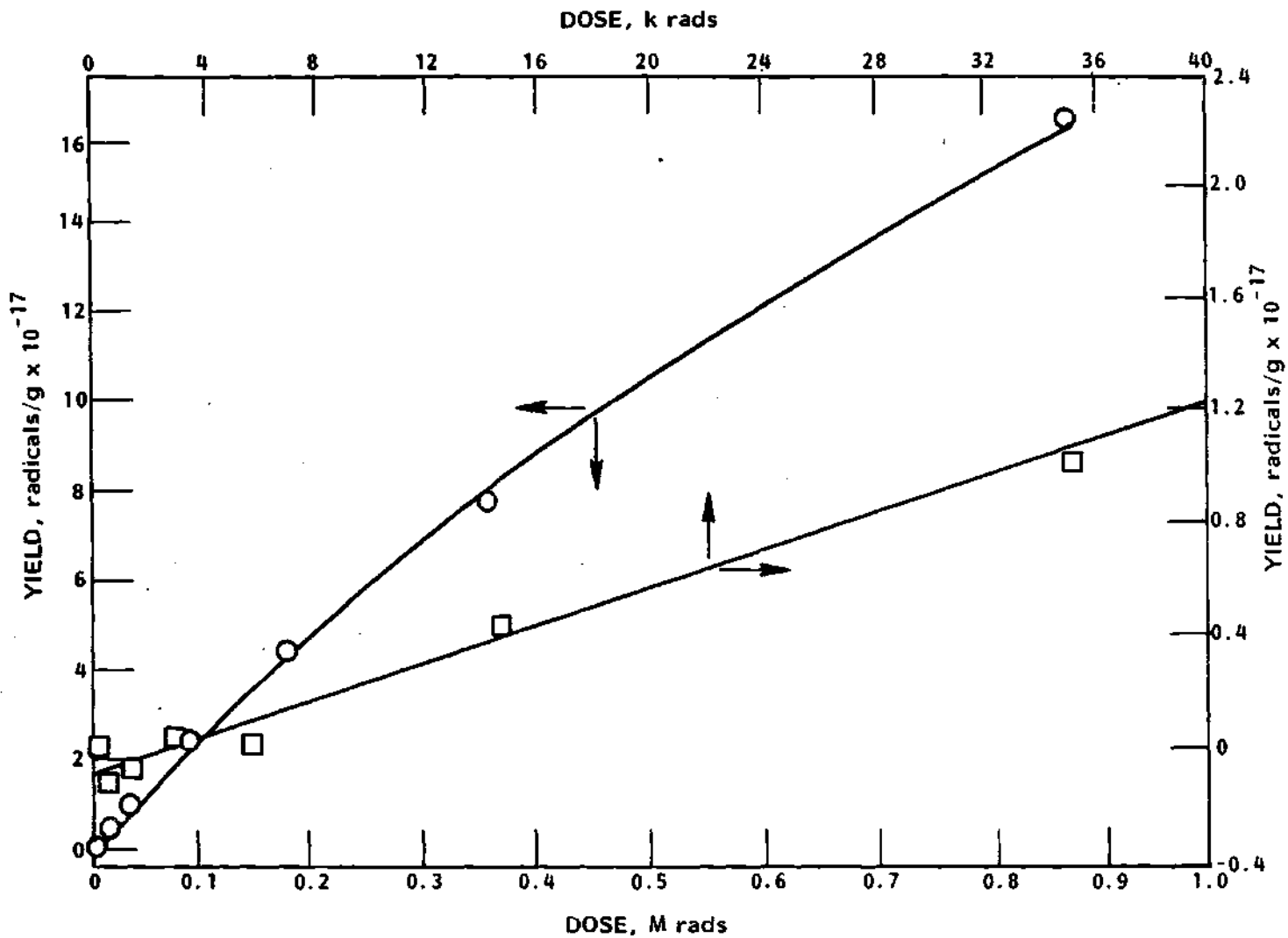


Figure 28. Build-up of Free Radicals at Room Temperature in Gamma Irradiated Membranes Dried at 80°C, HDM Sample

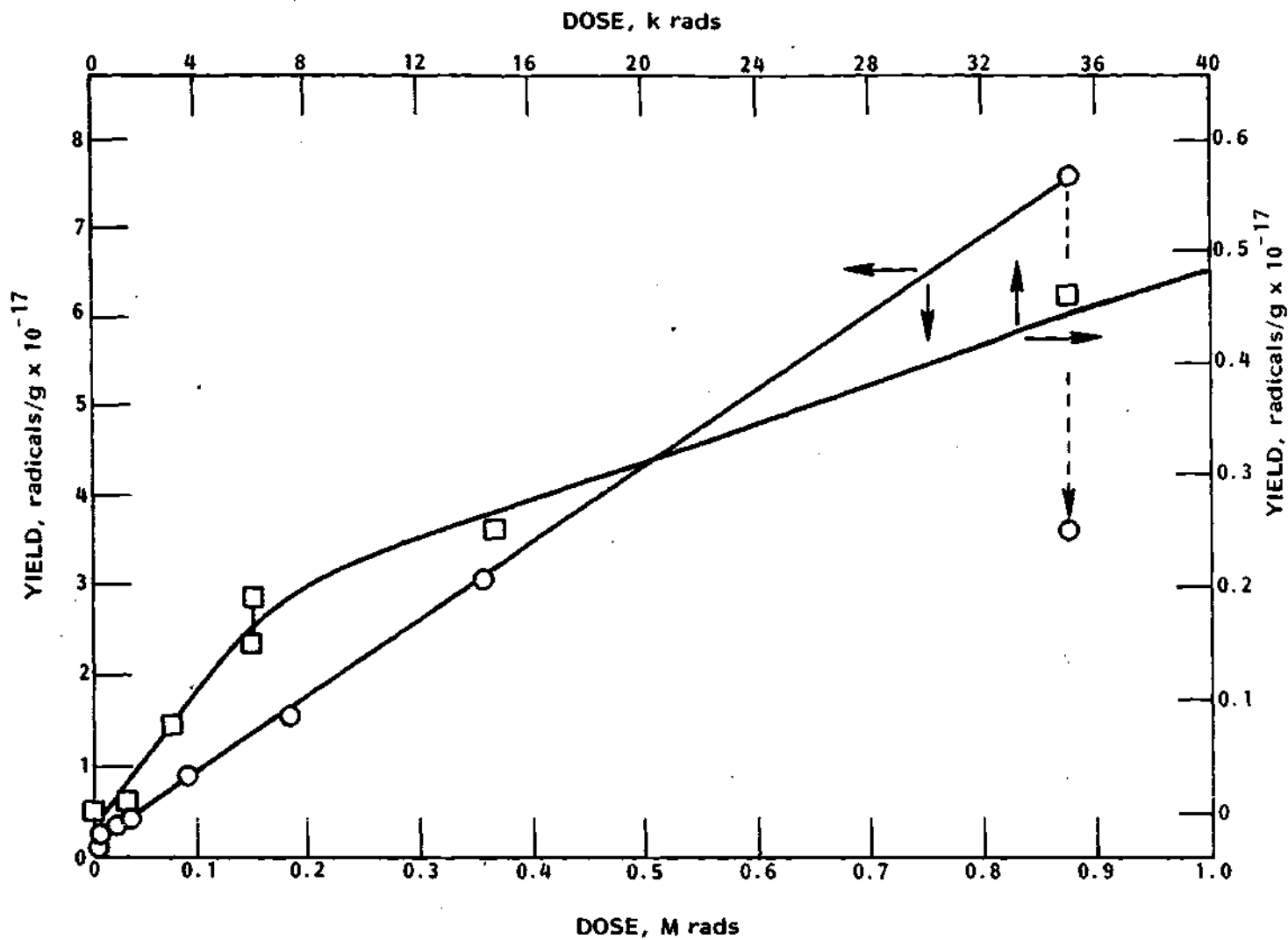


Figure 29. Build-up of Free Radicals at Room Temperature in Gamma Irradiated Lyophilized Membranes, FDM-1 Sample

Figure 29. All points at higher doses in Figure 29 had this amount of decay added to them in an effort to give the entire build-up curve a common basis. Similarly at the completion of irradiation, a one day waiting period produced the decay shown in Figure 29 at 0.875 Mrads. When the exposures were resumed, the resulting linear build-up produced a G-value of only 1.4 (Table 7). It is unknown whether this sudden change in G-value was a result of reactions occurring during the storage period or whether it would have occurred at that dose if little or no storage time had elapsed. It is appropriate to note that to give a sample a complete sequence of gamma exposures and determination of the associated ESR spectra required about 12 hours of exposure and analysis time. The reactions occurring during this time may have changed the sample in such a way as to produce different results from those that would be obtained if the analyses required very little time. If this is the case, the rate at which the dose is delivered will be important. Dose rate effects were beyond the scope of this investigation.

The lyophilized membrane exposed to gamma radiation at 77°K, particular evidence of saturation is seen in Figure 30. The half-value dose was about 0.19 krads (Table 6), which was the lowest observed in any sample. The initial build-up was approximately linear to about 14 krads and the resulting G-value was 2.9 (Table 7). The build-up equation that was fitted to all the data points did not fit the low dose data as well as was possible with a line segment. These two curves are compared in Figure 30. The G-value determined from the build-up equation was 1.4, which was about half that determined using only the low dose data and a

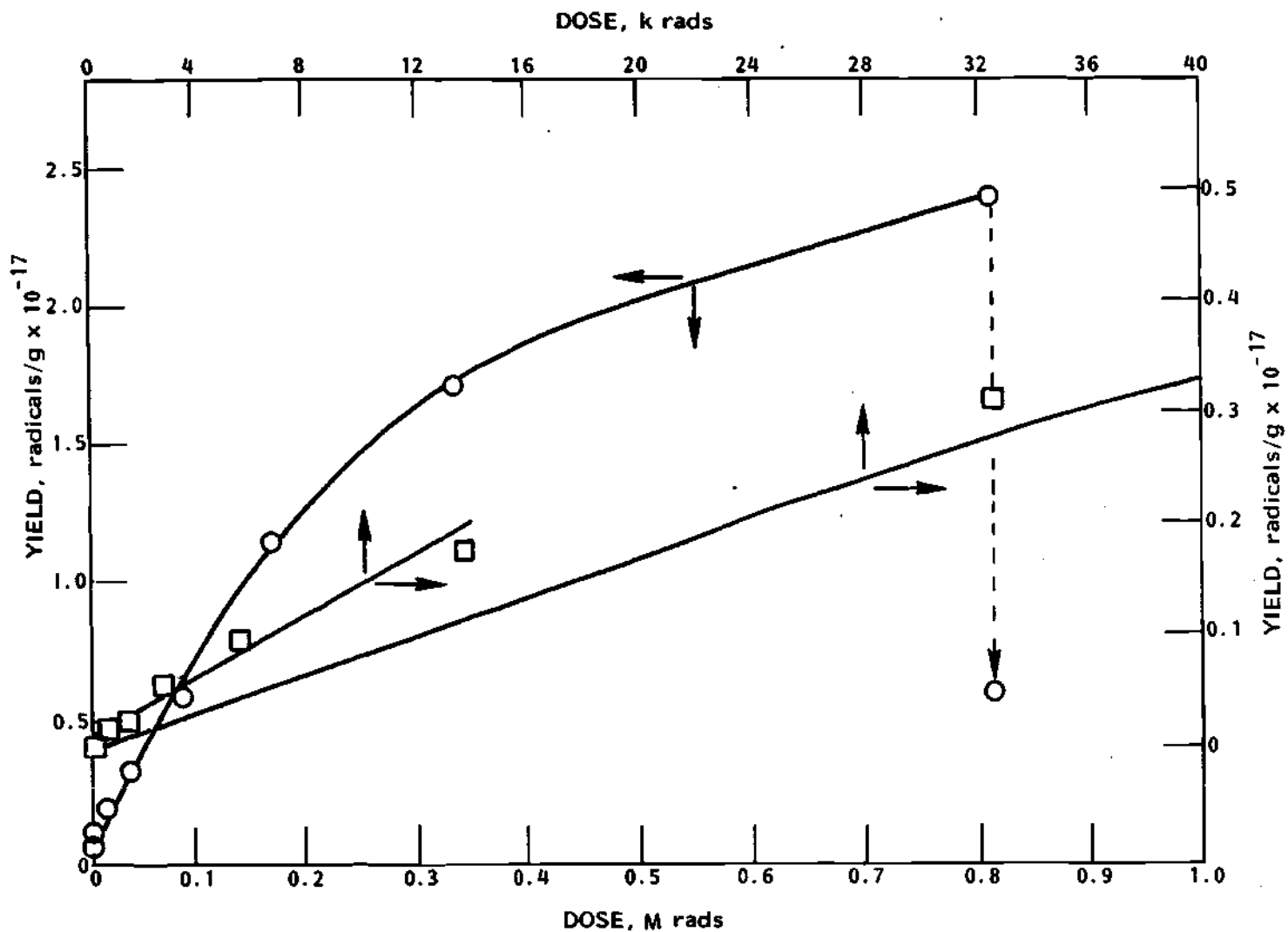


Figure 30. Build-up of Free Radicals at 77°K in Gamma Irradiated Lyophilized Membranes, FIM-2 Sample

straight line. Since the parameters in the build-up equation are determined using data from the high as well as the low dose region, the limited ability of this two parameter equation in fitting the data introduces additional uncertainty into any G-values determined from it. Hydrogen radicals were detectable in the membrane only at the highest dose. None were detectable in the Varian sample tube. Assuming a linear build-up to the dose where they were observed, the G-value for hydrogen radical production and trapping would be 0.0013. After warming of the sample to room temperature and refreezing, the hydrogen radicals were no longer detectable and the free radical population had also decreased to about one third its former value. The procedure of irradiation to 0.8 Mrad at 77°K followed by warming to room temperature produced a radical concentration about an order of magnitude lower than irradiation to the same dose at room temperature. This effect is partly attributable to radical saturation at 77°K since the two samples produced radical concentrations differing by less than a factor of two at doses below 30 krads. Another contributing cause is apparently different radical production pathways or different radical production efficiencies for the two exposure and annealing conditions.

The build-up of free radicals in the 1.5 percent membrane in water solution sample when gamma irradiated, was linear (Figure 31) to about 0.8 Mrad which constituted the upper limit of the range studied. The concentration of radicals in the solution without membranes was only slightly lower and the G-values of the samples were both approximately 0.3 (Table 7). An attempt to calculate the G-value of the membrane itself

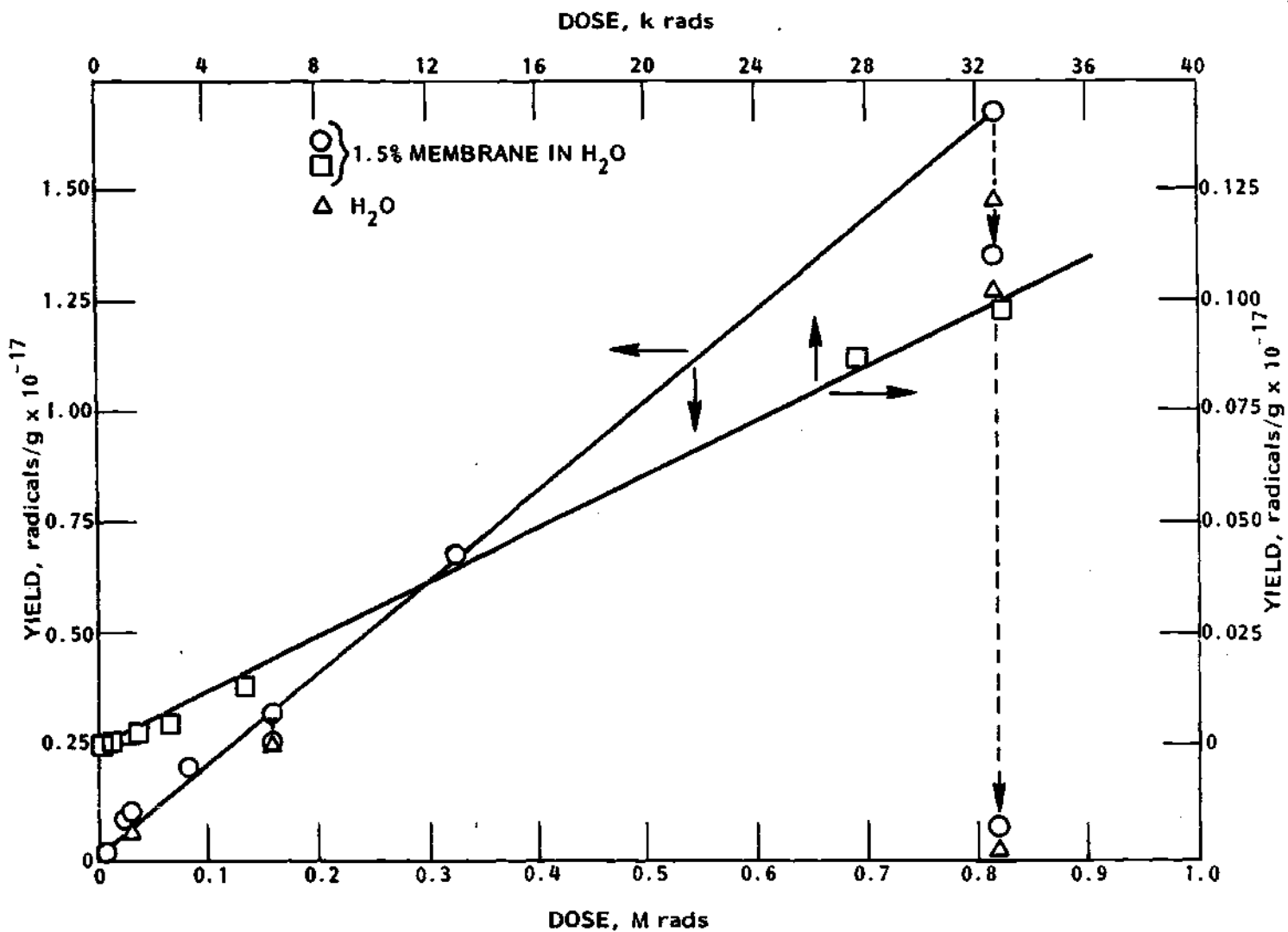


Figure 31. Build-up of Free Radicals at 77°K in Gamma Irradiated 1.5% Membrane Solution, LM Sample, and in Water, HS Sample

under highly restrictive necessary assumptions was made. It was assumed: (1) that the build-up of radicals in the membrane is independent of that in the surrounding solution, (2) that radicals generated in the membrane or water do not diffuse into nor attack and create radicals in the other entity, (3) that the water which may be absorbed in the membrane is either small or does not change its character of radical production from that of the pure water solution, and (4) that the energy absorbed by each the membrane and the water is proportional to the dry mass of the membrane and the mass of lyophilizable water respectively. The partition equation

$$G(E_m + E_w) = G_m E_m + G_w E_w$$

where G , G_m , G_w are the G -values of the membrane solution, the membrane, and the water, respectively; E_m , E_w are the radiological absorbed energies in membrane and water, was applied. From the data in Table 7, it was calculated that the G -value of the membrane component was three. However, assuming a ten percent error in the data, a range of G from zero to seven would result. In addition the reliability of this number would depend on how closely the above assumptions were satisfied.

Storage of the membrane solution at 77°K for 20 hours produced a decrease in the free radical concentration of about 20 percent indicating that not all free radical reactions were stopped at this temperature. After six days storage at 77°K the radical concentration decreased to about six percent of its former level in the membrane solution and to about two percent in the water sample.

Hydrogen radicals were detected in both the membrane and water samples. Build-up curves were linear for both (Figure 32). However the G-value for hydrogen radicals in the membrane sample was about 58 percent of that for the water sample (Table 7). Two very similar samples to be producing such very different results must indicate that radical reactions or trapping sites, rather than production rates, are influencing the build-up. Reactions removing hydrogen radicals are also indicated by the approximately 40 percent decrease in hydrogen radicals in samples stored for 20 hours at 77°K.

A similar 1.5 percent membrane in aqueous solution sample and an aqueous control were given a gamma dose of 0.875 Mrads at room temperature. After freezing at 77°K, the ESR spectra were observed to be practically identical. The number of radicals observed in the membrane sample was about ten percent less than in the control. Although this difference was the same magnitude as the expected error, there was a slight suggestion of possible radical scavenging by the membrane.

In order to prepare a sample which was intermediate in dryness between the lyophilized and normally wet states, water was added to some lyophilized membrane material until the sample consisted of 48 percent by mass of membrane material. This sample after freezing at 77°K was irradiated with gamma rays. The build-up of free radicals and hydrogen radicals was linear (Figure 33). The G-value for free radical build-up was about 0.7, about twice that for the wet sample, but about 0.2 of that for the dry membrane. This result is for the total sample material, membranes plus water, since there was no control sample with which to judge

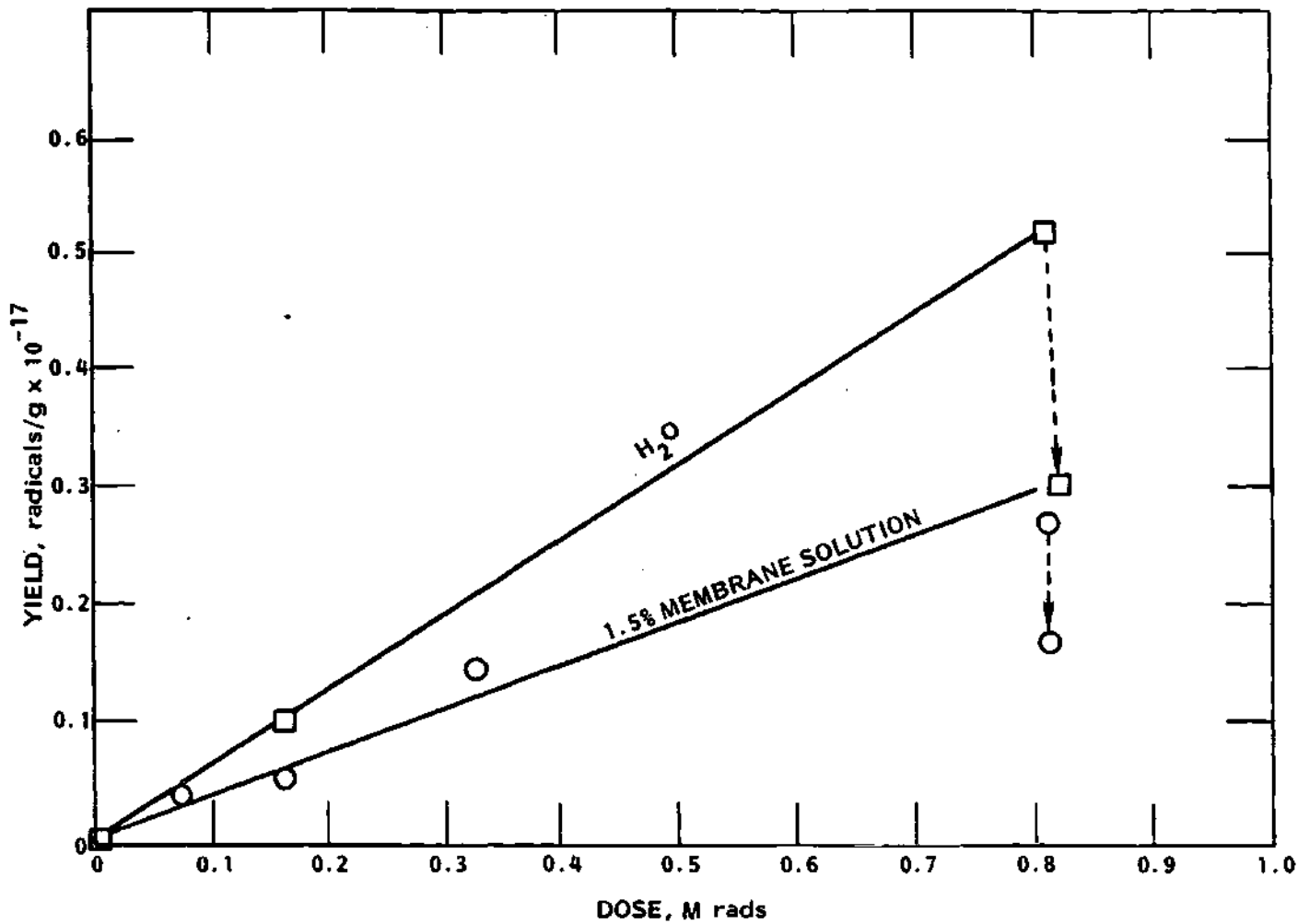


Figure 32. Build-up of Hydrogen Radicals at 77°K in Gamma Irradiated 1.5% Membrane Solution, LM Sample, and in Water, HS Sample

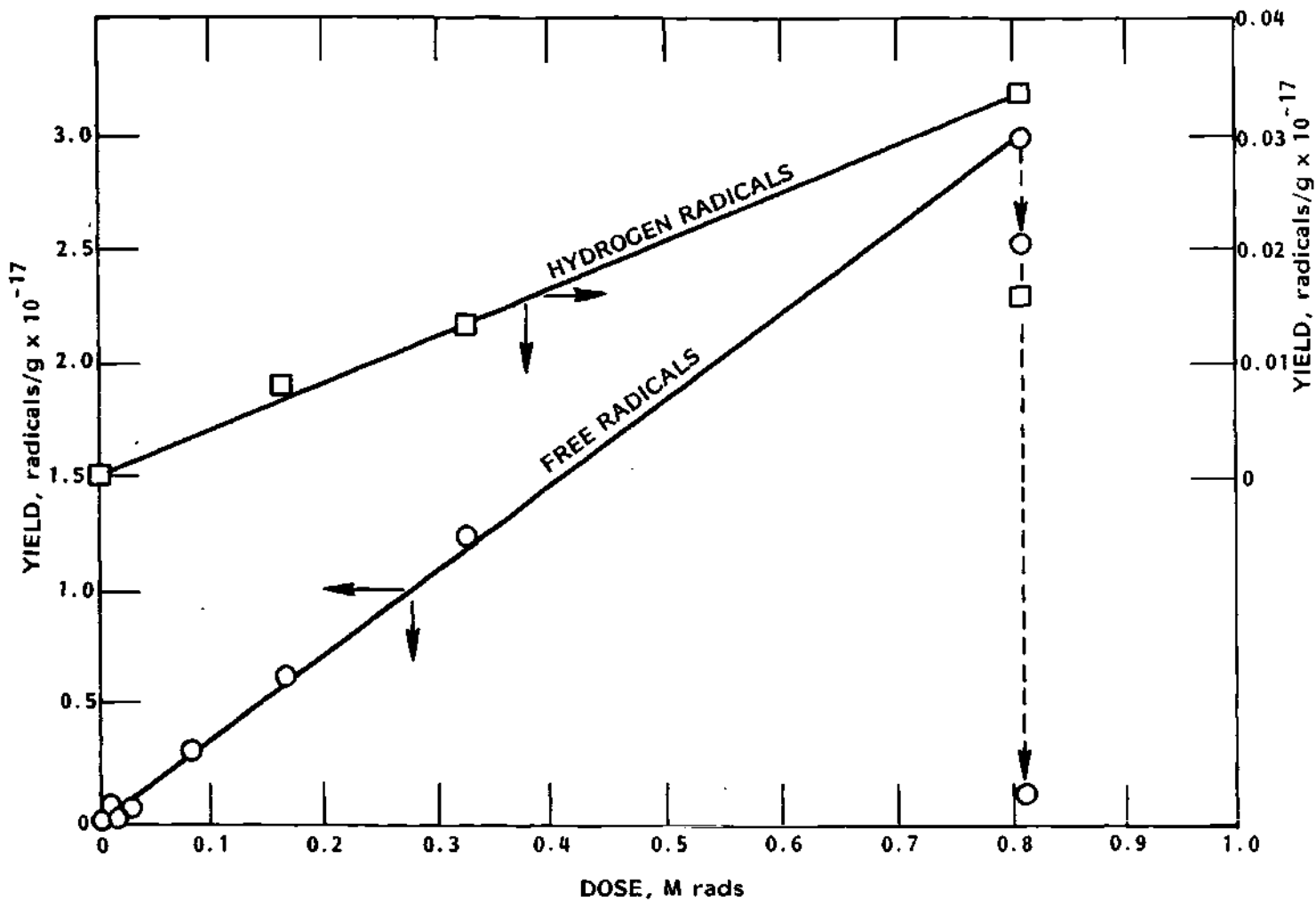


Figure 33. Build-up of Radicals at 77°K in Gamma Irradiated 48% Membrane in Aqueous Solution, 50-50 Sample

the effect on the individual components. However, if the assumptions discussed previously are made, then the G-value partition equation can be used. From this equation a G-value for the membrane component of 0.9 was derived. In case of ten percent error in the source terms, the resulting range of G-values is from 0.75 to 1.05. At 77°K free radicals decayed about 26 percent and hydrogen radicals decayed 53 percent in a day. Allowing the sample to reach room temperature reduced the free radical concentration by a factor of about 20.

Hydrogen radical production and trapping in the membrane samples at 77°K by gamma radiation was observed to be very low, being about 0.001 to 0.006 radicals/100 eV. No hydrogen radicals were observed in membranes exposed to high LET radiation.

The samples exposed to high LET radiation were placed in a neutron beam containing a gamma component. The dose rate from this beam was less than one percent of that of the high LET alpha and fission product particles. The build-up of radicals in freeze dried samples exposed to only the neutron and gamma field is shown in Figure 34 for room temperature exposures and in Figure 35 for exposures at 77°K. The radical build-up at 77°K occurs linearly with an estimated G-value of 1.5. This value was determined using the total dose, neutron plus gamma. It is probable that the gamma radiation is responsible for most of the radical build-up, since the G-value for neutron radiation is expected to be lower than that for gamma radiation. The G-value for neutrons may be calculated from the equation

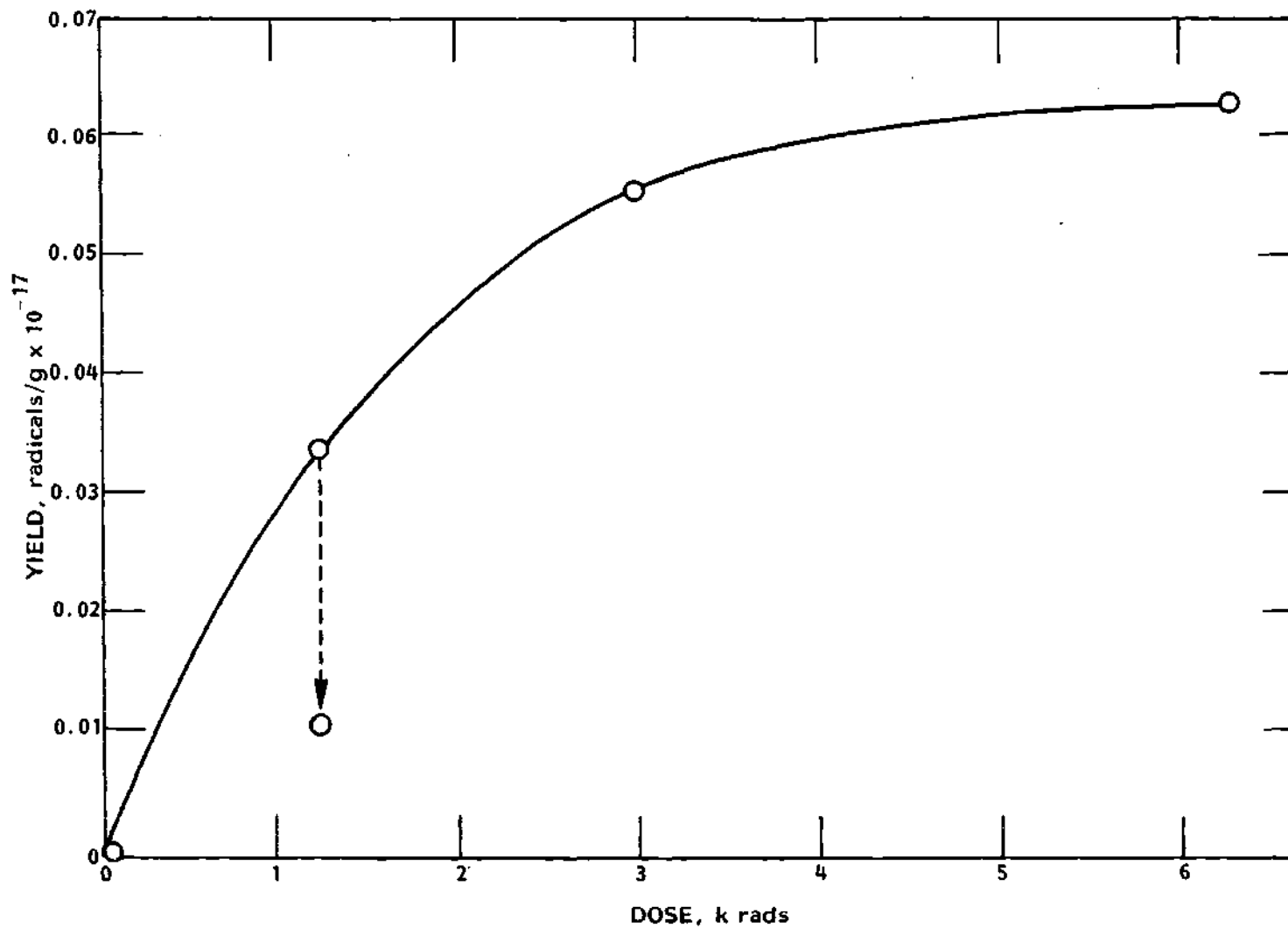


Figure 34. Build-up of Free Radicals at Room Temperature in $n+\gamma$ Irradiated Lyophilized Membranes, N-1 Sample

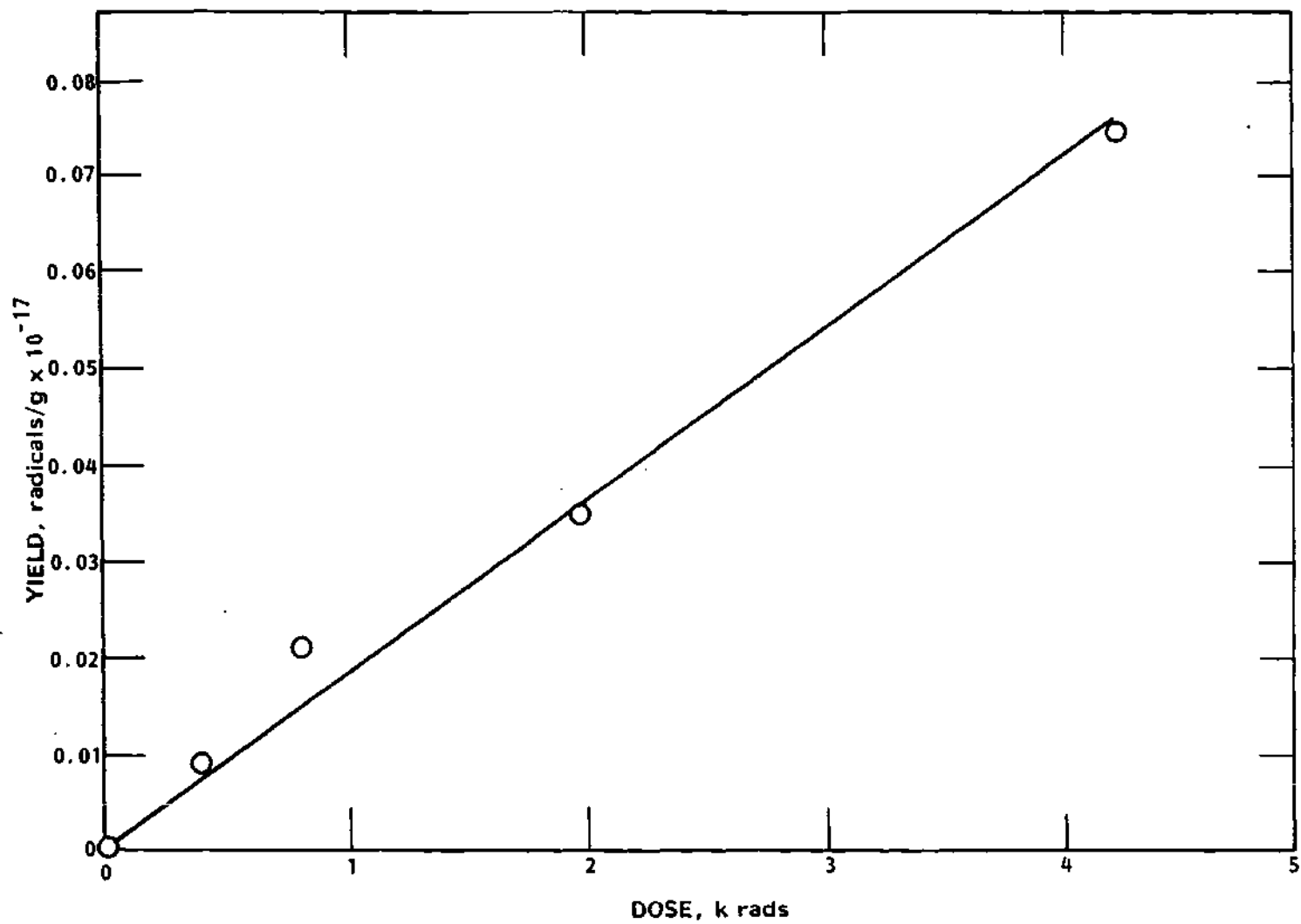


Figure 35. Build-up of Free Radicals at 77°K in n+ γ Irradiated Membranes, N-2 Sample

$$Y = G_n E_n + G_\gamma E_\gamma$$

where G_n and G_γ are G-values for neutrons and gamma rays

E_n and E_γ are the radiologically deposited energies for neutrons and gamma rays, and

Y is the total yield of radicals.

This equation results from assuming that the production of radicals by neutrons and gamma rays are independent of each other, that no synergism occurs, and that the build-up is linear in the range considered. Using this equation the G-value for neutron irradiation of lyophilized membranes at 77°K ranges from 0 to 0.9 with an average of 0.4. It is apparent then that most of the radicals are produced by the gamma component. In addition, at 77°K, the radicals generated in the sample tube accounted for 40 percent of the total. This introduced some inaccuracy after making this correction. At room temperature the radicals generated in the sample tube were very low and were easily taken into account without introducing additional error.

At 77°K free radical signal build-up occurred over a 90 G range. From the 2000 G scan, the ESR signal originally present was observed to decrease by 38 percent upon irradiation to about 4.2 krads neutron dose. This signal did not change on storage for a similar period of time before irradiation. No significant change in free radical concentration was observed upon storage for 5.6 days at 77°K after irradiation. Upon warming to room temperature the free radical concentration decreased by about a factor of two.

The irradiation of the samples exposed to high LET radiation occurred over a period of three days. This was necessitated by the work load involved. Some samples such as the one irradiated with neutrons and gamma rays at 77°K showed negligible decay upon storage overnight. Others such as the one irradiated with neutrons and gamma rays at room temperature showed a large decay on overnight storage (Figure 34). The decay is indicated by the arrow at 1.15 krads in Figure 34. This decay upon irradiation may be responsible for the highly non-linear build-up curve. Since there is doubt as to the nature of this curve and since the effect from the gamma component may be a large contributor to the total effect, the apparent G-values for this curve have unknown significance. If one were to calculate a G-value for this curve using the total neutron plus gamma dose then the initial G-value would be 2.4. If a straight line is fitted to all the data, then the G-value would be 0.83 (Table 7). Although only limited conclusions can be drawn from these samples due to the low doses available and to the large gamma dose fraction, these samples were useful in providing a control background for the alpha and fission product irradiated samples.

The lyophilized sample exposed to alpha radiation at room temperature exhibited radical saturation (Figure 36). The half-value dose was about one megarad (Table 6). The initial build-up gave a G-value of 0.6 while that determined from the fitted build-up curve was 0.8. This difference is attributable to the relatively poor fit between the curve and the data in the intermediate dose region between 0.1 and 0.5 Mrads. The total energy deposited by the alpha particle and ${}^7\text{Li}$ ion have been used

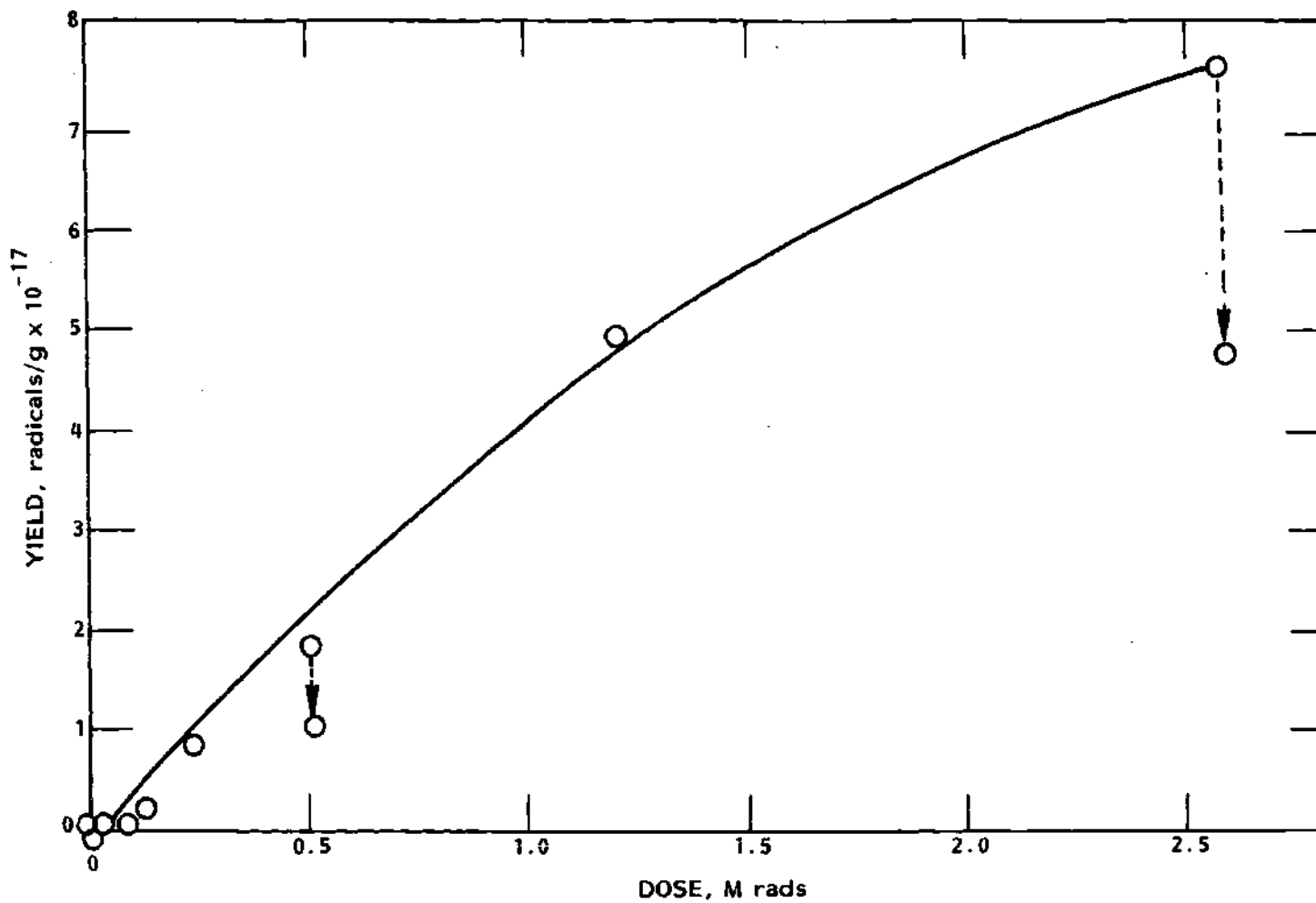


Figure 36. Build-up of Free Radicals at Room Temperature in Alpha Irradiated Lyophilized Membranes, A-1 Sample

in calculating these values. These values will be correct in the case that the Li ion is just as efficient in producing radicals as the alpha particle. If the Li ion produces no radicals, then the G-values would be 60 percent larger than those presented here and in Table 7. This applies to the sample irradiated at 77°K also. The decrease in radicals over a period of one day is seen to be 42 percent and over a period of 6.5 days, also 42 percent. This tends to indicate that there are two groups of radicals with very different lifetimes, although other explanations such as those given below are also possible.

Samples exposed to alpha radiation at 77°K produced a linear build-up curve (Figure 37). The associated G-value was 0.88. Not all reactions were completely stopped at 77°K. For example a 27 percent decrease occurred in one day and a six percent decrease occurred over 5.6 days. These two changes were observed after about 0.35 Mrads and 1.8 Mrads respectively. The absolute change in radicals was about the same in both cases. This tends to indicate that a radical species with a short lifetime is built up to equilibrium with relative small doses. The general increase is then due to a radical with a longer lifetime that has not reached an equilibrium concentration at the doses given. The relative amounts of each radical in the population are then changing with dose. After annealing the sample at room temperature the population of radicals decreased to 16 percent of its former level.

The build-up of radicals in the sample irradiated with fission products at room temperature (Figure 38) was not apparent until doses greater than 0.5 Mrad had been delivered. From the subsequent build-up

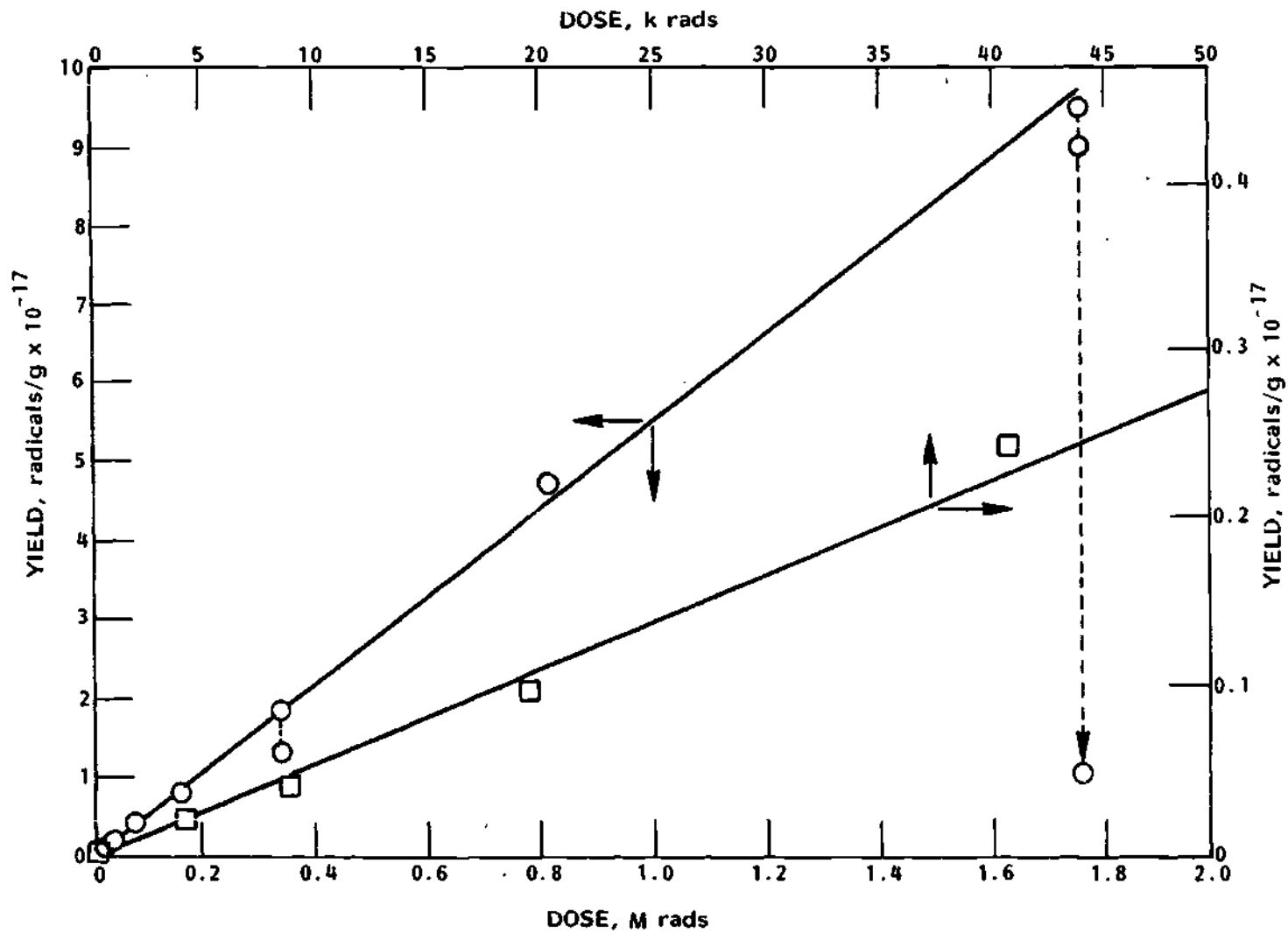


Figure 37. Build-up of Free Radicals at 77°K in Alpha Irradiated Lyophilized Membranes, A-2 Sample

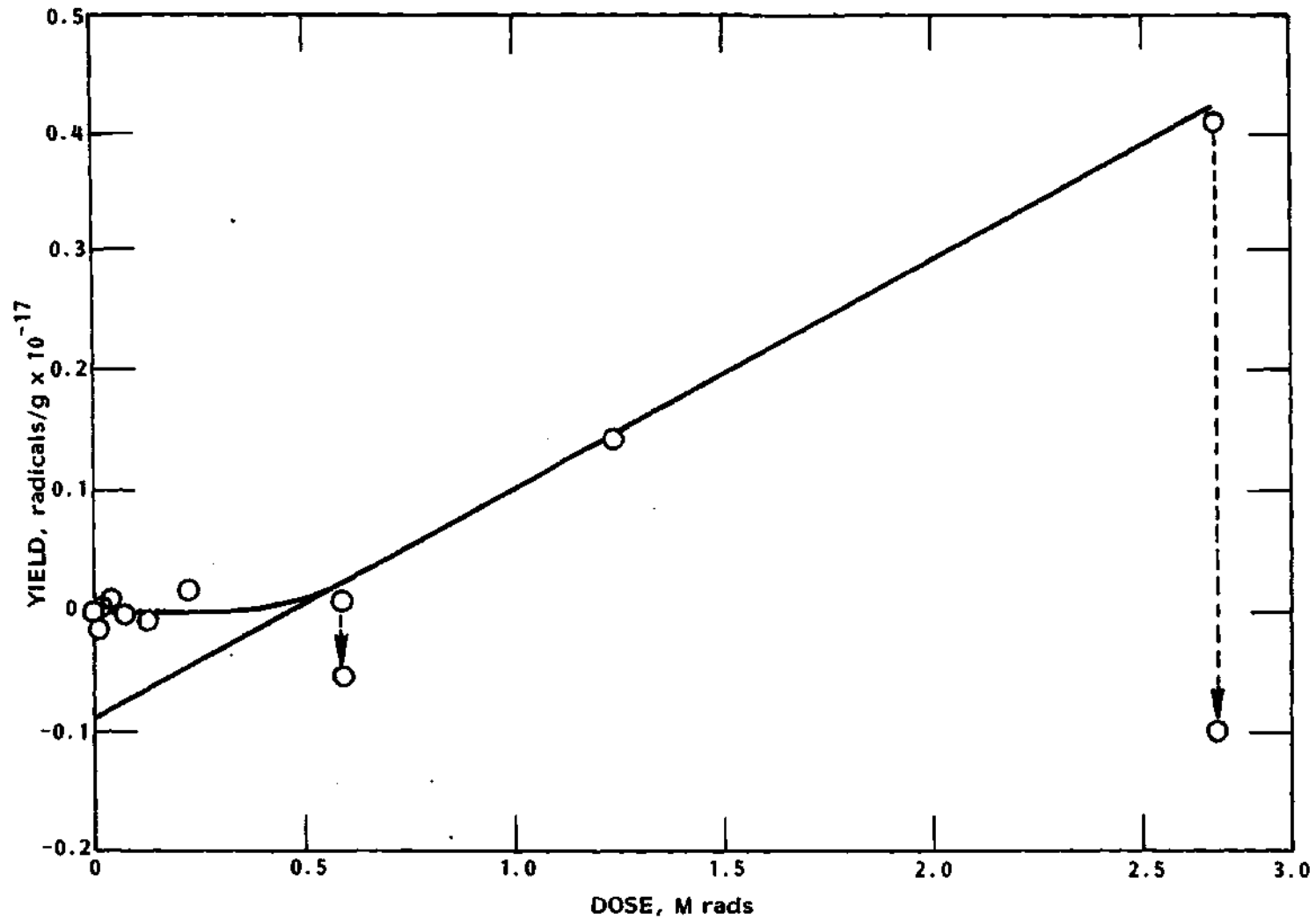


Figure 38. Build-up of Free Radicals at Room Temperature in Fission Product Irradiated Lyophilized Membranes, F-1 Sample

which occurred linearly with a G-value of 0.03, it should have been possible to observe this linear build-up at much lower doses. Apparently this did not occur. One explanation for the observed low dose response is that the observed radicals are being created following second or higher-order kinetics. This type of kinetics can originate because the observed radical is produced in a chain of chemical reactions or because the observed radical is produced in a chain of chemical reactions or because the radical is produced after a sequence of changes, each change caused by the radiation. Another possible reason for the peculiar response could be that radicals initially present were being destroyed either by the radiation or by other radiation-produced species resulting in little net production. A third explanation is that relatively fast reactions were occurring which eliminated the small number of radicals generated at low doses before they were detected by ESR. This last assertion is supported by the decay of radicals on storage at room temperature after doses of 0.5 and 2.7 Mrads. The second assertion is also supported by these decays since both decays ended with less radicals than were present initially. It seems likely then that radicals were being destroyed as a result of irradiation and that radical reactions were occurring at room temperature.

In contrast to the above observations at room temperature, fission-product irradiation at 77°K produced a linear build-up of radicals (Figure 39). No radical saturation was apparent, and the G-value was 0.43. Storage of the sample at 77°K for 5.6 days produced a three percent increase in radical concentration. Since this is within experimental

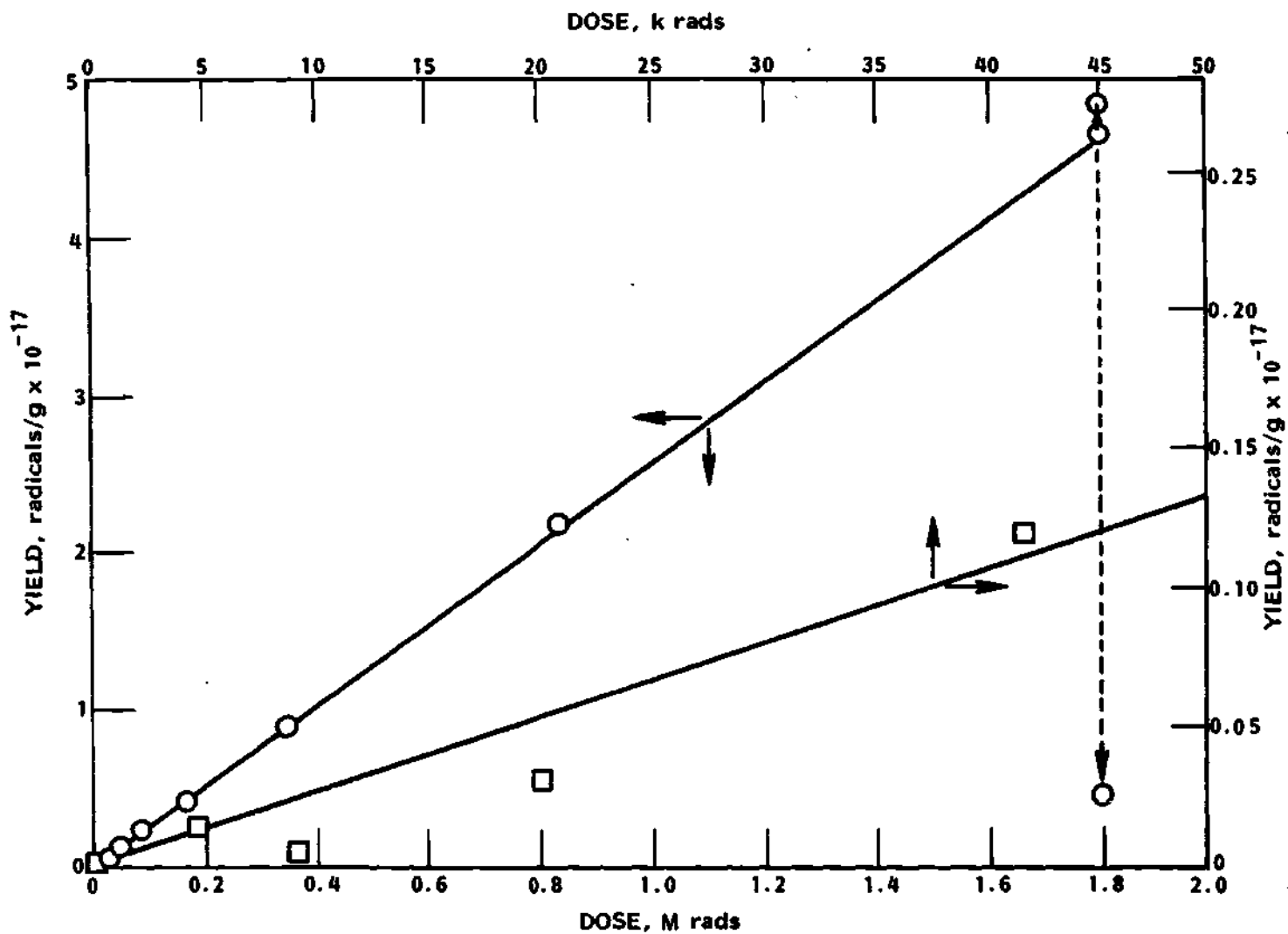


Figure 39. Build-up of Free Radicals at 77°K in Fission Product Irradiated Lyophilized Membranes, F-2 Sample

error, it is concluded that no change in radical concentration occurred. Upon annealing the sample at room temperature the radical concentration decreased by an order of magnitude.

CHAPTER VIII

CONCLUSIONS AND RECOMMENDATIONS

Conclusions

Biomembranes consisting of the plasma membrane or cell wall of erythrocytes were separated from human blood and lyophilized. This dry mass was irradiated under anoxic conditions with gamma rays, thermal neutrons, alpha particles, and recoil fission products. The subsequent build-up of free radicals at room temperature and at 77°K was observed by electron spin resonance spectroscopy. The observed build-up was not only a function of the production rate but also of the lifetime of the radical and of the trapping ability of the matrix.

Although lyophilized membrane preparations exhibited very broad ESR resonances extending over hundreds of Gauss, free radical signals near $g = 2$ were not detected in unirradiated samples. On irradiation the ESR spectrum was usually characterized by a few rather broad resonances within 100 Gauss of the free electron g -value of 2.0. The gamma irradiated sample exhibited a double peak near $g = 2$ at room temperature. At 77°K at least two peaks were apparent. One located at $g = 2.004$ was characteristic of many free radicals. The other, widely separated from the free electron g -value, occurred at $g = 2.015$ and was due to a strong interaction of the electron with the electronic and magnetic fields of the radical in which it was located. Common species which can produce

such shifts are oxygen, nitrogen, and sulfur. The principal g-value of the sulfur radical anion is 2.01, very close to that observed. This latter peak disappeared on warming to room temperature.

In x-irradiated proteins, the ESR spectrum is usually, but not exclusively, characterized by one of two types of spectra (Gordy, 1959). One type is a doublet with a splitting of 12 G, symmetrically situated about the free electron g-value. A spectrum similar to this was observed for the freeze dried membrane sample irradiated under vacuum with gamma rays at room temperature. The origin of this resonance is thought to be either due to protons associated with hydrogen bonds of the polypeptide chain or from unpaired electrons localized near a proton in a site along the protein back-bone. The other major type of spectrum from proteins is suggested to originate from sulfur radicals. This spectrum is broad and lacks detail and therefore is particularly difficult to associate with an observed spectrum especially when other interferences are present.

The alpha and fission product irradiated samples produced distinct spectra. The resonances produced at 77°K were broader than those produced at room temperature. Although this effect could be due to temperature as well as the kind of radical produced, the spectra produced upon warming was broadened to an even greater extent. The broadening illustrates that radical reactions occurring under room temperature irradiation may not be like those occurring on warming the sample after irradiation at 77°K.

In addition to the dry samples, membrane samples containing water were exposed to gamma rays. The spectra of samples so exposed exhibited

larger g-value shifts than the dry samples. More detail was resolvable in these spectra also. Hydrogen radicals, identifiable by a doublet with 507 G splitting, were most apparent in samples containing water. Hydrogen radicals were also observed at 77°K in dry samples exposed to gamma radiation. Radiation of higher LET produced no detectable hydrogen radicals in the membrane samples although such radiation was capable of producing hydrogen radicals in some organic glasses.

The build-up of radicals in the membrane samples was observed to occur linearly or to obey first order kinetics. At 77°K the build-up was linear for both low and high LET radiation in all cases except one. This exception was the lyophilized membrane exposed to gamma radiation in which the half-value dose was determined to be about 0.2 Mrad. Sample preparation can also affect the yield curve since at room temperature the oven-dried membrane sample exhibited radical saturation while the lyophilized sample did not. Of the samples exposed to high LET radiation, only the one irradiated with alpha particles at room temperature showed radical saturation effects.

In several cases extrapolation of the build-up curve, which fitted the high dose data very well, to lower doses resulted in inappropriate approximations in this region. A change of slope of the build-up curve below 20 krads was observed for the lyophilized membranes exposed to gamma radiation at both room temperature and 77°K. For fission product irradiation the radical concentration remained constant up to 0.5 Mrad. The cause of these low dose effects might be due to (1) radical decay during the irradiation and analysis period, or (2) a change of the

characteristics of the sample brought on by the radiation, or (3) destruction of pre-existing and created radicals caused by the radiation, or (4) second order kinetics associated with a chain of radical and radiation reactions.

From the linear portion of the build-up curve an estimate of the G-value was obtained. The G-value so determined is not only a measure of the production rate by the radiation but also of the trapping ability of the matrix. Thus the true G-value for the production rate will be equal to or greater than the effective G-value determined from the build-up curve. The G-value for total radicals produced by gamma radiation at room temperature was about five radicals/100 eV. For high LET radiation the G-value was 0.6 for alpha radiation and for fission product radiation it was 0.03. At 77°K the G-value was within 50 percent of that at room temperature for gamma and alpha radiation. However, for fission product radiation the G-value was over an order of magnitude greater at 77°K. The G-values for the samples containing water were less than for the dry samples by about an order of magnitude. Since this is for the membrane containing water, the G-value for the membrane component, if such an independent component exists, may well be of a larger magnitude.

In all the samples exposed to gamma radiation at 77°K, hydrogen radicals were detectable. In general the G-values for hydrogen radicals of from 0.001 to 0.006 were two to three orders of magnitude less than that for other free radicals. This may not entirely reflect a low production rate for hydrogen radicals. It has been indicated that trapping ability of the matrix will determine the number of such radicals subse-

quently observed at times on the order of tens of minutes after irradiation. Free radicals and hydrogen radicals in particular can participate in chemical reactions, even at 77°K, as indicated by the observed decay over a period of hours and days. Similarly there may be much faster reactions which have previously gone to completion by the time the ESR spectrum is recorded. If such reactions exist, then the apparent G-value observed will be lower than the true instantaneous one.

Of nine different amino acids irradiated with X-rays in vacuum at room temperature, six produced G-values of 3 to 7 and three ranged from 0.06 to 1.0 (Zimmer and Müller, 1965). G-values for six proteins ranged from 2 to 7 (Zimmer and Müller, 1965). The results for membranes, one component of which is protein, fall in this range. Irradiation of amino acids with alpha particles produced G-values of 0.1 to 0.4 times that for gamma radiation unless the amino acids contained aromatic rings. In this case the yields were about equal for high and low LET radiation. For the membrane sample the G-value for alpha radiation was 12 percent of that for gamma radiation.

The yield of free radicals in membranes is quite high, often exhibiting G-values greater than one radical per 100 eV absorbed energy. This supports the theory that free radicals are an important species in the chains of reactions leading to radiobiological effects. Radical yield and trapping decreased as the LET of the radiation increased. The ESR spectra at 77°K and room temperature were different indicating that the radicals initially formed are not the ones subsequently observed at room temperature.

In order to stabilize the free radicals generated by ionizing radiation at room temperature, dry membrane samples were used. Since these samples were opaque and since it was desirable to exclude oxygen, the ESR method was the method of choice. This method is also non-destructive permitting a sequence of exposures and analyses to be made on a particular sample. The sensitivity of the method required that doses in the krad range be used. An increase of sensitivity would have permitted determinations at lower doses. Working in this range may be particularly useful since biological effects can occur there and since some peculiar build-up patterns were observed in the low dose region. Greater sensitivity can be achieved by using longer ESR scan times. However, one must then contend with radical reactions during this longer time. Although the relative accuracy of data obtained is estimated to be 10 percent, the absolute precision may be about 30 percent which is the state-of-the-art for similar systems and samples.

Determination of free radicals generated in vivo is an ideal objective. However the low concentration of membranes in vivo, the rapid disappearance of radicals in aqueous solution, the contribution of radicals in the aqueous phase, and the reduced sensitivity of the ESR method for aqueous samples forces one to consider non-ideal systems such as dry material. Lyophilized material was considered the material of choice since the freeze-drying procedure produced a membrane material with a lower number of radicals than did the drying at 80°C.

Free radicals were found for all types of irradiation. Production of G-value varied inversely as the LET of the radiation. Moisture also had a negative effect on the production and trapping of radicals. Low

temperature enhanced trapping somewhat, and more so in some cases than others. However the effect is perhaps more related to the rapidity of reactions occurring at the higher temperature. For example, the apparently much greater trapping of fission product produced radicals at 77°K than at 295°K when compared to the same values for alpha radiation, may be due to the greater reaction rate of fission product produced radicals than of alpha produced radicals at 295°K. Hydrogen radicals in membranes were observed only for gamma radiation exposures and then with very low G-values. Hydrogen radicals were most apparent in wet samples.

It is apparent that free radicals are generated in membrane material in sufficient quantity to be possible agents in causing biological effects. The G-value for membranes is the same order as the G-values of many other cellular constituents such as DNA or amino acids. Of the biological materials that have been examined, the results for membranes are most nearly like those for protein.

Recommendations

In order to understand how damage to biological structures is produced, one must not only determine the yield of radicals but also determine the location of the radical in biomolecules or components. Thus it would be desirable to determine the effect of radiation on the protein and lipid portions of these components individually, in a mechanical mixture, and in seminatural configuration as was done here. Additionally, labeling specific molecules in the membrane with deuterium, carbon-13, or nitrogen-15 may provide information by way of the ESR spectrum as to which atoms are associated with the free radical.

Since organic single crystals are capable of supplying much more information than polycrystalline materials, it is highly desirable to use single crystals. Radical identification is more likely from single crystal studies. Although membranes do not ordinarily exist as single crystals, they do have a regular structure. Organizing the sheets of membrane into a repeating structure held together in a matrix of urea as was partially successfully done with DNA might be worthwhile. This might be more easily done with synthetic membranes than natural biomembranes. Additionally synthetic membranes whose composition and structure are known and could be varied at will would be desirable experimental materials.

Since some of the radicals studied were saturated even at 0.5 mW, it would be desirable to study these species in the microwatt range. Additionally, ESR spectral changes in this region would be informative. ENDOR, electron-nuclear double resonance, should also be applied. Measurement at K-band in addition to X-band would enable hyperfine splitting to be distinguished from multi-radical spectral lines.

Examination of the free radicals as the temperature is raised in a precisely controlled manner might prove informative. Pulse radiolysis or irradiation of the samples while they are in the spectrometer cavity could be very useful. Fast reactions could be studied in this manner. The decay of radicals, rather than the build-up of radicals should also be studied. Dose rate may affect the type of radical observed as well as the yield. There were indications in these experiments that radical decay or sample rearrangement by the radiation caused some low dose anomalies. The low dose region holds considerable interest although it

would be one of the most demanding in terms of time and technique in which to work. The effect of radioprotectors and radiosensitizers on the membrane would be of interest. Some of the chemical effects are already known and the extension to include free radical effects would probably be warranted.

Some of the most important effects of radiation perhaps occur in the aqueous state. To date there are no good solutions to the problem of radical build-up in the liquid state. ESR spectrometer sensitivity is limited for aqueous samples. Some biostructures such as membranes occupy a small fraction of the total aqueous mass in the natural state. This makes radical determination difficult. Irradiation of dry material with chemical species normally produced in water by radiation, such as low energy hydrogen ions, is a partial solution to the problem that could be used with membrane samples also.

Finally, the relationship of the radicals produced to biological damage must be considered. Comparison of membrane characteristics such as membrane integrity, ability to retain simple ions, or ability to participate in cellular metabolism, with the physically measured free radicals and chemical changes will sometimes be necessary. There seems to be no scarcity of possible experiments. However some questions that need resolving are unanswered because of our limited ability to effectively carry out experiments at the molecular and macromolecular level with small numbers of molecules in biological systems.

APPENDIX I

FREE RADICAL BUILD-UP

In Table 8 are yields for the free radicals generated by ionizing radiation as a function of dose. The sample identification may be correlated with the sample characteristics and type of radiation exposure by consulting Table 1. In the sample identification are the symbols RT and LN designating room temperature or liquid nitrogen temperature. The H' in the sample designation indicates that the concentration values refer to hydrogen radical concentrations. The radical concentrations are given above the background or pre-existing number present. The initial number of radicals is indicated by the additional concentration values at zero dose. Negative net concentration values are due to errors of measurement at low concentrations or are attributable to destruction of some of the pre-existing radicals. The time given in the dose column represents time elapsed from the previous measurement.

Table 8. Free Radicals Generated by Ionizing Radiation

HDM RT		FDM RT		FDM LN	
Dose	Radicals/g	Dose	Radicals/g	Dose	Radicals/g
0	0 + 37.8 E17	0	0 + 1.6 E17	0	0 + 2.0 E17
292	- 0.012 E17	1460	0.0082 E17	544	0.0158 E17
584	- 0.138 E17	2920	0.0766 E17	1360	0.0241 E17
1460	- 0.078 E17	5840	0.180 E17	2720	0.0559 E17
2920	0.030 E17	5840 + 1 day	0.147 E17	5440	0.0985 E17
5840	0.005 E17	14,600	0.221 E17	13,600	0.177 E17
24,600	0.434 E17	35,000	0.428 E17	32,640	0.311 E17
35,000	1.07 E17	87,500	0.884 E17	81,600	0.583 E17
87,500	2.36 E17	175,000	1.55 E17	163,200	1.14 E17
175,000	4.35 E17	350,000	3.09 E17	326,400	1.70 E17
350,000	7.86 E17	875,000	7.59 E17	816,000	2.33 E17
875,000	16.2 E17	875,000 + 1 day	3.97 E17	816,000 after RT	0.671 E17

LM LN		HS LN		LM LN H*	
0	0 + .50 E17	0	0	0	0
544	0.000793 E17	544	0.000759 E17	81,600	0.0393 E17
1360	0.00237 E17	5440	0.00970 E17	163,200	0.0593 E17
2720	0.00504 E17	32,640	0.0619 E17	163,200 + 1 day	0.0507 E17
5440	0.0131 E17	163,200	0.257 E17	326,400	0.144 E17
27,760	0.0867 E17	163,200 + 1 day	0.257 E17	816,000	0.266 E17
32,640	0.0985 E17	816,000	1.47 E17	816,000 + 20 hr	0.170 E17
81,600	0.195 E17	816,000 + 20 hr	1.25 E17		
163,200	0.325 E17	816,000 + 6 days	0.0216 E17		
163,200 + 1 day	0.269 E17				
326,400	0.621 E17				
816,000	1.61 E17				
816,000 + 20 hr	1.29 E17				
816,000 + 6 days	0.0748 E17				

HS LN H*	
0	0
163,200	0.100 E17
816,000	0.519 E17
816,000 + 20 hr	0.296 E17

Table 8. (Concluded)

N LN		A LN		F LN	
Dose	Radicals/g	Dose	Radicals/g	Dose	Radicals/g
0	0 + 1.6 E17	0	0 + 1.4 E17	0	0 + 1.5 E17
386 + 1 day	0.00903 E17	4445	0.0232 E17	4526	0.0156 E17
808 + 1 day	0.0211 E17	8891	0.0419 E17	9052	0.0056 E17
1955	0.0348 E17	19,580	0.0985 E17	19,936	0.0311 E17
4244	0.0753 E17	40,854 + 1 day	0.241 E17	41,595 + 1 day	0.120 E17
4244 + 5.7 day	0.0719 E17	80,174	0.441 E17	81,628	0.226 E17
4244 after RT	0.0362 E17	160,930	0.844 E17	163,850	0.415 E17
		336,780	1.86 E17	342,892	0.896 E17
		336,780 + 1 day	1.36 E17	342,892 + 1 day	0.896 E17
		814,600	4.19 E17	829,380	2.18 E17
		1,768,600	9.04 E17	1,800,700	4.70 E17
		1,768,600 + 5.7 day	8.52 E17	1,800,700 + 5.7 day	4.85 E17
		1,768,600 after RT	1.37 E17	1,800,700 after RT	0.475 E17

APPENDIX II

COMPUTER PROGRAMS

ESR Spectral Integration

The derivative ESR spectrum was integrated once to obtain the absorption curve. A second integration produced the cumulative absorption. The program for doing this which is written in FOCL/F for operation on a PDP-8/I computer is given below. The X axis representing magnetic field strength has the units of "channels" and along the Y axis is the ESR intensity. Correction is made in this program for spectrometer gain, V, and scan time, T. Drift DR, is the channel by channel increase in the base line. This may be equated to zero and the linear base line routine described below may be used. The start, P1, and end, N1, of integration are input variables. Although integration is stepwise, channel by channel, the teletype print out begins at channel P2, ends at N2, and is printed every R channels from P2 to N2. A linear base line may be used. The X-Y coordinates are X1, Y1, at the left hand side of the derivative spectrum and XN, YN at the right hand side. Theoretically any base line will suffice, as adjustment will be made in a subsequent program. Practically, it is numerically advantageous to choose a base line as close to the true one as possible.

A graphical X-Y plotter was available and a plot of the absorption curve was obtained. The input for this plot routine is the minimum

absorption, L, and the range, S, which is the desired full scale height of the graph. These values may simply be the ones printed out by the program or conveniently chosen values near to these values. However, one may invert the absorption spectrum by making the minimum absorption the maximum absorption printed out and making the scale the negative of the Max-Min range. After completion of the program, one may initiate another run by manually entering a go to line 1.1 command. The spectral integration program follows.

```

01.02 V L,410
01.04 V K;V 0,AB,1
01.06 J (FX(2,FX(10,6071))) ;BR 1.06;I (FDIS(A',B'))
01.07 T "ADJUST PLOTTER",!
01.08 L F0=1.06
01.09 D 5
01.10 T "ESR SPECTRAL INTEGRATION"!!
01.11 A "NO. CHANNELS=",M
01.12 A "DRIFT=",DR
01.14 A "GAJN=",V,"SCN T=",T,!
01.16 A "ABS CH:!" "START=",P1,"END=",N1,!
01.18 A "OUTPUT CH:!" "START=",P2,"END=",N2,"STEP=",R,!
01.20 S TV=1/T#V

02.10 T "BASE LINE SRT"!
02.20 A "INITIAL X,Y="!,X1,Y1,! "FINAL X,Y="!,XN,YN,!
02.30 S A=(YN-Y1)/(XN-X1);S B=(Y1*XN-YN*X1)/(XN-X1)
02.40 T Z,"          A=",A," B=",B,!
02.60 S A=A*TV;S B=B*TV;S DR=DR*TV
02.80 T #NORM LI ED; A=",A," B=",B,!!!
02.90 L I,R

03.90 G 10.1

04.10 SET NU=0; DO 4.15; DO 4.15; DO 4.15
04.15 SET Z=FX(3,127,F#N( ));S X=FX(3,Z,15)
04.20 IF (Z-FX(10,177)) 4.30, 4.15
04.30 IF (X-11) 4.40; RETURN
04.40 SET NU=NU*10+X; GOTO 4.15

05.10 F I=1,200;S Z=F0(1023,1023)
05.20 F I=1,200;S Z=F0(0,0)

```

```

10.10 T "ABS, CUM ABS"!!
10.20 T "8.04," CHANNEL DERIV ABS CUM ABS"!!
10.30 S Y=A*P1+B+UR;S I=P1;S J=P2

11.10 F Q=1,P1+1;D 4
11.20 S D1=NU*TV;S E1=D1-Y;S G1=.5*E1
11.30 S L=E1;S H=E1;S AB(I)=E1

12.10 I (I-N2)12.4,12.5,15.1
12.40 I (I-J)15.1,12.5,12.42
12.42 S J=J+R;I (I-J)15.1,12.5,12.42
12.50 T I,D1,E1,G1,I
12.60 S J=J+R

15.10 S Y=Y+A;S I=I+1
15.12 I (I-N1)15.2,15.2,20.1
15.20 D 4
15.21 I (NU-10000) 15.22,15.22,15.24
15.22 S D2=NU*TV
15.24 S E2=E1+D2-Y
15.26 S G2=G1+.5*(E2+E1)
15.28 S D1=D2;S E1=E2;S G1=G2
15.40 S L=.5*(L+E1-FABS(L-E1))
17.42 S H=.5*(H+E1+FABS(H-E1))
15.44 S AB(I)=E1;G 12.1

20.10 T I,"MAX ABS=",H,I
20.20 T "MIN ABS=",L,I
20.30 S DY=H-L
20.40 T "MAX - MJN =",DY,!!

21.10 T "PLOT READY",I
21.15 A "MIN ABS",L
21.20 A "MAX - MJN SCALE ",S,I
21.30 S S=1023/S
21.40 A "CH START",P3," END",N3,I
21.50 F I=P3,N3;D 22

22.10 S Z=F0(I+2.5639,(AB(I)-L)*S)

23.10 T "END"
#

```

Base Line Correction Program

After integration of the ESR derivative spectrum to obtain an absorption spectrum, it is possible to change the linear base line into another linear one without using the integration program with the new base line by applying the following program. Additionally the area under the absorption curve between any two values of the magnetic field can be obtained. In this program, sample identification is S. X1 and X2 are the two values of the magnetic field, in channels, that delimit the area desired. The ones refer to the left hand coordinates and the twos refer to the right hand ones. Y is the value of the absorption curve or the value through which the base line will pass. A is the cumulative area under the absorption curve. M is a slope in the absorption curve graph. M may be taken as the slope of the absorption curve provided the absorption curve is following the desired base line. The program determines the new area, called "Area True," under the absorption curve with the new base line in five ways. These are: (1) a linear base line in the absorption graph passing through Y1 and Y2 in the absorption graph, (2) a quadratic base line passing through Y1 and Y2 and having a slope of M1 at X1 in the absorption graph, (3) a quadratic base line passing through Y1 and Y2 and having a slope of M2 at X2 in the absorption graph, (4) a quadratic base line through Y1 and Y2 and fitting by least squares the slopes M1 and M2, (5) a quadratic base line passing through Y1 and Y2 and fitting by least squares the slopes M1 and M2 subject to the difference between the slope M1 and the slope of the base line at X1 must be equal to or greater than zero and subject to the difference between the slope M2

and the base line must be zero or less than zero. Then "Area BL" is the area between the new base line and the old base line. T is M minus the slope of the base line. Care must be used in using this program to make certain the base line does not inadvertently intersect the absorption curve, except possibly at the ends. If the absorption curve falls below the new base line, the integrated area in this region will be negative and correspondingly subtracted from the area. Negative areas are handled correctly mathematically and need not be considered separately. That is, the original base line can be above the absorption curve. Only the final base line, when it is desired to have the absorption curve entirely above the base line, must be placed with care. The program for making these base line corrections follows.

```

01.20 C A=AREA, M=CURVE SLOPE IN BL-1, N=DESIRED SLOPE
01.22 C IN :IL-2, T=ACTUAL SLOPE IN BL-2.
01.24 C GROUP 2 IS INPUT, 5 IS PROGRAM STRUCTURE, AND 9 IS PRINT OUT.
01.26 C GROUP 12 IS LINEAR BASE LINE) 14, 16, 18, AND 19 ARE QUADRATIC
01.28 C WHERE GROUP 14 USES LEFT END SLOPE, 16 USES RIGHT END SLOPE,
01.30 C AND 18 & 19 USE LEAST SQUARES OF SLOPES AT BOTH ENDS.
01.32 C SLOPE IN GROUP 19 IS CONSTRAINED > OR = 0 ON LEFT AND
01.34 C < OR = 0 ON RIGHT.
01.36 C GROUP 20 IS GENERAL QUADRATIC CALCULATION WHERE N IS SLOPE IN BL-1
01.38 C X2 MUST BE GREATER THAN X1.

02.10 A "SAMPLE",S
02.20 A "X1",X1,"X2",X2,
02.30 S DX=X2-X1

```

```

03.20 A "Y1",Y1,"A1",A1,"M1",M1,"Y2",Y2,"A2",A2,"M2",M2,I
05.10 C USE GROUPS 12, 14, 16, 18, AND 19 FOR CALCULATIONS AND 9
05.11 C FOR PRINT OUT.
05.20 D 12;D 9
05.30 D 14;D 9
05.40 D 16;D 9
05.50 D 18;D 9
05.60 D 19;D 9
06.97 C IF X1 AND X2 DO NOT CHANGE, CHANGE STATEMENT 2.1 TO 3.1 AND
05.98 C IN 5.99 DELETE G 2.1 AND WRITE G 3.1
05.99 T !!G 2.1

09.10 S C=Y1-X1*(B+C)*X1
09.20 S T1=M1-2*A*X1-B;S T2=M2-2*A*X2-B
09.30 S BT=((A*X2/3+B/2)*X2+C)*X2-((A*X1/3+B/2)*X1+C)*X1
09.40 S AC=A2-A1-AT
09.50 T 2,"T1=",T1," T2=",T2,I
09.60 T "AREC: BL=",BT," TRUE=",AC,!!

12.10 S N1=0;S N2=0
12.20 T "LINEAR",I
12.30 D 20

14.10 S N1=0;T "N1:",N1,I;S N1=M1-N1
14.20 S A=((Y2-Y1)/DX-N1)/DX
14.30 S B=N1-2*A*X1

16.10 S N2=0;T "N2:",N2,I;S N2=M2-N2
16.20 S A=-((Y2-Y1)/DX-N2)/DX
16.30 S B=N2-2*A*X2

18.10 T "QUAD",I
18.20 S N1=0;S N2=0;T "N1:",N1,I;"N2:",N2,I
18.30 S N1=M1-N1;S N2=M2-N2
18.40 D 20

19.10 T "CONSTRAINED QUAD",I
19.20 S A=.5*(M2-M1)/DX
19.22 S U1=((Y2-Y1)/DX-M1)/DX
19.24 S U2=-((Y2-Y1)/DX-M2)/DX
19.30 I (A-U1) 19.32,19.36,19.36
19.32 S A=U1
19.36 I (A-U2) 19.38,19.4,19.4
19.38 S A=U2
19.40 S B=(Y2-Y1)/DX-A*(X2+X1)

20.10 S A=.5*(N2-N1)/DX
20.20 S B=(Y2-Y1)/DX-A*(X2+X1)
#

```

Power Saturation Program

The power saturation program is a least squares fitting of the equation

$$Y = A \sqrt{\frac{kP}{1 + kP}}$$

where Y is the total ESR absorption

P is the microwave power incident on the cavity

A and k are constants to be determined.

In the program, sample identification is S, N is the number of points to be used, and Y(I) is the value of the measured total ESR absorption at power P(I). N must be at least two. The input should be ordered in terms of increasing power. Least squares determination of A and k are printed out. Also printed are the data at the first and last data points. Appearing are the original input data P and Y. In addition, the unsaturated total ESR absorption, S, is printed as well as the ratio S/Y. The unsaturated absorption is obtained from $S = A \sqrt{kP}$. The power saturation program follows.

```

01.30 T "POWER SATURATION PROGRAM",11
01.40 C GROUP 15 IS S=A*FSQT(K*P/(1+K*P))
01.50 C N GREATER OR EQUAL TO 2; Y(I) NOT EQUAL TO Y(J) FOR AT LEAST
01.60 C ONE I AND J; P(I) GREATER THAN ZERO

02.10 A "SAMPLE",S
02.20 A "N",N
02.30 F I=1,N;T 23.00, "P(",I,") " ;A P(I);T "Y(",I,") " ;A Y(I),I

04.20 D 15
04.30 T !!!!!;G 2.1

15.10 S SY=0;S Y2=0;S YP=0;S YQ=0
15.20 F I=1,N;D 16
15.30 D 19;S A=FSQT(A);D 20;F I=1,N-1,N;D 22

16.10 S T1=Y(I)+2; S SY=SY+T1;S Y2=Y2+T1+2;S T2=T1/P(I)
16.20 S YP=YP+J2;S YQ=YQ+T2*T1

19.10 S D=N*Y2-SY+2
19.20 S K=(SY+YP-N*YQ)/D
19.22 I (K) 19.23,19.24,19.3
19.23 T "K=NEGATIVE, NO SOLUTION",;!D 20.11;S K=0;S A=0;G 19.4
19.24 D 20.11;T "A*FSQT(K)=FINITE=NEW A",;S K=1
19.30 S A=(Y2*YP-SY*YQ)/(D*K)
19.40 R

20.10 T %, "A=",A,1
20.11 T %, "K=",K,!!
20.20 T " P(I) Y(I) S(I) S(I)/Y(I)",I

22.10 S S=A*FSQT(K*P(I));D 25

25.10 T P(I),Y(I),S,S/Y(I),!
#

```

Radical Build-up Program

Either a linear equation or the build-up equation

$$N = N_0(1 - \exp(-GD/N_0))$$

where N is the radical concentration

D is the radiological dose

N_0 and G are constants to be determined

was fitted by least squares to the data on radical build-up with increasing dose. The following program solves both of these problems. In the program the sample identification is A and the number of input points is M . The doses $D(I)$ at which the radical concentration $N(I)$ was measured are input in order of increasing dose. The first K points are used in fitting the linear function. The fitting of the build-up equation by least squares is done in three ways. They are: (1) by linearizing the build-up equation and solving exactly, (2) by least squares using an iterative technique based on Newton's method, and (3) by relative least squares fit using the same technique. In the least squares technique the variance is based on the difference in the radical concentration of the measured value and value from the equation. In the relative least squares the variance is based on this same difference divided by the experimental radical concentration value. Printout includes the basic data and the estimated concentration from the equation. The build-up program follows.

```

01.10 T Z,"FITTING  $N(D)=N_0*(1-EXP(-G*D/N_0))$ ",!!
01.12 C "N(D)=NUMBER OF RADICALS; D=DOSE, N0=N(INFINITY),"
01.14 C "G=RADICAL PRODUCTION RATE, M=NUMBER OF POINTS,"
01.16 C "K=NUMBER OF POINTS TO BE USED IN INITIAL LINEAR REGION,"
01.18 C "LA=G/N0, DER SIGMA2=DERIVATIVE(VARIANCE)/D N0
01.20 C GROUP 1 IS INPUT, 3 IS PROGRAM CONSTRUCTION, 9 IS OUTPUT,
01.22 C 15 IS LINEARISED EXPONENTIAL, 17 IS LEAST SQUARES,
01.24 C 18 IS RELATIVE LEAST SQUARES, 20 IS NEW APPROXIMATION,
01.26 C AND 25 IS BASIC LEAST SQUARES ARITHMETIC
01.28 C BUILD UP, B=INTERCEPT
01.30 L F0=25
01.32 S Z=0
01.40 A "SAMPLE #",A
01.50 A "NUMBER OF POINTS: ",I,"M ",M
01.52 F I=1,M;A "#D",D(I)
01.53 T Z,!!
01.54 F I=1,M;A "N",N(I)
01.55 T !!!

03.01 A "K ",K
03.02 I(K) 3.06,3.06,3.04
03.04 T "INITIAL LINEAR BUILD UP:",!;D 11
03.06 A "G",G,"B ",B
03.10 D 15;I "LINEAR: ",!,"N0=",N0,!,"LA=",LA,!,"D1/2=",D1,!,"B=",B,!!
03.20 T "LEAST SQUARES",!
03.30 T 16,"N0",:18,"LA",:31,"HALF D",:46,"NEW N0",:59,"DER SIGMA2",!!
03.40 S S=0;S N3=0;S N1=N0
03.42 F J=1,25;D 17;D 9;D 20
03.50 T !,"RELATIVE LEAST SQUARES",!;D 3.3
03.51 S S=0;S N3=0;S N1=N0
03.52 F J=1,25; D 18;D 9;D 20
03.54 T !;D 23
03.55 T !;D 24
03.99 G 30.1

09.10 S LA=G/N1;S D1=FLOG(2)/LA
09.20 T N1,LA,D1 .N2,2*S1,!

11.10 S X=0;S Y=0;S X2=0;S XY=0;S DN=0
11.20 F I=1,K;D 12
11.30 S G=Y/X;S B=0
11.32 T "LINE THRU ORIGIN: "; D 11.9
11.39 S DN=K*X2-X+2
11.40 S G=(K*XY-X+Y)/DN;S B=(X2+Y-XY*X)/DN
11.41 T "LINEAR LINE: "
11.90 T "G=",G," B=",B,!
11.91 T !!

12.10 S X=X+D(I);S Y=Y+N(I);S X2=X2+D(I)+2;S XY=XY+D(I)*N(I)

15.10 S T1=0;S T2=0;S T3=0
15.20 F I=K,M;S T1=T1+D(I);S T2=T2+D(I)+2;S T3=T3+N(I)-B
15.30 S N0=.5*G+2*T2/(G*T1-T3)
15.40 S LA=G/N0;S D1=FLOG(2)/LA

```

```

17.10 S S1=0;S S2=0
17.20 F I=K,M;S S2=S2+F0(D(I),N(I)-B);S S1=S1+Z
17.30 S N2=N1-S1/S2
17.40 I(N2) 17.5,17.6,17.6
17.50 S N2=.5*N1
17.60 R

18.10 S S1=0;S S2=0
18.20 F I=K,M;S C=N(I)-B;S S2=S2+F0(D(I),C)/C+2;S S1=S1+Z/C+2
18.30 S N2=N1-S1/S2
18.40 I(N2) 18.5,18.6,18.6
18.50 S N2=.5*N1
18.60 R

20.10 I(S1) 20.2,20.9,20.3
20.20 I(S) 20.5,20.5,20.4
20.30 I(S) 20.4,20.5,20.5
20.40 S N2=N3+S*(N1-N3)/(S-S1)
20.42 I(N2-N3) 20.5,20.9,20.5
20.50 I(N2-N1) 20.6,20.9,20.6
20.60 S N3=N1;S S=S1;S N1=N2;R
20.90 S J=25

23.09 T "LINEAR APPROX"
23.10 T !,;3,"D",;18,"N(D)",;32,"G*D",;!
23.20 F J=1,M;T D(I),N(I),G*D(I),!

24.10 A "N0 ",N1,"LA ",LA
24.20 T !,;3,"D",;18,"N(D)",;32,"N0(1-EXP(-LA*D))",!
24.30 F I=1,M;S T1=N1*(1-FEXP(-LA*D(I)))+B;T D(I),N(I),T1,!

25.20 S T1=G*A'/N1
25.30 S T2=FEXP(-T1)
25.40 S T3=B'-N1*(1-T2)
25.50 S T4=(T1*T2-1+T2)
25.60 S Z=T3*T4
25.70 S Z'=T4+2+T1+2*T2-T3/N1

30.10 C
#

```

BIBLIOGRAPHY

- P. Alexander and M. G. Ormerod, "Repair of the Primary Chemical Lesion: A Unitary Hypothesis for Radiosensitization by Oxygen and Protection by Sulphydryl Compounds," in Biological Effects of Ionizing Radiation at the Molecular Level, International Atomic Energy Agency, Vienna, 1962.
- R. S. Alger, "Trapped Radicals in Radiation Damage," in Formation and Trapping of Free Radicals, A. M. Bass and H. P. Broida, Ed., Academic Press, New York, 1960.
- K. J. Altman, G. B. Gerber, and S. Okoda, Radiation Biochemistry, Volume II Tissue and Body Fluids, Academic Press, New York, 1970.
- H. M. Assenheim, Introduction to Electron Spin Resonance, Hilger & Watts, Ltd., London, 1966.
- S. Ben-Yaakov, "Analog-to-frequency Converter is Accurate and Simple," Electronic Design, 14:96, (July 4, 1968).
- W. Bernhard, "Electron Microscope Studies on Thin Sections of Human Erythrocytes," Nature, 170:359 (1952).
- L. A. Blumenfeld and A. E. Kalmanson, "Electron Spin Resonance (ESR) Investigations on Radiation-Induced Chemical Effects in Biological Species," in The Initial Effects of Ionizing Radiation on Cells, R. J. C. Harris, Ed., Academic Press, New York, 1961.
- F. Bresciani, F. Auricchio, and C. Fiore, "Effect of X-rays on Movements of Sodium in Human Erythrocytes," Radiation Research, 21:394 (1964 a).
- F. Bresciani, F. Auricchio, and C. Fiore, "A Biochemical Study of the X-radiation-induced Inhibition of Sodium Transport (Na Pump) in Human Erythrocytes," Radiation Research, 22:463 (1964 b).
- T. G. Castner, Jr., "Saturation of the Paramagnetic Resonance of a V Center," Physical Review, 115:1506 (1959).
- D. Chapman, Introduction to Lipids, McGraw Hill, New York, 1969.
- G. Cividalli, "Effect of Gamma Irradiation on Glucose Utilization, Glutathione, and Electrolyte Content of the Human Erythrocyte," Radiation Research, 20:564 (1963).

BIBLIOGRAPHY (Continued)

- E. S. Copeland and H. M. Swartz, "Radical Formation in Cysteamine-HCl Gamma-Irradiated in the Dry State and in Frozen Aqueous Solution," Int. J. Rad. Biol., 16:293 (1969).
- J. F. Danielli and H. Davson, "A Contribution to the Theory of Permeability of Thin Films," J. of Cellular and Comparative Physiology, 5:495 (1935).
- J. F. Danielli and E. N. Harvey, "The Tension at the Surface of Mackerel Egg Oil, with Remarks on the Nature of the Cell Surface," J. Cellular and Comparative Physiology, 5:483 (1935).
- D. Daron, A. Nevo, and Y. Marikovsky, "Preparation of Erythrocyte Ghosts by Gradual Haemolysis in Hypotonic Aqueous Solution," Bull. Res. Council of Israel, Vol. 6E:36 (1956).
- H. Dertinger and H. Jung, Molecular Radiation Biology, Springer Verlag, New York, 1970.
- M. M. Dewey and L. Barr, "Some Considerations about the Structure of Cellular Membranes," in Current Topics in Membrane Transport, Vol. 1, F. Branner and A. Kleinzeller, Ed., Academic Press, New York, 1970.
- J. T. Dodge, C. Mitchell, and D. J. Hanahan, "The Preparation and Chemical Characteristics of Hemoglobin-Free Ghosts of Human Erythrocytes," Arch. Biochem. Biophys., 100:119 (1963).
- R. M. Dowben, "Composition and Structure of Membranes," in Biological Membranes, R. M. Dowben, Ed., Little Brown & Company, Boston, 1969.
- R. C. Drew and W. Gordy, "Electron Spin Resonance Studies of Radiation Effects on Polyamino Acids," Radiation Research, 18:552 (1963).
- W. Snipes, Ed., National Academy of Sciences Report 43, Washington, D. C., (1966 a).
- T. Henriksen, "Production of Free Radicals in Solid Biological Substances by Heavy Ions," Radiation Research, 27:676 (1966 b).
- T. Henriksen, "Effect of Oxygen on Radiation-Induced Free Radicals in Proteins," Radiation Research, 32:892 (1967 a).
- T. Henriksen, "Free Radicals and Their Interaction in Solid Molecular Mixtures," Radiation Research, 32:164 (1967 b).

BIBLIOGRAPHY (Continued)

- T. Henriksen, "The Mechanism for Radiation Damage and Repair in Solid Biological Systems as Revealed by ESR Spectroscopy," in Solid State Biophysics, S. J. Ward, Ed., McGraw-Hill, 1969.
- T. Henriksen, "Radicals Induced in Thymine and Some of Its Derivative by Ionizing Radiation and Thermal Hydrogen Atoms," Radiation Research, 40:11 (1969 b).
- T. Henriksen, P. K. Horan, and W. Snipes, "Free Radical Production by Heavy Ions at 77°K and Its Relation to Thermal Spike Theory," Radiation Research, 43:1 (1970).
- T. Henriksen, "Destruction of Free Radicals by Radiation," Int. J. Radiat. Biol., 19:301 (1971).
- R. Höber, "The Surface of the Protoplant, Its Properties and Its Architecture," in Physical Chemistry of Cells and Tissue, R. Höber, Ed., Blakiston, Philadelphia, 1945.
- C. J. Hochanadel, "Evidence for 'Thermal Spikes', in the Alpha-Particle Radiolysis of Nitrate Crystals," Radiation Research, 16:286 (1962).
- A. J. Hoff and D. C. Koningsberger, "Production of Free Radicals in DNA and Inactivation of Its Biological Activity by Gamma Rays," Int. J. Rad. Biol., 17:459 (1970).
- R. Holroyd, J. Glass, and P. Riesz, "Radicals Formed in Protein by Reaction with Hydrogen Atoms," Radiation Research, 44:59 (1970).
- P. K. Horan and W. Snipes, "Free Radical Destruction by Gamma-Irradiation at 77°K," Int. J. Rad. Biol., 15:157 (1969).
- P. K. Horan and W. Snipes, "On the Role of Hydrogen Atoms in Free Radical Site Migration," Int. J. Rad. Biol., 17:201 (1970).
- P. K. Horan and W. Snipes, "The Temperature Dependence of Radiation-Induced Free Radical Destruction," Int. J. Rad. Biol., 19:37 (1971).
- F. M. Huennekens, "In Vitro Aging of Erythrocytes," in The Biology of Aging, A Symposium, B. L. Strehler, Ed., American Institute of Biological Sciences Publication 6, 1960.
- C. A. Hutchison, "Paramagnetic Resonance Absorption in Crystals Colored by Irradiation," Phys. Rev., 75:1769 (1949).
- D. J. E. Ingram, Free Radicals as Studied by Electron Spin Resonance, Academic Press, New York, 1958.

BIBLIOGRAPHY (Continued)

- T. Kankura, W. Nakamura, H. Eto, and M. Nakao, "Effect of Ionizing Radiation on Passive Transport of Sodium Ion into Human Erythrocytes," Int. J. Rad. Biol., 15:125 (1969).
- J. S. Kirby-Smith and M. L. Randolph, "Production and Lifetime of Radiation-Induced Free Radicals in Some Molecules of Biological Importance," in Immediate and Low Level Effects of Ionizing Radiations, A. A. Buzzati-Traverso, Ed., Taylor & Francis Ltd., London, 1960.
- J. S. Kirby-Smith and M. L. Randolph, "Modification of Radiation Induced Electron Spin Resonance in Dry Materials," J. of Cellular and Comparative Physiology, 58:1 (Supplement 1, Dec., 1961).
- J. A. Knight, Jr., Personal Communication, Georgia Tech Engineering Experiment Station, Atlanta, Georgia, 1972.
- C. Kittel and E. Abrahams, "Dipolar Broadening of Magnetic Resonance Lines in Magnetically Diluted Crystals," Phys. Rev., 90:238 (1953).
- G. Kollmann, B. Shapiro, and D. Martin, "The Mechanism of Radiation Hemolysis in Human Erythrocytes," Radiation Research, 37:551 (1969).
- E. D. Korn, "Structure of Biological Membrane," Science, 153:1491 (1966).
- J. L. Kostyo, "Separation of the Effects of Growth Hormone on Muscle Amino Acid Transport and Protein Synthesis," Endocrinology, 75: 113 (1964).
- D. Libby, M. G. Ormerod, and A. Charlesby, "Electron-Spin Resonance Studies of Bovine Serum Albumin and Cystine Irradiated with X-rays at 77°K and at Room Temperature," Int. J. Rad. Biol., 4:21 (1961).
- F. G. Limming, Jr., "Free Radicals Formed in Aliphatic Polyamino Acids by Exposure to Hydrogen Atoms," Radiation Research, 39:252 (1969).
- Ralph Livingston, "The Potentialities and Limitations of the Paramagnetic Resonance Method in Radiation Research," Radiation Research, Supplement 1, 463 (1959).
- J. A. Lucy, "Theoretical and Experimental Models for Biological Membranes," in Biological Membranes Physical Fact and Function, D. Chapman, Ed., Academic Press, New York, 1968.
- G. McCormick and W. Gordy, "Electron Spin Studies of Radiation Damage to Peptides," J. of Physical Chemistry, 62:783 (1958).
- M. E. McLain, Jr., Personal Communication, Georgia Tech Nuclear Research Center, Atlanta, Georgia, 1972.

BIBLIOGRAPHY (Continued)

- P. Milvy and I. Pullman, "ESR Studies of Spin Transfer in Irradiated Nucleic Acid-Cysteamine Systems," Radiation Research, 34:265 (1968).
- P. Milvy, "Dose Dependence of the Transfer of Radiation-Induced Free Radicals from DNA to Cysteamine," Radiation Research, 47:83 (1971).
- A. Müller, "Efficiency of Radical Production by X-rays in Substances of Biological Importance," in Biological Effects of Ionizing Radiation at the Molecular Level, International Atomic Energy Agency, Vienna, 1962.
- A. Müller, "Observations on X-ray-induced Radicals in Whole Bacteriophage and Phage Nucleic Acid," Int. J. Rad. Biol., 6:137 (1963).
- A. Müller, P. E. Schambra, and E. Pietsch, "Comparative ESR Measurements of Radical Production in Amino Acids by ^{210}Po Alpha and ^{60}Co Gamma Radiation," Int. J. Rad. Biol., 7:587 (1964).
- D. K. Myers and R. W. Bide, "Biochemical Effects of X-irradiation on Erythrocytes," Radiation Research, 27:250 (1966).
- D. K. Myers and T. Karazin, "Comparison of the Effects of Radiation on the Cell Membrane and on the Reproductive Survival of Yeast," Radiation Research, 35:612 (1968).
- D. K. Myers, "Some Aspects of Radiation Effects on Cell Membranes," in Advances in Biological and Medical Physics, J. H. Lawrence and J. W. Gofman, Eds., Academic Press, New York, 1970.
- K. F. Nakken, "Radiation Damage to Erythrocyte Membranes and Its Modification," Strahlentherapie, 129:586 (1966).
- G. J. Nelson, "Composition of Neutral Lipids from Erythrocytes of Common Animals," J. Lipid Research, 8:374 (1967).
- S. O. Nielsen and B. V. Rasmussen, "Solid State Processes in Serum Albumin Irradiated at Low Temperatures," in Biological Effects of Ionizing Radiation at the Molecular Level, International Atomic Energy Agency, Vienna, 1962.
- M. G. Ormerod and P. Alexander, "On the Mechanism of Radiation Protection by Cysteamine: An Investigation by Means of Electron Spin Resonance," Radiation Research, 18:495 (1963).
- A. B. Pardee, "Membrane Transport Proteins," Science, 162:632 (1968).

BIBLIOGRAPHY (Continued)

- Frank Patten and Walter Gordy, "Temperature Effects on Free Radical Formation and Electron Migration in Irradiated Proteins," Proc. Nat. Acad. Sci. U.S.A., 46:1137 (1960).
- F. Patten and W. Gordy, "Temperature Effects on the Formation of Free Radicals in the Amino Acids," Radiation Research, 41:573 (1961 a).
- L. H. Piette, R. C. Rempel, H. E. Weaver, and J. M. Flournoy, "EPR Studies of Electron Irradiated Ice and Solid Hydrogen," J. of Chemical Physics, 30:1623 (1959).
- H. Porzig, "Calcium Efflux from Human Erythrocyte Ghosts," J. Membrane Biol., 2:324 (1970).
- T. A. J. Pranker, The Red Cell, Blackwell, Oxford, 1961.
- M. L. Randolph, "Quantitative Studies of Electron Spin Resonance Produced in Biologically Significant Materials by Ionizing Radiation," in Free Radicals in Biological Systems, M. S. Blois, Jr., H. W. Brown, R. M. Lemmon, R. O. Lindblom, and M. Weissbluth, Eds., pp. 249-61, Academic Press, New York, 1961.
- N. H. Rexroad and W. Gordy, Proc. Nat. Acad. Sci. U.S.A., 45:256 (1959).
- P. Riesz and F. H. White, Jr., "Radical Distributions in Gamma-Irradiated Dry Proteins at 195°K," Radiation Research, 44:24 (1970).
- J. D. Robertson, "The Ultrastructure of Cell Membranes and Their Derivatives," Biochemical Soc. Symp., 16:3 (1959).
- J. D. Robertson, "Unit Membranes: A Review with Recent New Studies of Experimental Alterations and a New Submit Structure of Synaptic Membranes, in Cellular Membranes in Development," Proceedings of XXII Symp. of the Society for the Study of Development & Growth, M. Locke, Ed., Academic Press, New York, 1964.
- J. D. Robertson, "Granulo-Fibrillar and Globular Substances in Unit Membranes," Ann. of N. Y. Acad. Sci., 137:429 (1966).
- J. Rotblat and J. A. Simmons, "Dose-Response Relationship in the Yield of Radiation-Induced Free Radicals in Amino Acids," Physics in Medicine and Biology, 7:489 (1964).
- A. Rothstein and R. I. Weed, "The Functional Significance of Sulphydryl Groups in the Cell Membrane," University of Rochester, U.S. AEC Research and Development Report UR-633 or TID-4500, 1963.

BIBLIOGRAPHY (Continued)

- A. Rothstein, "Sulfhydryl Groups in Membrane Structure and Function," in Current Topics in Membranes and Transport, F. Branner and A. Kleinzeller, Eds., Academic Press, New York, 1970.
- G. Rouse, G. J. Nelson, S. Fleischer, and G. Simon, "Lipid Composition of Animal Cell Membranes, Organelles and Organs," in Biological Membranes Physical Fact and Function, D. Chapman, Ed., Academic Press, 1968.
- E. E. Schneider, M. J. Day, and G. Stein, "Effect of X-rays upon Plastics," Nature, 168:644 (1951).
- J. F. Seitz, The Biochemistry of the Cells of Blood and Bone Marrow, Charles C. Thomas, Springfield, Ill., 1969.
- B. Shapiro, G. Kollmann, and J. Asnen, "Mechanism of the Effect of Ionizing Radiation on Sodium Uptake by Human Erythrocytes," Radiation Research, 27:139 (1966).
- B. Shapiro and G. Kollmann, "The Nature of the Membrane Injury in Irradiated Human Erythrocytes," Radiation Research, 34:335 (1968).
- H. Shields and W. Gordy, "Electron Spin Resonance Studies of Radiation Damage to Amino Acids," J. of Physical Chemistry, 62:789 (1958).
- H. Shields and P. J. Hamrick, Jr., "Relative Stability of the Characteristic Sulfur and Doublet Resonances in X-irradiated Native Proteins as Measured with ESR," Radiation Research, 41:259 (1970).
- L. S. Singer, "Synthetic Ruby as a Secondary Standard for the Measurement of Intensities in Electron Paramagnetic Resonance," J. Appl. Phys., 30:1463 (1959).
- R. L. Sinsheimer, "Bacteriophage ϕ X174 and Related Viruses," in Progress in Nucleic Acid Research and Molecular Chemistry, J. N. Davidson and W. E. Cohn, Eds., Academic Press, New York, 1968.
- F. S. Sjöstrand, "A New Ultrastructural Element of the Membranes in Mitochondria and Some Cytoplasmic Membranes," J. Ultrastructure Res., 9:340 (1963 a).
- F. S. Sjöstrand, "A Comparison of Plasma Membrane, Cytomembranes, and Mitochondrial Membrane Elements with Respect to Ultrastructural Features," J. Ultrastructure Res., 9:561 (1963 b).
- R. C. Smith and S. J. Wyard, "Electron Spin Resonance of Free Radicals Produced by Irradiation of Hydrogen-Perioxide-Water Solution in 90°K," in The Fifth International Symposium on Free Radicals July 6-7, 1961, Gordon and Breach, New York, 1961.

BIBLIOGRAPHY (Continued)

- W. Snipes and P. K. Horan, "Electron Spin Resonance Studies of Free Radical Turnover in Gamma-Irradiated Single Crystals of Alanine," Radiation Research, 30:307 (1967).
- S. Spiegelman, "Protein and Nucleic Acid Synthesis in Subcellular Fractions of Bacterial Cells," in Recent Progress in Microbiology (Symposia held at the VIIth International Congress for Microbiology, Stockholm, 1958), G. Tunevali, Ed., Almquist & Wiksells, Stockholm, 1959.
- B. O. Stuart and J. N. Standard, "On the Radioprotective Action of Cystamine at the Yeast Cell Membrane," Radiation Research, 34:459 (1968).
- R. M. Sutherland, J. N. Standard, and R. I. Weed, "Involvement of Sulfhydryl Groups in Radiation Damage to Human Erythrocyte Membrane," Int. J. Rad. Biol., 12:551 (1967).
- R. M. Sutherland and A. Pihl, "Repair of Radiation Damage to Erythrocyte Membranes: The Reduction of Radiation Induced Disulfide Groups," Radiation Research, 34:300 (1968).
- H. M. Swartz, "Cells and Tissues," in Biological Applications of Electron Spin Resonance, H. M. Swartz, J. R. Bolton, and D. C. Borg, Eds., John Wiley, New York, 1972.
- J. J. Ten Bosch, "Free Radical Yields in X-irradiated Glycine Peptides," Int. J. Rad. Biol., 13:93 (1967).
- D. S. Thompson and J. S. Waugh, "Adjustable Ruby Intensity Standard for ESR Spectra," Review of Scientific Instruments, 36:552 (1965).
- W. M. Watkins, "Blood Group Substances," in The Specificity of Cell Surfaces, B. D. Davis and L. Warren, Eds., Prentice-Hall, Englewood Cliffs, N. J., 1967.
- P. Ways and D. J. Hanahan, "Characterization and Quantification of Red Cell Lipids in Normal Man," J. Lipid Research, 5:319 (1964).
- R. I. Weed, C. F. Reed, and G. Berg, "Is Hemoglobin an Essential Structural Component of Human Erythrocyte Membranes," J. Clin. Invest., 42:581 (1963).
- E. D. Wills and J. Rotblat, "The Formation of Peroxide in Tissue Lipids and Unsaturated Fatty Acids by Irradiation," Int. J. Rad. Biol., 8:551 (1965).

BIBLIOGRAPHY (Concluded)

- E. D. Wills and A. E. Wilkinson, "The Effect of Irradiation on Lipid Peroxide Formation in Subcellular Fractions," Radiation Research, 31:732 (1967).
- S. J. Wyard, "Electron Spin Resonance Spectroscopy," in Solid State Biophysics, S. J. Wyard, Ed., McGraw-Hill, New York, 1969 a.
- S. J. Wyard and J. B. Cook, "Electron Spin Resonance Studies of Damage in Biological Materials," in Solid State Biophysics, S. J. Wyard, Ed., McGraw-Hill, New York, 1969.
- J. J. Yunis and W. G. Yasminch, "Glucose Metabolism in Human Erythrocytes," in Biochemical Methods in Red Cell Genetics, J. J. Yunis, Ed., Academic Press, New York, 1969.
- E. Zavoisky, "Paramagnetic Relaxation of Liquid Solutions for Perpendicular Fields," J. Phys. U.S.S.R., 9:211 (1945).
- A. Zermeno and A. Cole, "Radiosensitive Structure of Metaphase and Interphase Hamster Cells as Studied by Low-Voltage Electron Beam Irradiation," Radiation Research, 39:669 (1969).
- K. G. Zimmer, "Evidence for Free-Radical Production in Living Cells Exposed to Ionizing Radiation," Radiation Research, Supplement 1, 519 (1959).
- K. G. Zimmer, Studies on Quantitative Radiation Biology, Hafner Publishing Co., New York, 1961.
- K. G. Zimmer and A. Müller, "New Light on Radiation Biology from Electron Spin Resonance Studies," in Current Topics in Radiation Research, North Holland Publishing Co., Amsterdam, 1965.

VITA

Henry L. Fisher, Jr., born on February 26, 1938, is a native of Mt. Pleasant, North Carolina. After graduating from Mt. Pleasant High School, he attended North Carolina State University from 1956 to 1960 when he received the Bachelor of Science degree in Nuclear Engineering. After continuing his education at this university, he received the Master of Science degree in Applied Mathematics in 1962.

In 1962 Mr. Fisher was given a commission in the U. S. Public Health Service. Until 1969 he worked in this capacity for the National Center for Radiological Health. For two years during this period he was assigned by the Service to the Oak Ridge National Laboratory where he did studies in the Health Physics Division. In 1969 the Service assigned him to the Georgia Institute of Technology for additional graduate work. In 1973 he returned to begin research in the Experimental Biology Laboratory of the Environmental Protection Agency, Research Triangle Park, North Carolina.